UNIVERSITY OF CALIFORNIA, SAN DIEGO

Structured approaches to large-scale systems: Variational integrators for interconnected Lagrange-Dirac systems and structured model reduction on Lie groups

A dissertation submitted in partial satisfaction of the
requirements for the degree
Doctor of Philosophy

in

Mathematics

by

Helen Frances Parks

Committee in charge:

Professor Melvin Leok, Chair
Professor Scott Baden
Professor Randolph Bank
Professor Michael Holst
Professor Sonia Martínez

2015

The dissertation of Helen Frances Parks is approved, and it is acceptable in quality and form for publication on microfilm and electronically:

_____

_____

_____

_____

_____
Chair

University of California, San Diego

2015

DEDICATION

For my scientifically minded grandmothers, Joyce Parks and Betty Armstrong, gifters of puzzles and Legos.

EPIGRAPH

Ours, according to Leibniz, is the best of all possible worlds, and the laws of nature can therefore be described in terms of extremal principles.

—C.L. Siegel & J.K. Moser, *Lectures on Celestial Mechanics*

TABLE OF CONTENTS

LIST OF FIGURES

LIST OF TABLES

ACKNOWLEDGEMENTS

I want to thank Professor Melvin Leok for support and guidance throughout the past few years. I have thoroughly enjoyed our studies of geometric mechanics. I also want to thank Professors Elena Celledoni and Brynjulf Owren for their support of and dedication to the model reduction project presented in Chapter 4.

Chapters 2 and 3 are currently being prepared for submission for publication of the material. Parks, H.F.; Leok, M. The dissertation author was the primary investigator and author of this material.

Chapter 4 represents a portion of material currently being prepared for submission for publication. Parks, H.F.; Celledoni, E.; Owren, B. The dissertation author was the primary investigator and author of this portion.

Thanks to the many wonderful mentors who believed in me sooner and more than I did. Jamal Tajdaran, Jeffrey Gimble, Heinrich Jaeger, Juan Manfredi, Stuart Hastings, Csaba Szabó, Jonathan Rubin, and Bard Ermentrout.

Thanks also to my family and especially my wonderful parents for your love and support.

This dissertation, among many other wonderful things in my life, would not exist without Andy Wilson.

VITA

2010	B. S. in Mathematics with Honors, *summa cum laude*, University of Pittsburgh
2013	M. S. in Mathematics, University of California, San Diego
2015	Ph. D. in Mathematics, University of California, San Diego

PUBLICATIONS

Parks, H.F.; Ermentrout, B.; Rubin, J.E. (2011). The dynamics of a forced coupled network of active elements. *Physica D, 240*(7), 554-67

Wu, X.; Yu, G.; Parks, H.; Heber, T.; Goh, B.C.; Dietrich, M.A.; Pelled, G.; Izadpanah, R.; Gazit, D.; Bunnell, B.A.; Gimble, J.M. (2008). Circadian mechanisms in murine and human bone marrow mesenchymal stem cells following dexamethasone exposure. *Bone, 42*(5)

ABSTRACT OF THE DISSERTATION

Structured approaches to large-scale systems: Variational integrators for interconnected Lagrange-Dirac systems and structured model reduction on Lie groups

by

Helen Frances Parks

Doctor of Philosophy in Mathematics

University of California, San Diego, 2015

Professor Melvin Leok, Chair

This dissertation presents two projects related to the structured integration of large-scale mechanical systems. Structured integration uses the considerable differential geometric structure inherent in mechanical motion to inform the design of numerical integration schemes. This process improves the qualitative properties of simulations and becomes especially valuable as a measure of accuracy over long time simulations in which traditional Gronwall accuracy estimates lose their meaning. Often, structured integration schemes replicate continuous symmetries and their associated conservation laws at the discrete level.

Such is the case for variational integrators, which discretely replicate the

process of deriving equations of motion from variational principles. This results in the conservation of momenta associated to symmetries in the discrete system and conservation of a symplectic form when applicable. In the case of Lagrange-Dirac systems, variational integrators preserve a discrete analogue of the Dirac structure preserved in the continuous flow. In the first project of this thesis, we extend Dirac variational integrators to accommodate interconnected systems. We hope this work will find use in the fields of control, where a controlled system can be thought of as a "plant" system joined to its controller, and in the approach of very large systems, where modular modeling may prove easier than monolithically modeling the entire system.

The second project of the thesis considers a different approach to large systems. Given a detailed model of the full system, can we reduce it to a more computationally efficient model without losing essential geometric structures in the system? Asked without the reference to structure, this is the essential question of the field of model reduction. The answer there has been a resounding yes, with Principal Orthogonal Decomposition (POD) with snapshots rising as one of the most successful methods. Our project builds on previous work to extend POD to structured settings. In particular, we consider systems evolving on Lie groups and make use of canonical coordinates in the reduction process. We see considerable improvement in the accuracy of the reduced model over the usual structure-agnostic POD approach.

Chapter 1

Introduction and background

This thesis extends variational integrators to the setting of interconnected Dirac mechanical systems. These ideas are rooted in the geometric interpretation of mechanics and its use in the development of structured integrators. This specific project is motivated by the work of Jerry Marsden, and in particular by future objectives laid out at the end of [20]. In [19] and [20], Yoshimura and Marsden develop the theory of implicit Lagrangian systems, including both Dirac structures and variational principles. The authors hoped to extend this work to the settings of variational integrators and control by interconnection. Leok and Ohsawa developed variational integrators for implicit Lagrangian systems in [12], while Jacobs and Yoshimura developed the continuous theory of interconnections in [10]. The present work merges these two developments, and we hope that it will be useful in the practical study of interconnected systems, including in particular control systems.

This first chapter presents a detailed overview of the relevant background. We review the geometric perspective of continuous Lagrangian and Hamiltonian mechanics as well as the generalization to Lagrange-Dirac dynamics and Lagrange-Dirac interconnections. We briefly discuss the merits of structured integration in general before focusing on variational integrators in particular, including variational integrators for Lagrange-Dirac systems. We will revisit these concepts in the introductory portions of later chapters as needed.

1.1 Geometric mechanics

Sometimes referred to as the modern perspective of mechanics, geometric mechanics takes the view that mechanical systems evolve on manifolds. This simple shift from strictly Euclidean spaces to manifolds allows the many tools of differential geometry to be applied to mechanical analysis. The two fields intertwine in a remarkably rich and natural way.

1.2 Lagrangian and Hamiltonian mechanics from variational principles

We begin by reviewing classical Lagrangian and Hamiltonian mechanics from the geometric perspective. Let Q be an n-dimensional configuration manifold with local coordinates $(q^1, \ldots, q^n)$. The associated state and phase spaces are given by the tangent and cotangent bundles TQ and T^*Q, respectively. Denote coordinates on TQ by $(q^1, \ldots, q^n, v^1, \ldots, v^n)$ and coordinates on T^*Q by $(q^1, \ldots, q^n, p_1, \ldots, p_n)$. Let $L : TQ \to \mathbb{R}$ be a Lagrangian function and $H : T^*Q \to \mathbb{R}$ be a Hamiltonian. We can derive the equations of motion for both perspectives using variational principles.

On the Lagrangian side, we employ Hamilton's state space principle, most often referred to simply as Hamilton's principle. Define the action functional on curves in Q by

$$\mathfrak{S}(q) := \int_0^T L(q(t), \dot{q}(t))\ dt. \tag{1.1}$$

Hamilton's principle states that the curve joining fixed endpoints q_0 and q_1 in Q in a fixed time T is a stationary point of the action. That is,

$$\delta\mathfrak{S}(q) = \delta \int_0^T L(q(t), \dot{q}(t))\ dt = 0, \tag{1.2}$$

for variations with fixed endpoints. From this principle we can compute explicitly

the following

$$0 = \int_0^T \frac{\partial L}{\partial q}\delta q + \frac{\partial L}{\partial \dot{q}}\delta \dot{q}\ dt \tag{1.3}$$

$$= \int_0^T \left[\frac{\partial L}{\partial q} - \frac{d}{dt}\frac{\partial L}{\partial \dot{q}}\right]\delta q\ dt + \frac{\partial L}{\partial \dot{q}}\delta q\Big|_0^T. \tag{1.4}$$

Because we have assume that we have fixed endpoints and because this relationship must hold for any $\delta q(t)$, we conclude by the fundamental theorem of the calculus of variations that

$$\frac{\partial L}{\partial q} - \frac{d}{dt}\frac{\partial L}{\partial \dot{q}} = 0 \tag{1.5}$$

along the curve $q(t)$. These are the usual Euler-Lagrange equations of motion of Lagrangian mechanics.

On the Hamiltonian side, we turn to Hamilton's phase space principle. Again, the principle states that curves joining fixed endpoints in a fixed time interval are stationary points of an action integral. Again, we hold the endpoints $q_0, q_1 \in Q$ fixed. The action integral is given in terms of the Hamiltonian as

$$\int_0^T (\langle p, \dot{q}\rangle - H(q,p))\ dt. \tag{1.6}$$

Thus, the full principle is

$$\delta \int_0^T (\langle p, \dot{q}\rangle - H(q,p))\ dt = 0, \tag{1.7}$$

for variations that fix the endpoints. Once again we can explicitly compute the variations to derive the equations of motion. In this case, we arrive at Hamilton's canonical equations.

$$0 = \int_0^T \langle \delta p, \dot{q}\rangle + \langle p, \delta \dot{q}\rangle - \frac{\partial H}{\partial q}\cdot \delta q - \frac{\partial H}{\partial p}\cdot \delta p\ dt \tag{1.8}$$

$$= \int_0^T \left[\left(-\frac{\partial H}{\partial p} + \dot{q}\right)\cdot \delta p - \left(\frac{\partial H}{\partial q} + \dot{p}\right)\delta q\right]\ dt + p\cdot \delta q\Big|_{t=0}^{t=T}. \tag{1.9}$$

The boundary term comes from integrating $\langle p, \delta \dot{q}\rangle$ by parts. Under the assumption of fixed endpoints, $\delta q(0) = \delta q(T) = 0$, so the boundary term disappears. The remaining integral must then equal 0 for all variations $\delta p, \delta q$. Thus, by the fundamental theorem of the calculus of variations, we have Hamilton's equations,

$$\dot{q} = \frac{\partial H}{\partial p},\ \dot{p} = -\frac{\partial H}{\partial q}. \tag{1.10}$$

1.3 Symplectic structures in classical mechanics

The flow of Hamilton's equations evolving on a cotangent bundle T^*Q preserves the canonical symplectic form on T^*Q. This fact is quite central to the themes of this thesis, so we will spend some time exploring it in this section. You may, like me, find this interesting simply for the remarkable beauty of finding such high level mathematics in our daily experience. From a practical standpoint, the universality of symplectic conservation guides the development of structured integrators. Integrators which conserve a symplectic form along numerical solutions (called *symplectic integrators*) are one of the most widely applicable classes of structure-preserving numerical integrators. They offer impressive qualitative gains to any conservative Hamiltonian problem, sometimes with no more computational effort than a more naive approach. We'll talk about this more in the geometric integration sections below. For now, we define symplectic manifolds and discuss the ways in which both the cotangent bundle T^*Q and mechanical flows are symplectic.

1.3.1 Symplectic manifolds and T^*Q

Let M be a manifold, and Ω a nondegenerate two-form on M. If Ω is also closed, i.e. $\mathbf{d}\Omega = 0$, then Ω is called a *symplectic form*, and the pair (M, Ω) is called a *symplectic manifold*. A map $f : M \to M$ is called a *symplectic* or *canonical* map if $f^*\Omega = \Omega$. Recall the following definition of the pullback notation,

$$f^*\Omega_m(v_m, w_m) = \Omega_{f(m)}(Tf(v_m), Tf(w_m)), \tag{1.11}$$

where Ω_m denotes the form Ω at the point $m \in M$, $v_m, w_m \in T_mM$, and Tf denotes the tangent lift of the map f. Thus, f is a symplectic map if Tf preserves the symplectic structure in this way. We now review the way in which any cotangent bundle T^*Q is a symplectic manifold for a canonical symplectic form Ω_{T^*Q}.

Given a configuration manifold Q, coordinates on Q induce coordinates on T^*Q referred to as *canonical coordinates*. These are the coordinates (q^i, p_i) referred to in the previous section. Given a choice of canonical coordinates, there exists a

unique one-form Θ on T^*Q given in coordinates by

$$\Theta(q,p) = \sum_i p_i dq^i. \tag{1.12}$$

Here, (dq^i, dp_i) represents the canonical basis for T^*T^*Q induced from the coordinates (q^i, p_i) on T^*Q. Note that Θ can be intrinsically defined — for instance, we may require that $\Theta(v_{\alpha_q}) = \langle \alpha_q, T\pi_Q(v_{\alpha_q})\rangle$ — but that Θ will have the coordinate expression (1.12) for any choice of canonical coordinates.

The canonical symplectic form Ω_{T^*Q} is then given by $\Omega_{T^*Q} = -\mathbf{d}\Theta$. In any choice of canonical coordinates,

$$\Omega_{T^*Q} = \sum_i dq^i \wedge dp_i. \tag{1.13}$$

For nondegeneracy, we need to check that $\Omega_{\alpha_q}(v_{\alpha_q}, w_{\alpha_q}) = 0$ for all w_{α_q} implies $v_{\alpha_q} = 0$. This is a straightforward calculation in local coordinates. The form Ω_{T^*Q} is clearly a two-form, and it is closed by the $\mathbf{d}^2 = 0$ property of the exterior derivative. Thus, (T^*Q, Ω_{T^*Q}) is indeed a symplectic manifold.

1.3.2 Hamiltonian flows are symplectic

Given a symplectic manifold (M, Ω) and any function $H : M \to \mathbb{R}$, we denote by X_H the *Hamiltonian vector field* on M associated with H. We define the vector field through Ω by

$$\Omega_m(X_H(m), w) = \mathbf{d}H \cdot w \tag{1.14}$$

for all $w \in T_mM$. We can use contraction notation to write (1.14) more succinctly as $\mathbf{i}_{X_H}\Omega = \mathbf{d}H$. With this definition, we can write Hamilton's equations (1.10) equivalently as

$$(\dot{q}, \dot{p}) = X_H(q,p). \tag{1.15}$$

Thus, the flow of the Hamiltonian system determined by H is the flow of the vector field X_H. Denote by $\varphi_t : T^*Q \to T^*Q$ the time t flow of X_H. As the section title suggests, this flow map is symplectic, i.e. $\varphi_t^*\Omega_{T^*Q} = \Omega_{T^*Q}$.

To show this explicitly we rely on the Lie derivative and Cartan's magic formula. Recall the following fact about Lie derivatives for a given k-form α and vector field X with flow ψ_t [14],

$$\frac{d}{dt}\psi_t^*\alpha = \psi_t^*\mathcal{L}_X\alpha. \tag{1.16}$$

We also recall Cartan's magic formula for the Lie derivative,

$$\mathcal{L}_X\alpha = \mathbf{d}\mathbf{i}_X\alpha + \mathbf{i}_X\mathbf{d}\alpha. \tag{1.17}$$

Lastly, recalling that both Ω and $\mathbf{i}_{X_H}\Omega = \mathbf{d}H$ are closed, we compute

$$\mathcal{L}_{X_H}\Omega = \mathbf{d}\mathbf{i}_{X_H}\Omega + \mathbf{i}_{X_H}\mathbf{d}\Omega = 0. \tag{1.18}$$

Thus,

$$\frac{d}{dt}\varphi_t^*\Omega = 0. \tag{1.19}$$

To complete the argument, note that φ_0 is the identity, so $\varphi_0^*\Omega = \Omega$. Hence, for all t, $\varphi_t^*\Omega = \Omega$, and the Hamiltonian flow determined by H is symplectic on T^*Q.

We focus here on the symplectic nature of Hamiltonian mechanics in canonical coordinates because it bears an intimate relationship with the Dirac structure of Dirac mechanics central to this thesis. One should note that there exists a more general description of Hamiltonian mechanics via Poisson structures.The Poisson description allows for Hamiltonian systems in non-canonical coordinates, which can be useful for describing symmetry-reduced systems among other things. The Poisson description encompasses the symplectic one; every symplectic structure naturally induces a Poisson structure on the same underlying manifold.

1.3.3 The Legendre transform and symplectic Lagrangian flows

Hamiltonian and Lagrangian mechanics are related through the *fiber derivative* or *Legendre transform* $\mathbb{F}L : TQ \to T^*Q$ defined by

$$\mathbb{F}L(v) \cdot w = \frac{d}{ds}\Big|_{s=0} L(v + sw). \tag{1.20}$$

In coordinates,

$$\mathbb{F}L(q,\dot{q}) = \left(q, \frac{\partial L}{\partial \dot{q}}\right). \tag{1.21}$$

The variable

$$p = \frac{\partial L}{\partial \dot{q}} \tag{1.22}$$

is called the *conjugate momentum*. We also define an *energy function* associated to L by

$$E(v) = \mathbb{F}L(v) \cdot v - L(v) \tag{1.23}$$

for $v \in TQ$.

One might hope that the Hamiltonian dynamics of E in the canonical variables given by the conjugate momenta would be equivalent to the Lagrangian dynamics of L. This is the case locally when L is regular and globally if L is hyperregular. We say that L is *regular* if the quadratic form

$$\mathbf{D}_2\mathbf{D}_2 L = \frac{\partial^2 L}{\partial \dot{q}^2} \tag{1.24}$$

is nondegenerate. Otherwise we say that L is *degenerate*. Regularity implies that the Legendre transform $\mathbb{F}L$ is locally invertible. We say that L is *hyperregular* if the Legendre transform is a diffeomorphism and hence globally invertible.

In the case of a regular Lagrangian, we can use $\mathbb{F}L$ to pull back the forms Θ, Ω on T^*Q to define

$$\Theta_L = \mathbb{F}L^*\Theta \quad \text{and} \quad \Omega_L = \mathbb{F}L^*\Omega_{T^*Q}. \tag{1.25}$$

The exterior differential $\mathbf{d}$ commutes with the pullback operation, so we have $\Omega_L = -\mathbf{d}\Theta_L$, analogous to the Hamiltonian case. Thus, Ω_L is closed. It is clearly also a two-form on TQ. Regularity of the Lagrangian guarantees nondegeneracy of Ω_L, so that Ω_L is a symplectic form and (TQ, Ω_L) is a symplectic manifold.

With this in place, we take the Lagrangian vector field X_L to be the Hamiltonian vector field of E with respect to Ω_L, i.e.

$$\Omega_L(v)(X_L(v), w_v) = \mathbf{d}E(v) \cdot w_v \tag{1.26}$$

for all $w_v \in T_vTQ$. Note that nondegeneracy of Ω_L and hence regularity of L are needed for X_L to be well-defined in this way.

Because X_L is defined as the Hamiltonian vector field of some function via a symplectic form, the same Lie derivative arguments from above prove that the flow of X_L is symplectic on (TQ, Ω_L). The integral curves of X_L satisfy the Euler-Lagrange equations for L [14]. That is, the Euler-Lagrange equations are equivalent to the statement

$$\dot{v} = X_L(v) \tag{1.27}$$

for $v \in TQ$. Thus, the Lagrangian flow determined by L is symplectic. Clearly these arguments for symplecticity break down for degenerate Lagrangians. Indeed, the system becomes pre-symplectic rather than symplectic. Dirac mechanics, described below, addresses this situation.

1.4 Momentum preservation

We focus on the Lagrangian perspective, as that is the perspective we will use later. To talk about momentum conservation, we begin with symmetry. At the end of this section we will quote the famous Noether's theorem stating that symmetry results in momentum conservation. We take the geometric perspective and describe symmetry as invariance under the action of a Lie group G with Lie algebra $\mathfrak{g}$. Denote the left action of G on Q by $\Phi : G \times Q \to Q$ and the tangent lifted action by $\Phi^{TQ} : G \times TQ \to TQ$. We can write Φ^{TQ} as $\Phi_g^{TQ}(v_q) = T(\Phi_g) \cdot v_q$, where the subscript g denotes fixing the group variable, or in coordinates,

$$\Phi^{TQ}(g, (q, \dot{q})) = \left(\Phi^i(g, q), \frac{\partial \Phi^i}{\partial q^j}(g, q)\dot{q}^j \right). \tag{1.28}$$

We call the group action a *symmetry* of the Lagrangian if $L : TQ \to \mathbb{R}$ is *invariant* under the lifted action Φ^{TQ}, i.e. if $L \circ \Phi_g^{TQ} = L$ for all $g \in G$.

For each algebra element $\xi \in \mathfrak{g}$, we have the *infinitesimal generators* $\xi_Q : Q \to TQ$ and $\xi_{TQ} : TQ \to T(TQ)$ given by

$$\xi_Q(q) = \frac{d}{dg}\left(\Phi_g(q)\right) \cdot \xi, \tag{1.29}$$

$$\xi_{TQ}(v_q) = \frac{d}{dg}\left(\Phi_g^{TQ}(v_q)\right) \cdot \xi. \tag{1.30}$$

We often write ξ_Q more explicitly as

$$\xi_Q(q) = \frac{d}{dt}|_{t=0}\Phi_{\exp(t\xi)}(q). \tag{1.31}$$

Differentiating the invariance condition above shows that an invariant Lagrangian is also *infinitesimally invariant*, i.e. $\mathbf{d}L \cdot \xi_{TQ} = 0$ for all $\xi \in \mathfrak{g}$. The infinitesimal generators also allow us to define the *Lagrangian momentum map* $J_L : TQ \to \mathfrak{g}^*$ associated with the group action,

$$J_L(v_q) \cdot \xi = \left\langle \frac{\partial L}{\partial \dot{q}}, \xi_Q(q) \right\rangle. \tag{1.32}$$

Noether's theorem then states that when the group action is a symmetry, the Lagrangian flow preserves the association Lagrangian momentum map.

Theorem 1 (Noether's theorem [15])**.** Consider a Lagrangian system $L : TQ \to \mathbb{R}$ which is invariant under the lift of the (left or right) action $\Phi : G \times Q \to Q$. Then the corresponding Lagrangian momentum map $J_L : TQ \to \mathfrak{g}^*$ is a conserved quantity of the flow, so that $J_L \circ F_L^t = J_L$ for all times t.

Here F_L^t denotes the time t flow map of the Lagrangian system on Q determined by L. Conservation of the classical linear and angular momenta arises in this way, with linear momentum $J_L : T\mathbb{R}^n \to \mathbb{R}^n$ coming from $\mathbb{R}^n$ acting additively on itself and angular momentum $J_L : T\mathbb{R}^n \to \mathfrak{so}(n)^*$ coming from the action of $n \times n$ rotation matrices on $\mathbb{R}^n$. (The set of $n \times n$ rotation matrices is the Lie group $SO(n)$ with Lie algebra $\mathfrak{so}(n)$, the set of $n \times n$ skew-symmetric matrices.)

1.5 Forced Lagrangian systems

Again, we focus on the Lagrangian perspective. A *Lagrangian force* is a map $f_L : TQ \to T^*Q$ written in coordinates as

$$f_L : (q, \dot{q}) \mapsto (q, f_L(q, \dot{q})). \tag{1.33}$$

Thus, f_L is a fiber-preserving map over the identity. Any external forces acting on a mechanical system are modeled as such Lagrangian forces. In this case, we

expand Hamilton's principle to the *Lagrange-d'Alembert* principle,

$$\delta\left[\int_0^T L(q(t),\dot{q}(t))\ dt\right] + \int_0^T f_L(q(t),\dot{q}(t))\cdot\delta q(t)\ dt = 0. \tag{1.34}$$

As in Hamilton's principle, we consider only variations that fix the endpoints, so $\delta q(0) = \delta q(T) = 0$. Computing variations yields the *forced Euler-Lagrange equations*, given in coordinates as

$$\frac{\partial L}{\partial q}(q,\dot{q}) - \frac{d}{dt}\left(\frac{\partial L}{\partial \dot{q}}(q,\dot{q})\right) + f_L(q,\dot{q}) = 0. \tag{1.35}$$

Observe that for $f_L \equiv 0$, the Lagrange-d'Alembert principle reduces to Hamilton's principle, and the forced Euler-Lagrange equations reduce to the usual Euler-Lagrange equations.

Forcing terms affect the preservation of momentum, with only those symmetries whose group action is orthogonal to the forcing resulting in conserved momentum maps. We have the following forced Noether's theorem.

Theorem 2 ([15])**.** Consider a Lagrangian system $L : TQ \to \mathbb{R}$ with forcing $f_L : TQ \to T^*Q$ and a symmetry action $\Phi : G \times Q \to Q$ such that $\langle f_L(q,\dot{q}), \xi_Q(q)\rangle = 0$ for all $(q,\dot{q}) \in TQ$ and all $\xi \in \mathfrak{g}$. Then the Lagrangian momentum map $J_L : TQ \to \mathfrak{g}^*$ will be preserved by the flow, so that $J_L \circ F_L^t = J_L$ for all t.

Here F_L^t denotes the time t flow of the Lagrangian system on Q defined by L, f_L. If L is hyperregular, then L has an associated Hamiltonian H, and the forced Euler-Lagrange equations (1.35) are equivalent to the forced Hamiltonian equations for H. However, the flow no longer preserves the symplectic form in the presence of nonzero forcing.

1.6 Port-Hamiltonian mechanics

Port-Hamiltonian systems grew out of the control literature as a way to meld theoretical analysis via the Hamiltonian formalism with the practical habit of interconnected network modeling [6]. The port-Hamiltonian paradigm takes energy as the fundamental physical concept in modeling and focuses on modeling power flow [6]. A port-Hamiltonian system has internal energy storage and

dissipation ports as well as an external port for interacting with a controller and an external port for interacting with its surroundings [18]. The power-conserving structure of these systems is modeled using Dirac structures, and the formulation of a port-Hamiltonian system through a Dirac structure is often implicit, i.e. involving algebraic constraints [18]. One of the principal advantages of the port-Hamiltonian framework is that the power-conserving interconnection of two port-Hamiltonian systems via their external points is again a port-Hamiltonian system [18]. Thus, port-Hamiltonian systems can be used to model complex, large-scale systems in a way that keeps their geometry in full view [6]. The interconnected port-Hamiltonian framework can also be considered as a control paradigm in which the controllers themselves are port-Hamiltonian systems. Joining a controller port-Hamiltonian system to a "plant" port-Hamiltonian system via the plant's control ports produces, again, a port-Hamiltonian system. This has the advantage, as mentioned above, of maintaining a structured description of the full, controlled system. It also allows for a physical interpretation and thus, potentially, a physical realization of any controllers designed using this framework [18]. Helpfully, the framework itself suggests ways in which to construct such port-Hamiltonian controllers when the desired controller action has been found [18].

We review port-Hamiltonian systems here because Yoshimura and Marsden developed the Lagrange-Dirac mechanics of the next section as a way of understanding implicit port-Hamiltonian systems from the Lagrangian perspective [19, 20]. That aim is rooted partially in the natural desire to understand implicit systems from both classical perspectives. It also moves toward the goal of studying interconnections and control by interconnection using structured computations via variational integrators, which are most often derived from the Lagrangian perspective.

1.7 Dirac structures and Langrange-Dirac mechanics

Let V be a finite dimensional vector space with dual V^*. Denote the natural pairing between V and V^* by $\langle \cdot, \cdot \rangle$, and define the symmetric pairing $\langle\langle \cdot, \cdot \rangle\rangle$ on $V \oplus V^*$ by

$$\langle\langle (v_1, \alpha_1), (v_2, \alpha_2) \rangle\rangle = \langle \alpha_1, v_2 \rangle + \langle \alpha_2, v_1 \rangle \tag{1.36}$$

for $(v_1, \alpha_1), (v_2, \alpha_2) \in V \oplus V^*$. A Dirac structure on V is a subset $D \subset V \oplus V^*$ such that $D = D^\perp$ with respect to $\langle\langle \cdot, \cdot \rangle\rangle$.

Now let M be a smooth manifold. Denote by $TM \oplus T^*M$ the Pontryagin bundle over M, so the fiber over $x \in M$ is $T_xM \oplus T_x^*M$. Then a *Dirac structure on* M is a subbundle $D \subset TM \oplus T^*M$ such that every fiber $D(x)$ is a Dirac structure on T_xM. Dirac structures on manifolds were initially called almost Dirac structures in the literature. We omit the "almost" for brevity as it should be clear from context whether we are dealing with vector space or manifold Dirac structures.

Every manifold Dirac structure D has an associated distribution defined by

$$\Delta_D(x) = \{ v \in T_xM \mid (v, \alpha) \in D(x) \text{ for some } \alpha \}. \tag{1.37}$$

The Dirac structure D also defines a bilinear map on Δ_D,

$$\omega_{\Delta_D}(v, w) = \langle \alpha_v, w \rangle. \tag{1.38}$$

This holds for any α_v such that $(v, \alpha_v) \in D(x)$ and any $w \in \Delta_D(x)$. The form ω_{Δ_D} is well-defined on Δ_D even if there exist multiple such α_v. Suppose (v, α_v) and (v, β_v) are both in $D(x)$. By definition of $\Delta_D(x)$, there must exist $\alpha_w \in T_x^*M$ such that $(w, \alpha_w) \in D(x)$. Then because $D = D^\perp$ with respect to the symmetric pairing above, we have

$$\langle \alpha_v, w \rangle = -\langle \alpha_w, v \rangle = \langle \beta_v, w \rangle. \tag{1.39}$$

That is, if (v, α_v) and (v, β_v) are both in $D(x)$ and $w \in \Delta_D(x)$, then α_v and β_v have the same action on w, making ω_{Δ_D} well defined on Δ_D.

Conversely, given a two-form ω on M and a regular distribution $\Delta \subset TM$, we can define a Dirac structure D on M fiber-wise as

$$D(x) = \{(v, \alpha) \in T_xM \oplus T_x^*M \mid v \in \Delta(x) \text{ and } \langle \alpha, w \rangle = \omega_x(v, w) \text{ for all } w \in \Delta(x)\}. \tag{1.40}$$

Clearly, in this case $\Delta_D = \Delta$ and $\omega_{\Delta_D} = \omega|_{\Delta_D}$. We use this idea later to connect Dirac structures with constraint distributions.

1.7.1 Induced Dirac structures

Dirac structures are especially relevant in the case of Lagrangian systems with linear nonholonomic constraints, i.e. constraints of the form $\omega^a(q) \cdot \dot{q} = 0$, $a = 1, \ldots, m$ for $\{\omega^a\}$ one forms on Q. Such constraints can be equivalently expressed using the regular distribution $\Delta_Q \subset TQ$ defined by $\Delta_Q(q) = \cap_a \ker(\omega^a(q))$. Thus, the annihilator codistribution of Δ_Q is given by $\Delta_Q^\circ(q) = \text{span}\{\omega^a(q)\}$. The constraints are then written $\dot{q} \in \Delta_Q(q)$ or simply $\dot{q} \in \Delta_Q$. Nonholonomic constraints such as these cause the motion on T^*Q to be pre-symplectic rather than symplectic. The Dirac structure induced by Δ_Q gives a precise description of this pre-symplectic structure. Note that we may also have primary constraints on T^*Q if L is degenerate.

The constraints Δ_Q induce a Dirac structure on T^*Q as follows. From Δ_Q, define $\Delta_{T^*Q} \subset TT^*Q$ as

$$\Delta_{T^*Q} = (T\pi_Q)^{-1}(\Delta_Q) \tag{1.41}$$

for $\pi_Q : T^*Q \to Q$ the canonical projection and $T\pi_Q$ its tangent lift. We now apply the construction described in (1.40) using Δ_{T^*Q} and the canonical symplectic form Ω on T^*Q. This gives the following fiber-wise definition of D_{Δ_Q}, the Dirac structure on T^*Q induced by the constraint distribution Δ_Q.

$$D_{\Delta_Q}(q,p) = \{(v, \alpha) \in T_{(q,p)}T^*Q \oplus T^*_{(q,p)}T^*Q \mid v \in \Delta_{T^*Q}(q,p) \text{ and } \langle \alpha, w \rangle = \Omega(v, w) \text{ for all } w \in \Delta_{T^*Q}(q,p)\}. \tag{1.42}$$

1.7.2 Canonical local coordinate expressions

It will be useful to have expressions for $\Delta_{T^*Q}, \Delta^\circ_{T^*Q}$, and D_{Δ_Q} in terms of local canonical coordinates. Let V be a model vector space for the configuration manifold Q, and let $U \subset V$ be a chart around $q \in Q$. Then we have the following local representations near q,

$$\begin{aligned} TQ &\mapsto U \times V, \\ T^*Q &\mapsto U \times V^*, \\ TTQ &\mapsto (U \times V) \times (V \times V), \\ TT^*Q &\mapsto (U \times V^*) \times (V \times V^*), \\ T^*T^*Q &\mapsto (U \times V^*) \times (V^* \times V). \end{aligned}$$

In these coordinates $\pi_Q : (q,p) \mapsto q$ and $T\pi_Q : (q,p,\delta q,\delta p) \mapsto (q,\delta q)$, so that

$$\Delta_{T^*Q} = \{(q,p,\delta q,\delta p) \in T_{(q,p)}T^*Q \mid (q,\delta q) \in \Delta_Q\} \tag{1.43}$$

with the annihilator distribution

$$\Delta^\circ_{T^*Q}(q,p) = \{(q,p,\alpha_q,\alpha_p) \in T^*_{(q,p)}T^*Q \mid (q,\alpha_q) \in \Delta^\circ_Q \text{ and } \alpha_p = 0\}. \tag{1.44}$$

As indicated above, any $v \in T_{(q,p)}T^*Q$ has two coordinate components. We will write these as $(\delta q, \delta p)$ in the abstract case or (v_q, v_p) when referring to a particular v. Similarly, we will write $\alpha = (\alpha_q, \alpha_p)$ for $\alpha \in T^*_{(q,p)}T^*Q$. In this notation, $\Omega(v,w) = v_q \cdot w_p - v_p \cdot w_q$. So the condition $\langle \alpha, w \rangle = \Omega(v,w)$ for all $w \in \Delta_{T^*Q}$ translates to $(\alpha_q + v_p, \alpha_p - v_q) \in \Delta^\circ_{T^*Q}$. Thus the induced Dirac structure in (1.42) has the coordinate expression

$$\begin{aligned} D_{\Delta_Q}(q,p) = \{(v_q,v_p,\alpha_q,\alpha_p) \in T_{(q,p)}T^*Q \oplus T^*_{(q,p)}T^*Q \mid v_q \in \Delta_Q(q), \\ \alpha_p = v_q, \text{ and } \alpha_q + v_p \in \Delta^\circ_Q(q)\}. \end{aligned} \tag{1.45}$$

1.7.3 The Tulczyjew triple

We now introduce a set of three natural diffeomorphisms called the Tulczyjew triple. These maps are integral to the definition of Lagrange-Dirac systems. The Tulczyjew triple relates the spaces T^*T^*Q, TT^*Q, and T^*TQ and helps bridge

the gap between Lagrangian and Hamiltonian mechanics. These maps were first studied by Tulczyjew in the context of a generalized Legendre transform in [17]. The first map is the usual flat map derived from the symplectic form Ω on T^*Q. We write $\Omega^\flat : TT^*Q \to T^*T^*Q$ defined by

$$\Omega^\flat(v) \cdot w = \Omega(v, w). \tag{1.46}$$

In coordinates,

$$\Omega^\flat(v) = (-v_p, v_q) \in T^*T^*Q. \tag{1.47}$$

The second map, $\kappa_Q : TT^*Q \to T^*TQ$ is given locally by a simple coordinate shuffling,

$$\kappa_Q : (q, p, \delta q, \delta p) \mapsto (q, \delta q, \delta p, p). \tag{1.48}$$

A global definition of κ_Q can be found in [19]. A unique diffeomorphism κ_Q exists for any manifold Q [19]. The third map, $\gamma_Q : T^*TQ \to T^*T^*Q$ is defined in terms of the first two,

$$\gamma_Q := \Omega^\flat_{T^*Q} \circ \kappa_Q^{-1}. \tag{1.49}$$

1.7.4 Lagrange-Dirac dynamical systems

We are now equipped to define a Lagrange-Dirac dynamical system. Let $L : TQ \to \mathbb{R}$ be a given, possibly degenerate, Lagrangian. We define the Dirac differential of L to be

$$\mathfrak{D}L(q, v) := \gamma_Q \circ \mathbf{d}L : TQ \to T^*T^*Q. \tag{1.50}$$

Here $\mathbf{d}$ denotes the usual exterior derivative operator so that $\mathbf{d}L : TTQ \to T^*TQ$. For a curve $(q(t), v(t), p(t)) \in TQ \oplus T^*Q$, we define X_D to be the following partial vector field

$$X_D(q(t), v(t), p(t)) = (q(t), p(t), \dot{q}(t), \dot{p}(t)) \in TT^*Q. \tag{1.51}$$

Then the equations of motion for a Lagrange-Dirac dynamical system with Lagrangian L and constraint distribution Δ_Q are given by

$$(X_D(q(t), v(t), p(t)), \mathfrak{D}L(q(t), v(t))) \in D_{\Delta_Q}(q(t), p(t)). \tag{1.52}$$

In local coordinates $\mathbf{d}L(q,v) = (q, v, \frac{\partial L}{\partial q}, \frac{\partial L}{\partial v})$ and

$$\gamma_Q : (q, \delta q, \delta p, p) \mapsto (q, p, -\delta p, \delta q), \tag{1.53}$$

so we have

$$\mathfrak{D}L(q,v) = (q, \frac{\partial L}{\partial v}, -\frac{\partial L}{\partial q}, v). \tag{1.54}$$

Then using the coordinate expressions from (1.45), the equations determined by (1.52) are

$$\dot{q} = v \in \Delta_Q(q),\ \dot{p} - \frac{\partial L}{\partial q} \in \Delta_Q^\circ(q),\ p = \frac{\partial L}{\partial v}. \tag{1.55}$$

The last equation comes from matching the basepoints of $X_D(q,p)$ and $\mathfrak{D}L(q,v)$. This is a set of differential algebraic equations on $TQ \oplus T^*Q$ whereas the Euler-Lagrange equations give an ODE system on TQ. We see that the first and last equations explicitly enforce the second order curve condition and the Legendre transform, respectively. The middle equation reduces to the Euler-Lagrange equations in the absence of constraints. With constraints, the Euler-Lagrange relationship holds along the permissible directions. Explicit enforcement of the Legendre transform serves to enforce any primary constraints on the system.

1.7.5 The Hamilton-Pontryagin principle

Rather than the usual Hamilton's principle for curves on TQ, we apply the Hamilton-Pontryagin principle for curves on $TQ \oplus T^*Q$. This automatically incorporates a constraint distribution Δ_Q and any primary constraints coming from a degenerate Lagrangian. We have

$$\delta \int_0^T L(q(t), v(t)) - \langle p(t), \dot{q}(t) - v(t) \rangle \, dt = 0 \tag{1.56}$$

for variations $\delta q \in \Delta_Q(q)$ with fixed endpoints and arbitrary variations $\delta v, \delta p$ together with the constraint $\dot{q} \in \Delta_Q(q)$. This principle yields precisely the Lagrange-Dirac equations of motion (1.55).

1.7.6 The Lagrange-d'Alembert Pontryagin principle and Lagrange-Dirac systems with external forces

Suppose we have an external force field $F : TQ \to T^*Q$ acting on the system. As in the classical Lagrangian case [14], we take the horizontal lift of F to define $\tilde{F} : TQ \to T^*T^*Q$ by

$$\langle \tilde{F}(q,v), w \rangle = \langle F(q,v), T\pi_Q(w) \rangle. \tag{1.57}$$

In local coordinates $\tilde{F}(q,v) = (q,p,F(q,v),0)$. The equations of motion for the forced system are given by

$$(X_D(q,v,p), \mathfrak{D}L(q,v) - \tilde{F}(q,v)) \in D_{\Delta_Q}(q,p). \tag{1.58}$$

As before, we can derive the local coordinate equations from this, producing

$$\dot{q} = v \in \Delta_Q(q),\ \dot{p} - \frac{\partial L}{\partial q} - F \in \Delta_Q^\circ(q),\ p = \frac{\partial L}{\partial v}. \tag{1.59}$$

So only the second equation changes with the forcing. Equations (1.59) reduce to the usual forced Euler-Lagrange equations in the absence of constraints.

We must also incorporate the work of the forces into the variational principle. This is done in exactly the same way as forces are appended to Hamilton's principle in the usual forced Lagrangian setting [15]. In that setting, one obtains the Lagrange-d'Alembert principle. Here we arrive at the *Lagrange-d'Alembert-Pontryagin principle*,

$$\delta \int_0^T L(q,v) + \langle p, \dot{q} - v \rangle \ dt + \int_0^T \langle F(q,v), \delta q \rangle \ dt = 0 \tag{1.60}$$

for variations $\delta q \in \Delta_Q(q)$ with fixed endpoints and arbitrary variations $\delta v, \delta p$ together with the constraint $\dot{q} \in \Delta_Q(q)$. The addition of the forcing terms here again produces (1.59).

1.8 Interconnection of Lagrange-Dirac systems

In this section we review the interconnection of continuous Lagrange-Dirac systems laid out in [10]. Throughout this section we assume that we are connecting

two systems (L_1, Δ_{Q_1}) on Q_1 and (L_2, Δ_{Q_2}) on Q_2. The results easily extend to the interconnection of a finite number of systems, as shown in [10]. The interconnected system will then evolve on $Q = Q_1 \times Q_2$. The interconnection of the two systems has both a variational formulation and a formulation in terms of the interconnection of the two starting Dirac structures, $D_{\Delta_{Q_1}}$ and $D_{\Delta_{Q_2}}$. This interconnection of Dirac structures in turn involves the direct sum of $D_{\Delta_{Q_1}}$ and $D_{\Delta_{Q_2}}$, a product on Dirac structures, and an interaction Dirac structure D_{int}.

1.8.1 Standard interaction Dirac structures

Let $\Sigma_Q \subset TQ$ be a regular distribution on Q describing the interaction between systems 1 and 2. Lift this distribution to T^*Q to define

$$\Sigma_{\text{int}} = (T\pi_Q)^{-1}(\Sigma_Q) \subset TT^*Q. \tag{1.61}$$

Then the *standard interaction Dirac structure* D_{int} on T^*Q is given by

$$D_{\text{int}}(q,p) = \Sigma_{\text{int}}(q,p) \oplus \Sigma_{\text{int}}^{\circ}(q,p) \tag{1.62}$$

for $\Sigma_{\text{int}}^{\circ}$ the annihilator of Σ_{int}.

As mentioned above, any Dirac structure on a manifold M defines an associated distribution $\Delta_M \subset TM$ and bilinear map $\omega_{\Delta_M} : \Delta_M \times \Delta_M \to \mathbb{R}$ defined on Δ_M. Taking $D = \Delta \oplus \Delta^\circ$ produces $\Delta_M = \Delta$ and $\omega_{\Delta_M} \equiv 0$. Thus, the distribution associated with D_{int} is Σ_{int}, and the associated two-form is the zero form. The zero form obviously extends to the whole of T^*Q, so D_{int} can equivalently be generated from Σ_{int} and $\omega \equiv 0$.

1.8.2 The direct sum of Dirac structures

Given two Dirac structures D_1 and D_2 on M_1 and M_2, the direct sum $D_1 \oplus D_2$ is the vector bundle over $M_1 \times M_2$ given by

$$\begin{aligned} &D_1 \oplus D_2(x_1, x_2) = \\ &\quad \{((v_1, v_2), (\alpha_1, \alpha_2)) \in T_{(x_1,x_2)}(M_1 \times M_2) \oplus T^*_{(x_1,x_2)}(M_1 \times M_2) \mid \\ &\quad (v_1, \alpha_1) \in D_1(x_1) \text{ and } (v_2, \alpha_2) \in D_2(x_2)\}. \end{aligned} \tag{1.63}$$

From [10] we have that $D_1 \oplus D_2$ is itself a Dirac structure over $M_1 \times M_2$. In the particular case of induced Dirac structures, $D_{\Delta_{Q_1}} \oplus D_{\Delta_{Q_2}} = D_{\Delta_{Q_1} \oplus \Delta_{Q_2}}$ [10].

1.8.3 The tensor product of Dirac structures

The interconnection of Dirac structures relies on a product operation on Dirac structures referred to as the *Dirac tensor product*. We have the following characterization of the Dirac tensor product.

Definition 1. ([10]). Let D_a, D_b be Dirac structures on M. We define the Dirac tensor product

$$\begin{aligned} D_a \boxtimes D_b = \{(v,\alpha) \in TM \oplus T^*M \mid \exists \beta \in T^*M \\ \text{such that } (v, \alpha+\beta) \in D_a, (v,-\beta) \in D_b\}. \end{aligned} \tag{1.64}$$

An equivalent definition is given in [8]. Let D_Δ be an induced Dirac structure on Q and D_{int} the standard interaction Dirac structure defined above. Then $D_\Delta \boxtimes D_{\text{int}}$ is a Dirac structure when $\Delta \cap \Sigma_Q$ is a regular distribution [10].

We also have the following properties related to the distributions and two-forms of the Dirac structures.

Proposition 1. ([10]). Let D_a and $D_b \in \text{Dir}(M)$ [i.e., D_a, D_b are Dirac structures on M]. Let $\Delta_a = \text{pr}_{TM}(D_a)$ and $\Delta_b = \text{pr}_{TM}(D_b)$. [These are the associated distributions.] Let Ω_{Δ_a} and Ω_{Δ_b} be the bilinear maps associated with D_a and D_b respectively. If $\Delta_a \cap \Delta_b$ has locally constant rank, then $D_a \boxtimes D_b$ is a Dirac structure with the smooth distribution $\text{pr}_{TM}(D_a \boxtimes D_b) = \Delta_a \cap \Delta_b$ and with the bilinear map $(\Omega_{\Delta_a} + \Omega_{\Delta_b})|_{\Delta_a \cap \Delta_b}$.

Corollary 1. ([10]). If $\Omega_{\Delta_b} = 0$, then it follows that $D_b = \Delta_b \oplus \Delta_b^\circ$ and also that $D_c = D_a \boxtimes D_b$ is induced from $\Delta_a \cap \Delta_b$ and $\Omega_a|_{\Delta_a \cap \Delta_b}$.

1.8.4 Interconnection of Dirac structures

Recall that we wish to connect the systems (L^1, Δ_{Q_1}) and (L^2, Δ_{Q_2}) with associated Dirac structures $D_{\Delta_{Q_1}}$ and $D_{\Delta_{Q_2}}$. The smooth distribution Σ_Q describes

their interaction and is used to define the interaction Dirac structure $D_{\text{int}} = \Sigma_{\text{int}} \oplus \Sigma_{\text{int}}^{\circ}$ for $\Sigma_{\text{int}} = (T\pi_Q)^{-1}(\Sigma_Q)$. As before, $Q = Q_1 \times Q_2$ will be the configuration manifold of the interconnected system.

Given two Dirac structures D_a and D_b on Q_a and Q_b and an interaction Dirac structure D_{int} on $Q = Q_a \times Q_b$, the *interconnection of D_a and D_b through D_{int}* is

$$(D_a \oplus D_b) \boxtimes D_{\text{int}}. \tag{1.65}$$

We noted above that $D_{\Delta_{Q_1}} \oplus D_{\Delta_{Q_2}} = D_{\Delta_{Q_1} \oplus \Delta_{Q_2}}$. We have the following proposition for the interconnection of $D_{\Delta_{Q_1}}$ and $D_{\Delta_{Q_2}}$ through the standard interaction Dirac structure $D_{\text{int}} = \Sigma_{\text{int}} \oplus \Sigma_{\text{int}}^{\circ}$. (Recall that $\Sigma_Q \subset TQ$ and $\Sigma_{\text{int}} = (T\pi_Q)^{-1}(\Sigma_Q) \subset TT^*Q$.)

Proposition 2. ([10]). If $\Delta_{Q_1} \oplus \Delta_{Q_2}$ and Σ_Q intersect cleanly [i.e. $(\Delta_{Q_2} \oplus \Delta_{Q_2}) \cap \Sigma_Q$ has locally constant rank], then the interconnection of $D_{\Delta_{Q_1}}$ and $D_{\Delta_{Q_2}}$ through D_{int} is locally given by the Dirac structure induced from $(\Delta_{Q_2} \oplus \Delta_{Q_2}) \cap \Sigma_Q$ as, for each $(q, p) \in T^*Q$,

$$\begin{aligned}(D_{\Delta_{Q_1}} \oplus D_{\Delta_{Q_2}}) \boxtimes D_{\text{int}}(q,p) = \{(w, \alpha) \in T_{(q,p)}T^*Q \times T^*_{(q,p)}T^*Q \mid \\ w \in \Delta_{T^*Q}(q,p) \text{ and } \alpha - \Omega^\flat(q,p) \cdot w \in \Delta^{\circ}_{T^*Q}(q,p)\},\end{aligned} \tag{1.66}$$

where $\Delta_{T^*Q} = (T\pi_Q)^{-1}((\Delta_{Q_2} \oplus \Delta_{Q_2}) \cap \Sigma_Q)$ and $\Omega = \Omega_1 \oplus \Omega_2$, where Ω_1 and Ω_2 are the canonical symplectic structures on T^*Q_1 and T^*Q_2.

Note that for $Q = Q_1 \times Q_2$, the canonical symplectic form $\Omega_{T^*Q} = \Omega_{T^*Q_1} \oplus \Omega_{T^*Q_2}$. Thus, if we define

$$\Delta_Q = (\Delta_{Q_1} \oplus \Delta_{Q_2}) \cap \Sigma_Q, \tag{1.67}$$

the previous proposition amounts to

$$(D_{\Delta_{Q_1}} \oplus D_{\Delta_{Q_2}}) \boxtimes D_{\text{int}} = D_{\Delta_Q}. \tag{1.68}$$

1.8.5 Interconnection of Lagrange-Dirac systems

Set $L(q, v) = L_1(q_1, v_1) + L_2(q_2, v_2)$ and $\Delta_Q = (\Delta_{Q_1} \oplus \Delta_{Q_2}) \cap \Sigma_Q$. Here, as usual, $(q, v) = (q_1, q_2, v_1, v_2) \in TQ = T(Q_1 \times Q_2)$ in coordinates. Then the

interconnected system satisfies

$$(X_D(q,v,p), \mathfrak{D}L(q,v)) \in D_{\Delta_Q}(q,p). \tag{1.69}$$

The interconnected system also satisfies the usual Hamilton-Pontryagin principle (1.56) for L and Δ_Q.

Should there be any external forces $F_i : TQ_i \to T^*Q_i$ acting on either subsystem, those can be lifted to Q as $\tilde{F}_i = \pi_{Q_i}^* F_i$. Then $F = \sum_i \tilde{F}_i$ represents the external forces acting on the interconnected system, and the total system solves the equations

$$(X_D(q,v,p), \mathfrak{D}L(q,v) - F) \in D_{\Delta_Q}(q,p) \tag{1.70}$$

and satisfies the Lagrange-d'Alembert-Pontryagin principle (1.60).

Note that in [10] the forces considered in the interconnection process are interaction forces between subsystems, not external forces. As demonstrated in [10] the constraints imposed by Σ_Q have an equivalent representation as the effect of internal interaction forces. We ignore the interaction force perspective for now, viewing interconnections as governed wholly by constraints Σ_Q. We will say more about bringing the interaction force perspective into discrete interconnections in the concluding sections.

1.9 Structured integration and variational integrators

Reframing analytic mechanics as geometric mechanics by allowing mechanical systems to evolve on manifolds reveals the depth of geometric structure in the physical world. Examining the range of geometric structures and their associated invariants–momenta, energy, symplectic forms, etc.–relevant to a particular mechanical motion gives a qualitative picture of the motion. Computational geometric mechanics allows these geometric structures to guide the development of numerical methods, leading to improved qualitative behavior of numerical solutions.

Analytical mechanics and its geometric properties can be derived from variational or almost-variational principles. Variational integrators mimic this process by deriving integrators as the discrete evolution equations implied by a discrete variational principle. This process was first developed for discretizing Hamilton's principle in the case of conservative, nondegenerate, unconstrained Lagrangian systems. The discrete Hamilton's principle produces a set of discrete evolution equations known as the Discrete Euler–Lagrange (DEL) equations. Considered as a one-step map, the DEL equations are symplectic, approximately energy conserving, and satisfy a discrete Noether's theorem. This mirrors the symplecticity, energy conservation, and momentum conservation at the continuous level.

1.9.1 Classic variational integrators

Consider a conservative, unconstrained, nondegenerate Lagrangian system. In this case, variational integrators are constructed from the discrete Hamilton's principle, which states that

$$\delta \sum_{k=0}^{N-1} L_d(q_k, q_{k+1}) = 0, \tag{1.71}$$

for fixed endpoints, $\delta q_0 = \delta q_N = 0$, and $L_d : Q \times Q \to \mathbb{R}$ the discrete Lagrangian. Taking continuous variations δq_k then yields the discrete Euler–Lagrange equations,

$$D_2 L_d(q_{k-1}, q_k) + D_1 L_d(q_k, q_{k+1}) = 0. \tag{1.72}$$

Here $D_1 L_d$ and $D_2 L_d$ denote the derivative of the discrete Lagrangian L_d with respect its first and second argument, respectively. We view $Q \times Q$ as the discrete analog of the tangent bundle TQ and the discrete Euler–Lagrange equations as a one-step map from $Q \times Q$ to itself that determines (q_k, q_{k+1}) from (q_{k-1}, q_k).

One can also define a discrete flow along T^*Q by introducing two discrete Legendre transforms, $\mathbb{F}^{\pm} L_d : Q \times Q \to T^*Q$,

$$\mathbb{F}^{+} L_d(q_k, q_{k+1}) = (q_{k+1}, D_2 L_d(q_k, q_{k+1})), \tag{1.73a}$$

$$\mathbb{F}^{-} L_d(q_k, q_{k+1}) = (q_k, -D_1 L_d(q_k, q_{k+1})). \tag{1.73b}$$

These give two possible definitions for the momentum at the point q_k, which are defined in terms of the data (q_k, q_{k+1}) and (q_{k-1}, q_k),

$$p^-_{k,k+1} = \mathbb{F}^- L_d(q_k, q_{k+1}) = -D_1 L_d(q_k, q_{k+1}), \tag{1.74a}$$

$$p^+_{k-1,k} = \mathbb{F}^+ L_d(q_{k-1}, q_k) = D_2 L_d(q_{k-1}, q_k). \tag{1.74b}$$

Then, the DEL equations enforce a momentum matching condition along the discrete flow, i.e.,

$$p^+_{k-1,k} = p^-_{k,k+1}. \tag{1.75}$$

Thus, the momentum $p_k = p^+_{k-1,k} = p^-_{k,k+1}$ is well-defined along solutions of the DEL equations, and we can define a one-step map in phase space by

$$p_{k+1} = D_2 L_d(q_k, q_{k+1}), \tag{1.76a}$$

$$p_k = -D_1 L_d(q_k, q_{k+1}). \tag{1.76b}$$

This map is called the discrete Hamiltonian map corresponding to the DEL equations.

The discrete Euler–Lagrange equations and discrete Hamiltonian map each preserve the appropriate symplectic form and satisfy a discrete Noether's theorem, so that symmetries in the discrete Lagrangian L_d result in conservation of the component of the discrete momenta in the direction of the infinitesimal generators of the symmetry. As symplectic integrators, they also approximately conserve energy over exponentially long time scales. These conservation properties hold and ensure that the qualitative behavior of the Lagrangian system is well-approximated for any choice of L_d.

The choice of L_d is guided by the existence of an exact discrete Lagrangian, L^E_d, which yields a discrete Hamiltonian map that samples the exact Hamiltonian flow. For points $q_0, q_1 \in Q$, and h sufficiently small, let $q_{01}(t)$ be the unique curve such that $q_{01}(0) = q_0,\ q_{01}(h) = q_1$, and $q_{01}(t)$ satisfies the Euler–Lagrange equations for L on $[0, h]$. Then L^E_d is given by

$$L^E_d(q_0, q_1; h) = \int_0^h L(q_{01}(t), \dot{q}_{01}(t))\ dt. \tag{1.77}$$

One can approximate the exact discrete Lagrangian L_d^E by incorporating a wide variety of standard numerical techniques in order to obtain a computable discrete Lagrangian L_d, [13, 9]. By the variational error analysis described in [15], it can be shown that if the discrete Lagrangian $L_d(q_0, q_1; h) = L_d^E(q_0, q_1; h) + \mathcal{O}(h^{r+1})$, then the associated discrete Hamiltonian map is an order r approximation of the exact flow map.

1.9.2 Forced variational integrators

The forced discrete Euler–Lagrange equations are derived from the discrete Lagrange–d'Alembert principle,

$$\delta \sum_{k=0}^{N-1} L_d(q_k, q_{k+1}) + \sum_{k=0}^{N-1} [f_d^-(q_k, q_{k+1}) \cdot \delta q_k + f_d^+(q_k, q_{k+1}) \cdot \delta q_{k+1}] = 0, \tag{1.78}$$

where the additional terms correspond to the virtual work associated with the discrete forces $f_d^{\pm} : Q \times Q \to T^*Q$. The forced discrete Euler–Lagrange equations are given by

$$D_2 L_d(q_{k-1}, q_k) + f_d^+(q_{k-1}, q_k) + D_1 L_d(q_k, q_{k+1}) + f_d^-(q_k, q_{k+1}) = 0. \tag{1.79}$$

The discrete Legendre transforms and discrete Hamiltonian map now incorporate the contribution of the discrete forces,

$$p_{k+1} = \mathbb{F}^{f+} L_d(q_k, q_{k+1}) = D_2 L_d(q_k, q_{k+1}) + f_d^+(q_k, q_{k+1}), \tag{1.80a}$$

$$p_k = \mathbb{F}^{f-} L_d(q_k, q_{k+1}) = -D_1 L_d(q_k, q_{k+1}) - f_d^-(q_k, q_{k+1}). \tag{1.80b}$$

With these momentum definitions, the forced DEL equations can again be viewed as a momentum matching condition.

These equations reduce to the DEL equations in the absence of forcing, and they satisfy a forced discrete Noether's theorem for symmetries of the discrete Lagrangian where the discrete forces do no work in the direction of the infinitesimal generators of the symmetry. Forced variational integrators exhibit better energy behavior than non-geometric integrators in practice, in the sense that the discrete energy evolution better reflects the exact energy evolution of the system. This

lacks rigorous explanation since the forced equations are no longer symplectic nor energy preserving at either the continuous or the discrete level.

Once again, exact discrete quantities guide both the error analysis and the practical choice of L_d and $f_d^{\pm}$. For points $q_0, q_1 \in Q$, define $q_{01}(t)$ as above, except that we now require $q_{01}(t)$ to satisfy the *forced* Euler–Lagrange equations for L and f_L on $[0, h]$. Then, L_d^E and $f_d^{E\pm}$ are given by

$$L_d^E(q_0, q_1, h) = \int_0^h L(q_{01}(t), \dot{q}_{01}(t))\ dt, \tag{1.81a}$$

$$f_d^{E+}(q_0, q_1, h) = \int_0^h f_L(q_{01}(t), \dot{q}_{01}(t)) \cdot \frac{\partial q_{01}(t)}{\partial q_1}\ dt, \tag{1.81b}$$

$$f_d^{E-}(q_0, q_1, h) = \int_0^h f_L(q_{01}(t), \dot{q}_{01}(t)) \cdot \frac{\partial q_{01}(t)}{\partial q_0}\ dt. \tag{1.81c}$$

We obtain computable L_d and $f_d^{\pm}$ by approximating the curve $q_{01}(t)$ that satisfies the forced Euler–Lagrange boundary-value problem and the integrals that arise in the definition of $L_d^E, f_d^{E\pm}$. Again, the orders of these approximations determine the order of accuracy of the discrete Hamiltonian map. The authors mention this fact without proof in [15], and we provide an explicit proof in the following section.

1.9.3 Nonholonomic integrators

As mentioned above, Dirac mechanics encompasses the case of nonholonomic mechanics. However, one need not consider Dirac structures in order to study nonholonomic mechanics. There exists a considerable literature studying the geometric discretization of nonholonomic systems. We mention several of those results here because the Dirac variational integrators presented next and used in the research of chapters 2 and 3 generalize some of these integrators. We also mention these methods because they constitute several different approaches to nonholonomic structure. In future work we hope to compare and contrast these approaches with our Dirac structure approach with the aim of shedding light on both.

In [4], Cortés and Martìnez present variational nonholonomic integrators

based on the following discrete Lagrange-d'Alembert principle,

$$\delta \sum_{k=0}^{N-1} L_d(q_k, q_{k+1}) = 0 \tag{1.82}$$

for variations $\delta q_k \in \Delta_Q$ and $(q_k, q_{k+1}) \in \Delta_Q^d$. Here $\Delta_Q^d \subset Q \times Q$ is some discretization of the continuous constraint. This discrete Lagrange-d'Alembert principle generalizes the discrete Hamilton's principle above. The principles of discrete Dirac mechanics below further generalize this discrete Lagrange-d'Alembert principle, and our discrete Dirac mechanics recovers the discrete nonholonomic integrators of [4]. In [4] the authors show that their nonholonomic integrators obey a discrete version of the nonholonomic momentum equation and preserve the appropriate structure in the evolution of a discrete symplectic form.

In [16], McLachlan and Perlmutter further study the integrators presented in [4]. They demonstrate the benefits of preserving reversibility as well as satisfying the conditions of [4]. They derive a general exact discrete constraint distribution and an exact discrete Lagrange-d'Alembert principle for reversible systems. In [5], the authors take a different approach and construct nonholonomic integrators by approximating generating functions and the work of the constraint *forces* rather than the constraint *distribution*. The exact constraint force terms approximated in [5] are the same as the exact forcing terms of [16], but [5] does not rely on reversibility in its results. For a hyperregular Lagrangian, the nonholonomic constraints can be written as constraints on the conjugate momenta p. In this case, the authors of [5] use projection techniques to develop integrators on T^*Q that exactly preserve the constraints. Dirac mechanics, and, thus, the discrete Dirac mechanics below, purposefully allows for degenerate Lagrangians. It would be interesting to explore how the constraint preservation of [5] may relate to the discrete Dirac structure preservation below.

1.10 Dirac variational integrators

In this section we review the discrete Dirac mechanics of [12]. We begin with a Lagrangian function $L : TQ \to \mathbb{R}$ and a continuous constraint distribution

$\Delta_Q \subset TQ$. The authors also define a discrete Tulczyjew's triple using generating functions. This is used to define both a discrete Dirac differential on a given discrete Lagrangian and a discrete induced Dirac structure. We arrive at two formulations, $(+)$ and $(-)$-discrete Dirac mechanics, stemming from a choice of generating function used to define the discrete analogue of the symplectic flat map, $\Omega^\flat_{d\pm}$. In each formulation of discrete Dirac mechanics, we construct discrete annihilating one-forms $\omega^a_{d\pm}$ based on the continuous one-forms ω^a and a choice of retraction $\mathcal{R} : TQ \to Q$.

1.10.1 A discrete Tulczyjew triple

Recall the continuous Tulczyjew triple, summarized in the following diagram.

$$T^*TQ \xleftarrow{\kappa_Q} TT^*Q \xrightarrow{\Omega^\flat_{T^*Q}} T^*T^*Q, \qquad \gamma_Q : T^*TQ \to T^*T^*Q \tag{1.83}$$

This is used to define the continuous Dirac differential $\mathfrak{D}L = (\gamma_Q \circ \mathbf{d})L$.

The discrete analogue of the Tulczyjew triple makes use of generating functions for a given symplectic map $F : T^*Q \to T^*Q$ [12]. We write $F : (q_0, p_0) \mapsto (q_1, p_1)$. Assuming that Q is a vector space or that we are operating within a single chart, we can write $T^*Q \cong Q \times Q^*$, so that $F : Q \times Q^* \to Q \times Q^*$. We have four maps associated with F related to the four types of generating functions. We will only use types 1-3 in defining the discrete triple.

The first map is $F_1 : Q \times Q \to Q^* \times Q^*$ defined by $F_1(q_0, q_1) = (p_0, p_1)$ for $(q_1, p_1) = F(q_0, p_0)$. The type 1 generating function of F is the map defined on the domain of F_1 such that

$$-p_0 dq_0 + p_1 dq_1 = dS_1(q_0, q_1). \tag{1.84}$$

This map exists if and only if F is symplectic. Define the following additional map related to F_1.

$$i_{F_1} : (q_0, q_1) \mapsto ((q_0, p_0), (q_1, p_1)). \tag{1.85}$$

Then $\kappa_Q^d : T^*Q \times T^*Q \to T^*(Q \times Q)$ is defined so that the following diagram commutes,

$$\begin{array}{ccc} T^*Q \times T^*Q & \xrightarrow{\kappa_Q^d} & T^*(Q \times Q) \\ & {\scriptstyle i_{F_1}} \nwarrow \quad \nearrow {\scriptstyle dS_1} & \\ & Q \times Q & \end{array} \tag{1.86}$$

In coordinates,

$$\kappa_Q^d : ((q_0, p_0), (q_1, p_1)) \mapsto (q_0, q_1, -p_0, p_1). \tag{1.87}$$

The second map is $F_2 : Q \times Q^* \to Q^* \times Q$ defined by $F_2(q_0, p_1) = (p_0, q_1)$ for $(q_1, p_1) = F(q_0, p_0)$. The type 2 generating function of F is the map defined on the domain of F_2 such that

$$p_0 dq_0 + q_1 dp_1 = dS_2(q_0, p_1). \tag{1.88}$$

This map exists if and only if F is symplectic. Define the following additional map related to F_2.

$$i_{F_2} : (q_0, p_1) \mapsto ((q_0, p_0), (q_1, p_1)). \tag{1.89}$$

Then $\Omega_{d+}^\flat : T^*Q \times T^*Q \to T^*(Q \times Q^*)$ is defined so that the following diagram commutes,

$$\begin{array}{ccc} T^*Q \times T^*Q & \xrightarrow{\Omega_{d+}^\flat} & T^*(Q \times Q^*) \\ & {\scriptstyle i_{F_2}} \nwarrow \quad \nearrow {\scriptstyle dS_2} & \\ & Q \times Q^* & \end{array} \tag{1.90}$$

In coordinates,

$$\Omega_{d+}^\flat : ((q_0, p_0), (q_1, p_1)) \mapsto (q_0, p_1, p_0, q_1). \tag{1.91}$$

The third map is $F_3 : Q^* \times Q \to Q \times Q^*$ defined by $F_3(p_0, q_1) = (q_0, p_1)$ for $(q_1, p_1) = F(q_0, p_0)$. The type 3 generating function of F is the map defined on the domain of F_3 such that

$$-q_0 dp_0 - p_1 dq_1 = dS_3(p_0, q_1). \tag{1.92}$$

This map exists if and only if F is symplectic. Define the following additional map related to F_3.

$$i_{F_3} : (p_0, q_1) \mapsto ((q_0, p_0), (q_1, p_1)). \tag{1.93}$$

Then $\Omega^\flat_{d-} : T^*Q \times T^*Q \to T^*(Q^* \times Q)$ is defined so that the following diagram commutes,

$$\begin{array}{ccc} T^*Q \times T^*Q & \xrightarrow{\quad\Omega^\flat_{d-}\quad} & T^*(Q^* \times Q) \\ & {\scriptstyle i_{F_3}} \nwarrow \quad \nearrow {\scriptstyle dS_3} & \\ & Q^* \times Q & \end{array} \tag{1.94}$$

In coordinates,

$$\Omega^\flat_{d-} : ((q_0, p_0), (q_1, p_1)) \mapsto (p_0, q_1, -q_0, -p_1). \tag{1.95}$$

These maps define the (+) and (-) discrete Tulczyjew triples,

$$T^*(Q \times Q) \xleftarrow{\kappa_Q} T^*Q \times T^*Q \xrightarrow{\Omega^\flat_{d+}} T^*(Q \times Q^*) \qquad \gamma^{d+}_Q : T^*(Q \times Q) \to T^*(Q \times Q^*) \tag{1.96}$$

and

$$T^*(Q \times Q) \xleftarrow{\kappa_Q} T^*Q \times T^*Q \xrightarrow{\Omega^\flat_{d-}} T^*(Q^* \times Q). \qquad \gamma^{d-}_Q : T^*(Q \times Q) \to T^*(Q^* \times Q) \tag{1.97}$$

We use $\gamma^{d\pm}_Q$ to define a ($\pm$) discrete Dirac differential on L_d and $\Omega^\flat_{d\pm}$ to define ($\pm$) discrete induced Dirac structures.

1.10.2 Discrete constraint distributions and discrete induced Dirac structures

Recall that a continuous Lagrange-Dirac system on a manifold Q has an associated constraint distribution $\Delta_Q \subset TQ$. With this we have a set of associated constraint one-forms $\{\omega^a\}$ such that

$$\Delta^\circ_Q(q) = \text{span}\{\omega^a(q)\}^m_{a=1}, \quad \text{i.e.} \;\; \Delta_Q = \cap_a \ker(\omega^a(q)). \tag{1.98}$$

We define a discrete constraint distribution by discretizing these constraint one-forms. In the theory of [12], we do this using a retraction $R : TQ \to Q$. As with

the Tulczyjew triple, we have a (+) and a (-) way of doing this, resulting in discrete forms $\omega^a_{d\pm} : Q \times Q \to \mathbb{R}$.

$$\omega^a_{d+}(q_0, q_1) = \omega^a(q_0)\left(R^{-1}_{q_0}(q_1)\right), \quad \omega^a_{d-}(q_0, q_1) = \omega^a(q_1)\left(-R^{-1}_{q_1}(q_0)\right). \tag{1.99}$$

The discrete constraint distribution is then defined as

$$\Delta_Q^{d\pm} = \{(q_0, q_1) \in Q \times Q \mid \omega_{d\pm}(q_0, q_1) = 0,\ a = 1, \ldots, m\}. \tag{1.100}$$

In classical variational integrator theory, the pair (q_0, q_1) is thought of as the discrete analogue to a tangent vector in TQ. The $(\pm)$ formulation here can be thought of as a right and left formulation based on treating one of q_0, q_1 as the basepoint and the other as a representative of the velocity. Indeed, the distribution Δ_Q^{d+} constrains only q_1, while Δ_Q^{d-} constrains only q_0 [12].

Recall that a continuous Dirac structure on T^*Q relies on the distribution $\Delta_{T^*Q} = (T\pi_Q)^{-1}(\Delta_Q) \subset TT^*Q$ for π_Q the canonical projection on T^*Q. At the discrete level, we define

$$\begin{aligned} \Delta^{d+}_{T^*Q} &= (\pi_Q \times \pi_Q)^{-1}(\Delta_Q^{d\pm}) \\ &= \left\{((q_0, p_0), (q_1, p_1)) \in T^*Q \times T^*Q \mid (q_0, q_1) \in \Delta_Q^{d\pm}\right\} \end{aligned} \tag{1.101}$$

and

$$\begin{aligned} \Delta^{\circ}_{Q\times Q^*} &= \left\{(q, p, \alpha_q, 0) \in T^*(Q \times Q^*) \mid \alpha_q \mathrm{d}q \in \Delta^{\circ}_Q(q)\right\}, \\ \Delta^{\circ}_{Q^*\times Q} &= \left\{(q, p, 0, \alpha_q) \in T^*(Q^* \times Q) \mid \alpha_q \mathrm{d}q \in \Delta^{\circ}_Q(q)\right\} \end{aligned} \tag{1.102}$$

The distributions $\Delta^{d\pm}_{T^*Q}$ serve as the discrete analogues of Δ_{T^*Q}, while $\Delta^{\circ}_{Q\times Q^*}$ and $\Delta^{\circ}_{Q^*\times Q}$ are the (+) and (-) discrete analogues of $\Delta^{\circ}_{T^*Q}$, respectively.

We then define discrete induced Dirac structures using these discrete distributions and the discrete maps $\Omega^{\flat}_{d\pm}$ defined earlier. We have

$$\begin{aligned} D^{d+}_{\Delta_Q} = \{&\left((z, z^+), \alpha_{\hat{z}}\right) \in (T^*Q \times T^*Q) \times T^*(Q \times Q^*) \mid \\ &(z, z^+) \in \Delta^{d+}_{T^*Q},\ \alpha_{\hat{z}} - \Omega^{\flat}_{d+}(z, z^+) \in \Delta_{Q\times Q^*}\} \end{aligned} \tag{1.103}$$

and

$$\begin{aligned} D^{d-}_{\Delta_Q} = \{&\left((z^-, z), \alpha_{\tilde{z}}\right) \in (T^*Q \times T^*Q) \times T^*(Q^* \times Q) \mid \\ &(z^-, z) \in \Delta^{d-}_{T^*Q},\ \alpha_{\tilde{z}} - \Omega^{\flat}_{d-}(z^-, z) \in \Delta_{Q^*\times Q}\}. \end{aligned} \tag{1.104}$$

Given $z = (q, p)$ and $z^+ = (q^+, p^+)$ then $\hat{z} = (q, p^+)$. Given $z^- = (q^-, p^-)$ and $z = (q, p)$ then $\tilde{z} = (p^-, q)$.

1.10.3 The discrete Dirac differential and discrete Dirac mechanics

We have two versions of the discrete Dirac differential,

$$\mathfrak{D}^+ L_d = \gamma_Q^{d+} \circ \mathbf{d}L_d \quad \text{and} \quad \mathfrak{D}^- L_d = \gamma_Q^{d-} \circ \mathbf{d}L_d. \tag{1.105}$$

Using the discrete vector field

$$X_d^k = ((q_k, p_k), (q_{k+1}, p_{k+1})) \in T^*Q \times T^*Q \tag{1.106}$$

we then have the following systems. A *(+)-discrete Lagrange-Dirac system* satisfies

$$(X_d^k, \mathfrak{D}^+ L_d(q_k, q_k^+)) \in D_{\Delta_Q}^{d+}. \tag{1.107}$$

A $(-)$-*discrete Lagrange-Dirac system* satisfies

$$(X_d^k, \mathfrak{D}^- L_d(q_{k+1}^-, q_{k+1})) \in D_{\Delta_Q}^{d-}. \tag{1.108}$$

The variables q_k^+ and q_{k+1}^- are the discrete analogues of the velocity variable. In coordinates, equation (1.107) produces the *(+)-discrete Lagrange–Dirac equations of motion*,

$$0 = \omega_{d+}^a(q_k, q_{k+1}), \tag{1.109a}$$

$$q_{k+1} = q_k^+ \tag{1.109b}$$

$$p_{k+1} = D_2 L_d(q_k, q_k^+), \tag{1.109c}$$

$$p_k = -D_1 L_d(q_k, q_k^+) + \mu_a \omega^a(q_k), \tag{1.109d}$$

where μ_a are Lagrange multipliers, and the last equation uses the Einstein summation convention. Equation (1.108) produces the $(-)$-*discrete Lagrange–Dirac equations of motion*,

$$0 = \omega_{d-}^a(q_k, q_{k+1}), \tag{1.110a}$$

$$q_k = q_{k+1}^- \tag{1.110b}$$

$$p_k = -D_1 L_d(q_{k+1}^-, q_{k+1}), \tag{1.110c}$$

$$p_{k+1} = D_2 L_d(q_{k+1}^-, q_{k+1}) + \mu_a \omega^a(q_{k+1}). \tag{1.110d}$$

Again, μ_a are Lagrange multipliers, and the last equation makes use of the Einstein summation convention. Later we will write these equations with the q_k^+ and q_{k+1}^- variables eliminated for simplicity.

Both $(\pm)$ equations simplify to the DEL equations in the unconstrained case, and they recover the nonholonomic integrators of [4].

1.10.4 Variational discrete Dirac mechanics

The $(+)$-discrete Lagrange–d'Alembert–Pontryagin principle is

$$\delta \sum_{k=0}^{N-1} [L_d(q_k, q_k^+) + p_{k+1}(q_{k+1} - q_k^+)] = 0, \tag{1.111}$$

with variations that vanish at the endpoints, i.e. $\delta q_0 = \delta q_N = 0$, and the discrete constraints $(q_k, q_{k+1}) \in \Delta_Q^{d+}$. We also impose the constraint $\delta q_k \in \Delta_Q(q_k)$ after computing variations inside the sum. The variable q_k^+ serves as the discrete analog to the introduction of v in the continuous principle.

The $(-)$-discrete Lagrange-d'Alembert-Pontryagin principle is

$$\delta \sum_{k=0}^{N-1} [L_d(q_{k+1}^-, q_{k+1}) - p_k(q_k - q_{k+1}^-)] = 0 \ . \tag{1.112}$$

The variable q_k^- now plays the role of the discrete velocity. Again we take variations that vanish at the endpoints and impose the constraint $\delta q_k \in \Delta_Q(q_k)$. We now impose the discrete constraints $(q_k, q_{k+1}) \in \Delta_Q^{d-}$.

Computing variations of (1.111) yields (1.109). Computing variations for (1.112) yields (1.110) [12]. Thus, in direct analogy with the continuous case, we have equivalent variational and Dirac structure formulations of discrete Lagrange-Dirac mechanics.

Chapter 2

Constructing equivalence-preserving Dirac variational integrators with forces

Mechanical motion possesses underlying geometric structures, and preserving these structures in numerical integration improves qualitative behavior and reduces long-time simulation error. For a single mechanical system, structure preservation can be achieved by adopting the variational integrator construction. This construction has been generalized to more complex systems involving forces or constraints as well as to the setting of Dirac mechanics. Variational integrators have not yet been applied to interconnected systems, an important class of practically useful mechanical systems whose Dirac mechanical structure was recently elucidated in [10]. This paper establishes the components necessary for ongoing work on interconnecting discrete Dirac systems. Specifically, we revisit some of the properties of forced variational integrators important for interconnected applications and derive Dirac variational integrators with forces. We close with a discussion of ongoing and future research based on these findings.

2.1 Introduction

Reframing analytic mechanics as geometric mechanics by allowing mechanical systems to evolve on manifolds reveals the depth of geometric structure in the physical world. Examining the range of geometric structures and their associated invariants–momenta, energy, symplectic forms, etc.–relevant to a particular mechanical motion gives a qualitative picture of the motion. Computational geometric mechanics allows these geometric structures to guide the development of numerical methods, leading to improved qualitative behavior of numerical solutions.

Analytical mechanics and its geometric properties can be derived from variational or almost-variational principles. Variational integrators mimic this process by deriving integrators as the discrete evolution equations implied by a discrete variational principle. This process was first developed for discretizing Hamilton's principle in the case of conservative, nondegenerate, unconstrained Lagrangian systems. The discrete Hamilton's principle produces a set of discrete evolution equations known as the Discrete Euler–Lagrange (DEL) equations. Considered as a one-step map, the DEL equations are symplectic, approximately energy conserving, and satisfy a discrete Noether's theorem. This mirrors the symplecticity, energy conservation, and momentum conservation at the continuous level.

The variational construction has been extended to accommodate forcing, holonomic constraints [15], and nonholonomic constraints [4]. Most recently, the variational construction was applied to Lagrange–Dirac mechanical systems, which is the Lagrangian view of Dirac mechanics [12]. Dirac mechanics generalizes both Lagrangian and Hamiltonian mechanics to a formulation that accommodates forces and constraints as well as degeneracy. Forces, constraints, and degeneracy each change the geometric structure of the system away from straightforward conservation laws, and Dirac mechanics elucidates the specifics of these changes [19, 20].

Dirac mechanics was also recently shown to be a useful setting for the study of interconnected systems [10]. Interconnected systems consist of multiple mechanical components joined together to operate as a whole. Many practical engineering systems can be conceptualized this way, and often it is more natural to model

each component individually than to attempt to model the entire large-scale system monolithically. In ongoing and future work, we hope to bring that ease of subsystem-level modeling to geometric integration through an interconnected discrete Dirac simulation framework. That framework will be based on incorporating the ideas of [10] into the discrete foundation developed in [12].

This chapter takes the first step by extending Dirac variational integrators to a formulation that includes discrete forcing. Connected subsystems exert interaction forces on one another, so accommodating forces may prove useful in interconnected applications. We can also view the interconnected modeling process as breaking a large (possibly conservative) system into smaller, more manageable parts. From this point of view, interaction forces are artificial modeling constructs, and we should ensure that they cancel properly in the final integration, so as to ensure that the large monolithic model is equivalent to the model based on interconnecting the component subsystems. This paper addresses that concern by examining notions of equivalence at both the continuous and discrete levels and providing a criterion for defining forced variational or Dirac integrators which are well defined with respect to changes in representation of equivalent systems.

The paper begins with a review of classic, forced, and Dirac variational integrators in Section 2. Section 3 examines order of accuracy and equivalence preservation in forced variational integrators, including several numerical examples. This study informs the later design and implementation of forced Dirac variational integrators. Section 4 describes the extension of Dirac variational integrators to forced Dirac variational integrators, closing with a numerical example. Section 5 summarizes the implications of this work and suggests future research directions.

2.2 Background: A review of variational integrators

2.2.1 Classic variational integrators

Consider a conservative, unconstrained, nondegenerate Lagrangian system. In this case, variational integrators are constructed from the discrete Hamilton's principle, which states that

$$\delta \sum_{k=0}^{N-1} L_d(q_k, q_{k+1}) = 0, \tag{2.1}$$

for fixed endpoints, $\delta q_0 = \delta q_N = 0$, and $L_d : Q \times Q \to \mathbb{R}$ the discrete Lagrangian. Taking continuous variations δq_k then yields the discrete Euler–Lagrange equations,

$$D_2 L_d(q_{k-1}, q_k) + D_1 L_d(q_k, q_{k+1}) = 0. \tag{2.2}$$

Here $D_1 L_d$ and $D_2 L_d$ denote the derivative of the discrete Lagrangian L_d with respect its first and second argument, respectively. We view $Q \times Q$ as the discrete analog of the tangent bundle TQ and the discrete Euler–Lagrange equations as a one-step map from $Q \times Q$ to itself that determines (q_k, q_{k+1}) from (q_{k-1}, q_k).

One can also define a discrete flow along T^*Q by introducing two discrete Legendre transforms, $\mathbb{F}^{\pm} L_d : Q \times Q \to T^*Q$,

$$\mathbb{F}^{+} L_d(q_k, q_{k+1}) = (q_{k+1}, D_2 L_d(q_k, q_{k+1})), \tag{2.3a}$$

$$\mathbb{F}^{-} L_d(q_k, q_{k+1}) = (q_k, -D_1 L_d(q_k, q_{k+1})). \tag{2.3b}$$

These give two possible definitions for the momentum at the point q_k, which are defined in terms of the data (q_k, q_{k+1}) and (q_{k-1}, q_k),

$$p^{-}_{k,k+1} = \mathbb{F}^{-} L_d(q_k, q_{k+1}) = -D_1 L_d(q_k, q_{k+1}), \tag{2.4a}$$

$$p^{+}_{k-1,k} = \mathbb{F}^{+} L_d(q_{k-1}, q_k) = D_2 L_d(q_{k-1}, q_k). \tag{2.4b}$$

Then, the DEL equations enforce a momentum matching condition along the discrete flow, i.e.,

$$p^{+}_{k-1,k} = p^{-}_{k,k+1}. \tag{2.5}$$

Thus, the momentum $p_k = p^+_{k-1,k} = p^-_{k,k+1}$ is well-defined along solutions of the DEL equations, and we can define a one-step map in phase space by

$$p_{k+1} = D_2 L_d(q_k, q_{k+1}), \tag{2.6a}$$

$$p_k = -D_1 L_d(q_k, q_{k+1}). \tag{2.6b}$$

This map is called the discrete Hamiltonian map corresponding to the DEL equations.

The discrete Euler–Lagrange equations and discrete Hamiltonian map each preserve the appropriate symplectic form and satisfy a discrete Noether's theorem, so that symmetries in the discrete Lagrangian L_d result in conservation of the component of the discrete momenta in the direction of the infinitesimal generators of the symmetry. As symplectic integrators, they also approximately conserve energy over exponentially long time scales. These conservation properties hold and ensure that the qualitative behavior of the Lagrangian system is well-approximated for any choice of L_d.

The choice of L_d is guided by the existence of an exact discrete Lagrangian, L^E_d, which yields a discrete Hamiltonian map that samples the exact Hamiltonian flow. For points $q_0, q_1 \in Q$, and h sufficiently small, let $q_{01}(t)$ be the unique curve such that $q_{01}(0) = q_0,\ q_{01}(h) = q_1$, and $q_{01}(t)$ satisfies the Euler–Lagrange equations for L on $[0, h]$. Then L^E_d is given by

$$L^E_d(q_0, q_1; h) = \int_0^h L(q_{01}(t), \dot{q}_{01}(t))\ dt. \tag{2.7}$$

One can approximate the exact discrete Lagrangian L^E_d by incorporating a wide variety of standard numerical techniques in order to obtain a computable discrete Lagrangian L_d, [13, 9]. By the variational error analysis described in [15], it can be shown that if the discrete Lagrangian $L_d(q_0, q_1; h) = L^E_d(q_0, q_1; h) + \mathcal{O}(h^{r+1})$, then the associated discrete Hamiltonian map is an order r approximation of the exact flow map.

2.2.2 Forced variational integrators

The forced discrete Euler–Lagrange equations are derived from the discrete Lagrange–d'Alembert principle,

$$\delta \sum_{k=0}^{N-1} L_d(q_k, q_{k+1}) + \sum_{k=0}^{N-1} [f_d^-(q_k, q_{k+1}) \cdot \delta q_k + f_d^+(q_k, q_{k+1}) \cdot \delta q_{k+1}] = 0, \tag{2.8}$$

where the additional terms correspond to the virtual work associated with the discrete forces $f_d^{\pm} : Q \times Q \to T^*Q$. The forced discrete Euler–Lagrange equations are given by

$$D_2 L_d(q_{k-1}, q_k) + f_d^+(q_{k-1}, q_k) + D_1 L_d(q_k, q_{k+1}) + f_d^-(q_k, q_{k+1}) = 0. \tag{2.9}$$

The discrete Legendre transforms and discrete Hamiltonian map now incorporate the contribution of the discrete forces,

$$p_{k+1} = \mathbb{F}^{f+} L_d(q_k, q_{k+1}) = D_2 L_d(q_k, q_{k+1}) + f_d^+(q_k, q_{k+1}), \tag{2.10a}$$

$$p_k = \mathbb{F}^{f-} L_d(q_k, q_{k+1}) = -D_1 L_d(q_k, q_{k+1}) - f_d^-(q_k, q_{k+1}). \tag{2.10b}$$

With these momentum definitions, the forced DEL equations can again be viewed as a momentum matching condition.

These equations reduce to the DEL equations in the absence of forcing, and they satisfy a forced discrete Noether's theorem for symmetries of the discrete Lagrangian where the discrete forces do no work in the direction of the infinitesimal generators of the symmetry. Forced variational integrators exhibit better energy behavior than non-geometric integrators in practice, in the sense that the discrete energy evolution better reflects the exact energy evolution of the system. This lacks rigorous explanation since the forced equations are no longer symplectic nor energy preserving at either the continuous or the discrete level.

Once again, exact discrete quantities guide both the error analysis and the practical choice of L_d and $f_d^{\pm}$. For points $q_0, q_1 \in Q$, define $q_{01}(t)$ as above, except that we now require $q_{01}(t)$ to satisfy the *forced* Euler–Lagrange equations for L

and f_L on $[0, h]$. Then, L_d^E and $f_d^{E\pm}$ are given by

$$L_d^E(q_0, q_1, h) = \int_0^h L(q_{01}(t), \dot{q}_{01}(t))\ dt, \tag{2.11a}$$

$$f_d^{E+}(q_0, q_1, h) = \int_0^h f_L(q_{01}(t), \dot{q}_{01}(t)) \cdot \frac{\partial q_{01}(t)}{\partial q_1}\ dt, \tag{2.11b}$$

$$f_d^{E-}(q_0, q_1, h) = \int_0^h f_L(q_{01}(t), \dot{q}_{01}(t)) \cdot \frac{\partial q_{01}(t)}{\partial q_0}\ dt. \tag{2.11c}$$

We obtain computable L_d and $f_d^{\pm}$ by approximating the curve $q_{01}(t)$ that satisfies the forced Euler–Lagrange boundary-value problem and the integrals that arise in the definition of $L_d^E, f_d^{E\pm}$. Again, the orders of these approximations determine the order of accuracy of the discrete Hamiltonian map. The authors mention this fact without proof in [15], and we provide an explicit proof in the following section.

2.2.3 Dirac variational integrators

Dirac variational integrators were developed in [12] and generalize the variational integrator construction to the case of Dirac mechanics. In [12] the authors develop both the variational theory of discrete Dirac mechanics and explicit discrete analogues of Dirac structures. The authors arrive at two formulations, (+) and (-)-discrete Dirac mechanics, stemming from a choice of generating function used to define the discrete analogue of the symplectic flat map, $\Omega_{d\pm}^{\flat}$.

Discretization begins from a continuous problem described by a Lagrangian function $L : TQ \to \mathbb{R}$ and a continuous constraint distribution $\Delta_Q \subset TQ$. The constraint distribution is determined by its annihilator, which we write as $\Delta_Q^\circ = \text{span}\{\omega^a\}_{a=1}^m \subset T^*Q$. In each formulation of discrete Dirac mechanics, we construct a discrete Lagrangian L_d and discrete annihilating one-forms $\omega_{d\pm}^a$ based on the continuous problem and a choice of retraction $\mathcal{R} : TQ \to Q$.

(+)-discrete Dirac mechanics

In (+)-discrete Dirac mechanics, we define the discrete one-forms as

$$\omega_{d+}^a(q_k, q_{k+1}) = \omega^a(q_k, \mathcal{R}_{q_k}^{-1}(q_{k+1})). \tag{2.12}$$

These then define a discrete distribution as follows

$$\Delta_Q^{d+} = \{(q_k, q_{k+1}) \in Q \times Q \mid \omega_{d+}^a(q_k, q_{k+1}) = 0,\ a = 1, \ldots, m\}. \tag{2.13}$$

The (+)-discrete Lagrange–d'Alembert–Pontryagin principle is

$$\delta \sum_{k=0}^{N-1} [L_d(q_k, q_k^+) + p_{k+1}(q_{k+1} - q_k^+)] = 0, \tag{2.14}$$

with variations that vanish at the endpoints, $\delta q_0 = \delta q_N = 0$, and discrete constraints $(q_k, q_{k+1}) \in \Delta_Q^{d+}$. We also impose a constraint on the variations $\delta q_k \in \Delta_Q(q_k)$ after computing variations inside the sum. The variable q_k^+ serves as the discrete analog to the introduction of v in the continuous principle. This process produces the (+)-discrete Lagrange–Dirac equations of motion,

$$0 = \omega_{d+}^a(q_k, q_{k+1}), \tag{2.15a}$$

$$q_{k+1} = q_k^+ \tag{2.15b}$$

$$p_{k+1} = D_2 L_d(q_k, q_k^+), \tag{2.15c}$$

$$p_k = -D_1 L_d(q_k, q_k^+) + \mu_a \omega^a(q_k), \tag{2.15d}$$

where $a = 1, \ldots, m$, and the last equation uses the Einstein summation convention. These equations simplify to the DEL equations in the unconstrained case, and they recover the nonholonomic integrators of [4]. They can also be expressed in terms of discrete Dirac structures as

$$(X_d^k, \mathfrak{D}^+ L_d(q_k, q_k^+)) \in D_{\Delta_Q}^{d+}. \tag{2.16}$$

where $X_d^k = ((q_k, p_k), (q_{k+1}, p_{k+1}))$ is the discrete vector field, $\mathfrak{D}^+ L_d$ is the (+)-discrete Dirac differential, and $D_{\Delta_Q}^{d+}$ is the (+)-discrete Dirac structure induced by the continuous distribution Δ_Q. The discrete symplectic flat map, $\Omega_{d+}^\flat$, contributes to the definition of $D_{\Delta_Q}^{d+}$. We show (3.50) now to highlight its similarity to the continuous expression for constrained Dirac mechanics, $(X, \mathfrak{D}L) \in D_{\Delta_Q}$. We provide explicit descriptions of the discrete objects as needed in the development of forced Dirac integrators below.

(-)-discrete Dirac mechanics

This formulation defines the discrete one-forms as

$$\omega^a_{d-}(q_k, q_{k+1}) = \omega^a(q_{k+1}, \mathcal{R}^{-1}_{q_{k+1}}(q_k)) \tag{2.17}$$

and uses the (-)-discrete Lagrange-d'Alembert-Pontryagin principle

$$\delta \sum_{k=0}^{N-1} [L_d(q^-_{k+1}, q_{k+1}) - p_k(q_k - q^-_{k+1})] = 0 \ . \tag{2.18}$$

We impose the same constraints on the variations of the discrete principle as in the (+) case, using Δ_Q^{d-} defined from $\{\omega^a_{d-}\}_{a=1}^m$ instead of Δ_Q^{d+}. The variable q_k^- now plays the role of the discrete velocity. This yields the (-)-discrete Lagrange–Dirac equations

$$0 = \omega^a_{d-}(q_k, q_{k+1}), \tag{2.19a}$$

$$q_k = q^-_{k+1} \tag{2.19b}$$

$$p_k = -D_1 L_d(q^-_{k+1}, q_{k+1}), \tag{2.19c}$$

$$p_{k+1} = D_2 L_d(q^-_{k+1}, q_{k+1}) + \mu_a \omega^a(q_{k+1}). \tag{2.19d}$$

Equivalently,

$$(X^k_d, \mathfrak{D}^- L_d(q^-_{k+1}, q_{k+1})) \in D^{d-}_{\Delta_Q}. \tag{2.20}$$

Again, we avoid defining each discrete object until necessary.

2.3 Forced Integrators revisited

In [15], the authors assert without proof the existence of a theorem relating the order of a forced variational integrator to the order of approximation of $L_d, f_d^{\pm}$ to $L_d^E, f_d^{E\pm}$. Here, we provide an explicit proof of the most practical direction of that theorem and a recipe for constructing forced integrators of known order. We then analyze the conditions under which this process yields a well-defined, equivalence preserving integrator and discuss the implications of equivalence preservation in interconnected applications. The section closes with several numerical examples illustrating both our construction process and the consequences of equivalence preservation.

2.3.1 Determining the order of a forced variational integrator

Theorem 3 below explicitly proves that the orders of approximation of L_d and $f_d^\pm$ to L_d^E and $f_d^{E\pm}$ determine the order of accuracy of the discrete Hamiltonian map they define. This gives the most useful direction of the order theorem mentioned in [15], since the order of L_d and $f_d^\pm$ are easier to calculate than the order of the integrator.

We need a few preliminary definitions before we state the theorem. First, we explicitly define what we mean by the order of $L_d, f_d^\pm$ and $\mathbb{F}^{f\pm}L_d$, using the same definitions as in [15]. Thus, a given L_d is of order r if there exist constants $C_L > 0$, $h_L > 0$ and an open subset $U_L \subset TQ$ with compact closure such that

$$||L_d(q(0), q(h), h) - L_d^E(q(0), q(h), h)|| \leq C_L h^{r+1}, \tag{2.21}$$

for all solutions $q(t)$ of the forced Euler–Lagrange equations with initial conditions satisfying $(q(0), \dot{q}(0)) \in U_L$, and for all $h \leq h_L$. Similarly, $f_d^\pm$ are of order r if there exist constants $C_{f\pm} > 0$, $h_{f\pm} > 0$ and open subsets $U_{f\pm} \subset TQ$ with compact closure such that

$$||f_d^\pm(q(0), q(h), h) - f_d^{E\pm}(q(0), q(h), h)|| \leq C_{f\pm} h_{f\pm}^{r+1}, \tag{2.22}$$

for all solutions $q(t)$ of the forced Euler–Lagrange equations with initial conditions satisfying $(q(0), \dot{q}(0)) \in U_f^\pm$, and for all $h \leq h_f^\pm$. We will say that $L_d, f_d^\pm$ are *simultaneously of order* r if there exists $U \subset U_L \cap U_f^+ \cap U_f^-$ such that U is a nontrivial open set with compact closure.

For the discrete Legendre transforms to be of order r, we require constants $C^\pm > 0, h^\pm > 0$ and an open set $U^\pm \subset TQ$ such that

$$||\mathbb{F}^{f\pm}L_d(q(0), q(h), h) - \mathbb{F}^{f\pm}L_d^E(q(0), q(h), h)|| \leq C^\pm (h^\pm)^{r+1} \tag{2.23}$$

for all solutions $q(t)$ of the forced Euler–Lagrange equations with initial conditions satisfying $(q(0), \dot{q}(0)) \in U^\pm$, and for all $h \leq h^\pm$.

Theorem 3. Consider a hyperregular Lagrangian L with force f_L, corresponding Hamiltonian H, and corresponding Hamiltonian force f_H. If L_d and $f_d^\pm$ are simultaneously of order r, then

a. the forced discrete Legendre transforms $\mathbb{F}^{f\pm}L_d$ are of order r.

b. the discrete Hamiltonian map is of order r.

Proof. a. Assume that L_d and $f_d^{\pm}$ are simultaneously of order r. Then L_d of order r implies existences of a function e such that

$$L_d(q(0), q(h), h) = L_d^E(q(0), q(h), h) + h^{r+1}e(q(0), q(h), h) \tag{2.24}$$

and $||e(q(0), q(h), h)|| \leq C_L$ on U. Similarly, f_d^+ of order r implies the existence of a function e^+ such that

$$f_d^+(q(0), q(h), h) = f_d^{E+}(q(0), q(h), h) + h^{r+1}e^+(q(0), q(h), h) \tag{2.25}$$

and $||e^+(q(0), q(h), h)|| \leq C_{f+}$ on U.

Taking derivatives of (2.24) with respect to $q(h)$ gives

$$D_2L_d(q(0), q(h), h) = D_2L_d^E(q(0), q(h), h) + h^{r+1}D_2e(q(0), q(h), h)\ . \tag{2.26}$$

We assume both L_d and L_d^E have continuous derivatives in $q(h)$, so, by the definition of e in (2.24), D_2e is continuous and bounded on the compact set $cl(U)$. Combining this with (2.25), we have

$$\begin{aligned} &D_2L_d(q(0), q(h), h) + f_d^+(q(0), q(h), h) \\ &\qquad = D_2L_d^E(q(0), q(h), h) + f_d^{E+}(q(0), q(h), h) \\ &\qquad\qquad + h^{r+1}[D_2e(q(0), q(h), h) + e^+(q(0), q(h), h)]\ . \end{aligned} \tag{2.27}$$

From the above arguments, $D_2e(q(0), q(h), h) + e^+(q(0), q(h), h)$ is bounded on the set $cl(U)$. Thus, $\mathbb{F}^{f+}L_d$ is of order r. Taking derivatives of L_d with respect to $q(0)$ and using a similar calculation with f_d^- shows that $\mathbb{F}^{f-}L_d$ is of order r.

b. Let $F_{L_d}^f$ denote the integrator defined by the forced discrete Euler Lagrange equations and $\tilde{F}_{L_d}^f$ denote the discrete Hamiltonian integrator defined by the forced discrete Legendre transforms in (2.11). Then from the definitions of $F_{L_d}, \tilde{F}_{L_d}$, and

$\mathbb{F}^{f\pm}L_d$, we have the commutative diagram (2.28), which is the forced equivalent of diagram (1.5.3) in [15].

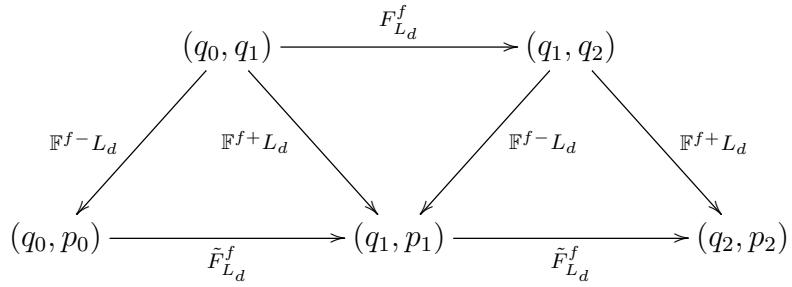

(2.28)

Thus, we can express the forced discrete Hamiltonian map as $\tilde{F}^f_{L_d} = \mathbb{F}^{f+}L_d \circ (\mathbb{F}^{f-}L_d)^{-1}$, directly analogous to the unforced discrete Hamiltonian map, $\tilde{F}_{L_d} = \mathbb{F}^{+}L_d \circ (\mathbb{F}^{-}L_d)^{-1}$. As such, the proof of b. from a. given in [15] carries over exactly, and we choose not to reproduce it here. □

The next theorem provides a recipe for constructing forced triples $(L_d, f_d^{\pm})$ of known order.

Theorem 4. Consider a p^{th} order accurate boundary-value solution method and a q^{th} order accurate quadrature formula. Assume both the Lagrangian and the forcing function are Lipschitz continuous in both variables. Use the boundary-value solution method to obtain approximations $(q^i, v^i) \approx (q(c_i h), v(c_i h))$, at the quadrature nodes c_i of the solution $(q(t), v(t))$ of the forced Euler–Lagrange boundary-value problem. Then the associated discrete Lagrangian given by

$$L_d(q_0, q_1; h) = h \sum_{i=0}^{n} b_i L(q^i, v^i) \ ,$$

and the discrete forces given by

$$f_d^+(q_0, q_1; h) = h \sum_{i=0}^{n} b_i f(q^i, v^i) \frac{\partial q^i}{\partial q_1},$$
$$f_d^-(q_0, q_1; h) = h \sum_{i=0}^{n} b_i f(q^i, v^i) \frac{\partial q^i}{\partial q_0},$$

all have order of accuracy $\min(p + 1, q)$.

Proof. The result follows from a few straightforward calculations. We begin with L_d.

$$\begin{aligned}
L_d^E(q_0, q_1, h) &= \int_0^h L(q_{01}(t), \dot{q}_{01}(t))\ dt \\
&= \left[h \sum_{i=1}^{m} b_i L(q_{01}(c_i h), \dot{q}_{01}(c_i h)) \right] + \mathcal{O}(h^{q+1}) \\
&= \left[h \sum_{i=1}^{m} b_i L(q^i + \mathcal{O}(h^{p+1}), v^i + \mathcal{O}(h^{p+1})) \right] + \mathcal{O}(h^{q+1}) \\
&= h \sum_{i=1}^{m} b_i L(q^i, v^i) + h \sum_{i=1}^{m} b_i \mathcal{O}(h^{p+1}) + \mathcal{O}(h^{q+1}) \\
&= L_d(q_0, q_1, h) + \mathcal{O}(h^{p+2}) + \mathcal{O}(h^{q+1})\ .
\end{aligned}$$

For f_d^+,

$$\begin{aligned}
f_d^{E+}(q_0, q_1, h) &= \int_0^h f(q_{01}(t), \dot{q}_{01}(t)) \cdot \frac{\partial q_{01}(t)}{\partial q_1}\ dt \\
&= \left[h \sum_{i=1}^{m} b_i f(q_{01}(c_i h), v_{01}(c_i h)) \cdot \frac{\partial q_{01}(c_i h)}{\partial q_1} \right] + \mathcal{O}(h^{q+1}) \\
&= \left[h \sum_{i=1}^{m} b_i f(q^i + \mathcal{O}(h^{p+1}), v^i + \mathcal{O}(h^{p+1})) \cdot \left(\frac{\partial q^i}{\partial q_1} + \mathcal{O}(h^{p+1}) \right) \right] \\
&\quad + \mathcal{O}(h^{q+1}) \\
&= \left[h \sum_{i=1}^{m} b_i \left(f(q^i, v^i) + \mathcal{O}(h^{p+1}) \right) \cdot \left(\frac{\partial q^i}{\partial q_1} + \mathcal{O}(h^{p+1}) \right) \right] + \mathcal{O}(h^{q+1}) \\
&= h \sum_{i=1}^{m} b_i f(q^i, v^i) \cdot \frac{\partial q^i}{\partial q_1} + \mathcal{O}(h^{p+2}) + \mathcal{O}(h^{2p+3}) + \mathcal{O}(h^{q+1}) \\
&= f_d^+(q_0, q_1, h) + \mathcal{O}(h^{p+2}) + \mathcal{O}(h^{q+1}).
\end{aligned}$$

A similar calculation shows that

$$f_d^{E-}(q_0, q_1, h) = f_d^-(q_0, q_1, h) + \mathcal{O}(h^{p+2}) + \mathcal{O}(h^{q+1})\ .$$

□

Taken together, Theorems 3 and 4 show that we can construct forced variational integrators of known order from a choice of a quadrature rule and

a boundary-value solution method. In fact, we could choose up to three different quadrature rules and boundary-value solution methods to define L_d, f_d^+, and f_d^-. The proofs above would still apply, and the resulting integrator would have order $\min(p_1+1, p_2+1, p_3+1, q_1, q_2, q_3)$ for p_i the orders of the boundary-value solutions and q_i the orders of the quadrature rules. However, this produces integrators with unpredictable results, as discussed in the next section.

2.3.2 Notions of equivalence and equivalence preservation

A forced Lagrangian system has equations of motion

$$\frac{\partial L}{\partial q}(q,\dot{q}) - \frac{d}{dt}\left(\frac{\partial L}{\partial \dot{q}}(q,\dot{q})\right) + f(q,\dot{q}) = 0. \tag{2.29}$$

Since the equations of motion are defined by the combination of L and f, it is possible for pairs (L^1, f^1) and (L^2, f^2) with $L^1 \neq L^2$ and $f^1 \neq f^2$ to define the same equations of motion. We refer to this as *equivalence* of the pairs (L^1, f^1) and (L^2, f^2). Most numerical methods simulate mechanics by numerically integrating the differential equations of motion, so they produce the same numerical approximation whether the motion was originally described using (L^1, f^1) or (L^2, f^2).

Variational integrators simulate mechanics using the discrete equations of motion defined by a particular choice of L_d and f_d. Thus, a variational integrator is defined by the choice of discretizations $L \mapsto L_d$ and $f \mapsto f_d$. It is therefore natural to ask which discretization schemes for the discrete Lagrangian and discrete forces when applied to equivalent representations of forced Euler–Lagrange systems lead to equivalent discrete equations of motion. This reflects whether or not the resulting variational integrator is well-defined on the equivalence class of representations of forced Euler–Lagrange systems.

More explicitly, given two equivalent representations (L^1, f^1) and (L^2, f^2) of a forced Euler–Lagrange system, the resulting solution trajectories are the same. Since a variational integrator for a forced Euler–Lagrange system aims to approximate that solution, it is desirable to consider well-defined variational integrators that produce the same approximation irrespective of which of the two equivalent representations (L^1, f^1) or (L^2, f^2) it is applied to. Well-definedness in this sense

will be important in interconnected applications where we intentionally alter the forced representation of a system to view it as a collection of interacting subsystems. In particular, if we considered a system with many components in terms of the constituent free-body diagrams, it is essential when combining the free-body diagrams for the internal forces to cancel out in order to recover the original system.

We discuss the implications of equivalence at the continuous and discrete levels. Then, we provide a simple criterion for constructing well-defined forced variational integrators.

Continuous equivalence

Suppose we have two canonical Lagrangians, $L^i = \frac{1}{2}\dot{q}^T M^i \dot{q} - V^i(q)$. Then equality of the equations of motion implies

$$-\nabla V^1(q) + M^1\ddot{q} + f^1(q,\dot{q}) = -\nabla V^2(q) + M^2\ddot{q} + f^2(q,\dot{q}) \ , \tag{2.30}$$

so that

$$f^1(q,\dot{q}) - f^2(q,\dot{q}) = \nabla(V^2 - V^1)(q) + (M^2 - M^1)\ddot{q}. \tag{2.31}$$

Comparing variables on each side, we conclude that $M^2 = M^1$ and $f^1(q,v) - f^2(q,v) = \nabla V^1(q) - \nabla V^2(q)$.

More generally, assume two Lagrangians of the form $L^i(q,v) = K(q,v) - V^i(q) = \frac{1}{2}g(v,v) - V^i(q)$ for some metric tensor g. Then, continuous equivalence again implies $f^1(q,v) - f^2(q,v) = \nabla V^2(q) - \nabla V^1(q)$.

Notions of discrete equivalence.

In [15], the authors define *strongly equivalent* discrete Lagrangians to be those that generate equivalent discrete Hamiltonian maps and *weakly equivalent* discrete Lagrangians to be those that generate equivalent discrete Lagrangian maps. That is to say that strongly equivalent discrete Lagrangians will generate the same discrete sequence $\{(q_k,p_k)\}_{k=0}^N \subset T^*Q$, whereas weakly equivalent discrete Lagrangians will only generate the same sequence $\{q_k\}_{k=0}^N \subset Q$.

We can define strong and weak equivalence of discrete triples $(L_d^i, f_d^{i\pm})$ in the same way. From diagram (2.28), we see that we have strong equivalence if

and only if we have equivalence of the forced discrete Legendre transforms, $\mathbb{F}^{f\pm}L_d$, just as in the unforced case. Then, Theorem 3 still holds for triples which are strongly equivalent to a triple meeting the assumptions. Moreover, Dirac variational integrators directly generalize the discrete Hamiltonian implementation of forced variational integrators. Thus, we focus on strong equivalence.

Strongly equivalent discrete triples $(L_d^1, f_d^{1\pm})$ and $(L_d^2, f_d^{2\pm})$ have equivalent forced discrete Legendre transforms, i.e. $\mathbb{F}^{f\pm}L_d^1 = \mathbb{F}^{f\pm}L_d^2$. This implies that

$$f_d^{2-}(q_k, q_{k+1}) - f_d^{1-}(q_k, q_{k+1}) = D_1 L_d^1(q_k, q_{k+1}) - D_1 L_d^2(q_k, q_{k+1}), \tag{2.32}$$

and

$$f_d^{1+}(q_k, q_{k+1}) - f_d^{2+}(q_k, q_{k+1}) = D_2 L_d^2(q_k, q_{k+1}) - D_2 L_d^1(q_k, q_{k+1}). \tag{2.33}$$

So each difference in discrete forcing in two strongly equivalent triples must be integrable in at least one of the position variables. If we think of $f_d^{\pm}$ as right and left discrete forces, then each discrete force difference must be integrable in its base-point variable, mirroring the continuous conclusion that $f^1(q, v) - f^2(q, v) = \nabla V^2(q) - \nabla V^1(q)$.

Preserving continuous equivalence

Theorems 3 and 4 provide a means of constructing forced variational integrators of known order by choosing quadrature rules and boundary-value solution methods. It is tempting to try to optimize the overall discretization by tailoring the discretization of L_d, f_d^+, and f_d^- individually, but the resulting integrator is no longer well-defined with respect to the equivalence relation defined above. The simplest way to generate an integrator that preserves continuous equivalence by our method is to choose the same quadrature rule and boundary-value solution method for all three discrete quantities.

In this case, we have

$$L_d(q_0, q_1; h) = h \sum_{i=0}^{n} b_i L(q^i, v^i) \ ,$$

and

$$f_d^+(q_0, q_1; h) = h \sum_{i=0}^{n} b_i f(q^i, v^i) \frac{\partial q^i}{\partial q_1}$$
$$f_d^-(q_0, q_1; h) = h \sum_{i=0}^{n} b_i f(q^i, v^i) \frac{\partial q^i}{\partial q_0}.$$

Suppose (L^1, f^1) and (L^2, f^2) are equivalent, so

$$f^1(q, \dot{q}) - f^2(q, \dot{q}) = \nabla V^1(q) - \nabla V^2(q).$$

Constructing $(L_d^1, f_d^{1\pm})$ and $(L_d^2, f_d^{2\pm})$ from (L^1, f^1) and (L^2, f^2), we then have

$$\begin{aligned} f_d^{1+}(q_0, q_1; h) - f_d^{2+}(q_0, q_1; h) &= h \sum_{i=0}^{n} b_i (f^1(q^i, v^i) - f^2(q^i, v^i)) \frac{\partial q^i}{\partial q_1} \\ &= h \sum_{i=0}^{n} b_i (\nabla V^2(q^i) - \nabla V^1(q^i)) \frac{\partial q^i}{\partial q_1} \\ &= D_2 L_d^2(q_0, q_1; h) - D_2 L_d^1(q_0, q_1; h). \end{aligned}$$

Similarly, $f_d^{2-}(q_0, q_1; h) - f_d^{1-}(q_0, q_1; h) = D_1 L_d^1(q_0, q_1; h) - D_1 L_d^2(q_0, q_1; h)$. Thus, $(L_d^1, f_d^{1\pm})$ and $(L_d^2, f_d^{2\pm})$ are strongly equivalent.

2.3.3 Numerical examples

We construct our implementations by choosing a quadrature rule and a one-step map, using shooting to solve the boundary-value problem, which is analogous to the shooting-based variational integrator proposed in [13]. Quadrature of order q and a one-step map of order p produce an integrator of order $\min(p, q)$ since the shooting solution is order $p - 1$.

Table 2.1 shows this construction converges as predicted. The second-order integrator uses trapezoidal quadrature and a second-order Taylor's method shooting solution. The fourth-order integrator uses Simpson's Rule quadrature and a fourth-order Taylor's method shooting solution. Both were run on a damped harmonic oscillator with mass $m = 1$, spring constant $k = 1$, and damping coefficient $c = 0.01$. The table shows the effect of doubling the number of time steps per

Table 2.1: Fourth and second-order forced integrators show the expected convergence rates. The second-order integrator uses Trapezoidal quadrature and second-order Taylor shooting. The fourth-order integrator uses Simpson's Rule quadrature and fourth-order Taylor shooting. Both methods simulate a damped harmonic oscillator with $m = k = 1$ and damping coefficient $c = 0.01$.

Steps per period	20	40	80	160
2^{nd} order error at $t = 5T$	0.2275	0.0557	0.0138	0.0035
error ratio	–	4.0844	4.0362	3.9429
4^{th} order error at $t = 5T$	0.6551×10^{-4}	0.0516×10^{-4}	0.0034×10^{-4}	0.0002×10^{-4}
error ratio	–	12.696	15.176	17

period T on the error after five periods. In both cases, the error decreases at the predicted rate.

Figure 2.1 illustrates the unpredictability of the results of non-equivalence preserving discretizations. Two implementations use second-order Taylor's method shooting as the boundary-value solution method for both L_d and $f_d^{\pm}$ with a Trapezoidal and/or Midpoint quadrature. The equivalence-preserving discretization uses Trapezoidal quadrature on both L_d and $f_d^{\pm}$. The non-equivalence preserving implementation uses a Trapezoidal quadrature on L_d and Midpoint quadrature on $f_d^{\pm}$. Both integrators were run on a conservative harmonic oscillator eleven times, with the potential force increasingly represented as an external force, i.e.

$$L(q,v) = \frac{1}{2}v^T M v - (1-\alpha)V(q)\ ,\ \ f(q,v) = -\alpha\nabla V(q) \tag{2.34}$$

for $\alpha = 0, 0.1, 0.2 \ldots, 1$. The step size was $h = 0.05$ for all runs. All values of α produce the same continuous equations of motion. The equivalence preserving discretization produces the same solution regardless of α. The non-equivalence preserving discretization produces α-dependent solutions which veer away from the unforced representation's solution as α increase. We also compared a Midpoint-Midpoint construction to a Midpoint-Trazezoidal construction in the same way. The results lie directly atop the Trap-Trap vs. Trap-Mid results shown. This unpredictability of results makes non-equivalence-preserving integrators unsuited for applications like interconnected systems in which a system's forced representation

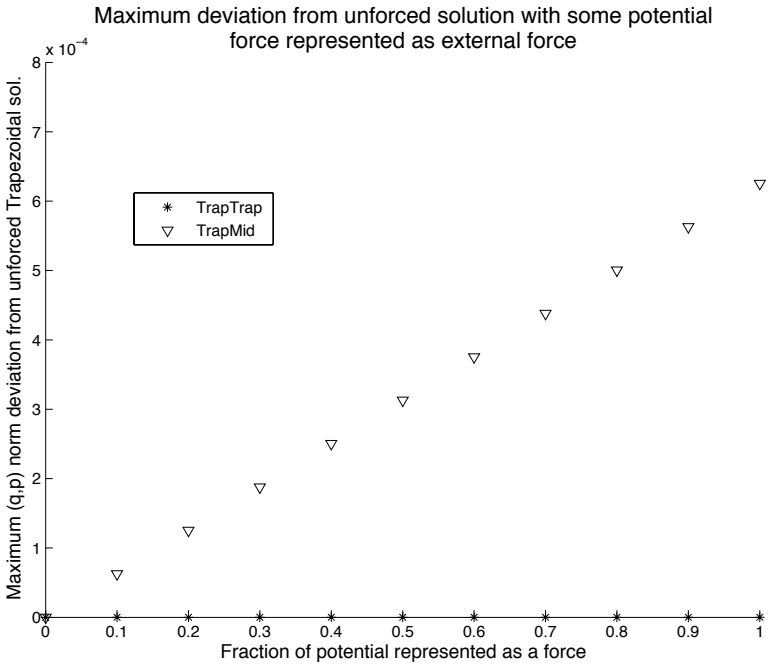

Figure 2.1: As the system's potential is increasingly represented as an external force, the non-equivalence-preserving construction produces solutions that veer further and further from the solution of an unforced representation. The equivalence-preserving construction produces the same solution whether the potential force is represented entirely through a potential within the Lagrangian or entirely as an external force.

will purposely be modified by modeling the component subsystems individually, with internal forces to account for the interaction with other subsystems.

Figure 2.2 shows a different example where failure to preserve equivalence produces wildly unpredictable results. A fourth-order equivalence-preserving integrator and a second-order non-equivalence-preserving integrator both simulate a system whose equations of motion simplify to an unforced harmonic oscillator. We inserted an artificial potential of $100q^5$, then canceled that potential force with a forcing function. The non-equivalence-preserving formulation fails to capture the motion beyond what can reasonably be explained by its lower order. The example is artificial, but it highlights the need to preserve equivalence in developing a well-defined integrator.

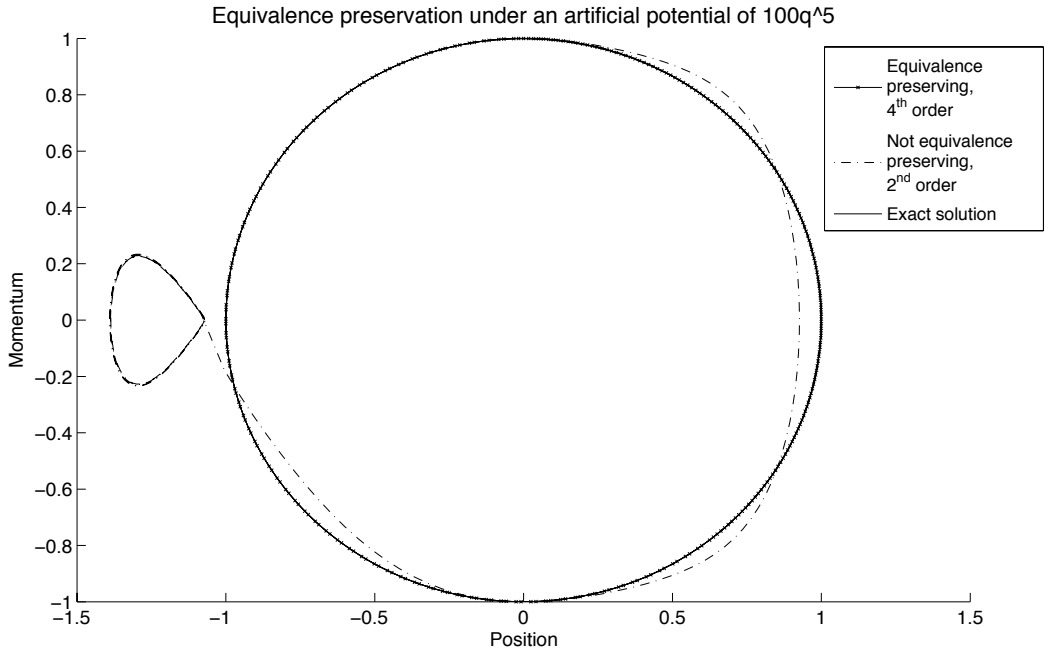

Figure 2.2: Two integrators simulate a system whose equations of motion simplify to an undamped harmonic oscillator. An artificial potential of $100q^5$ was added to the Lagrangian, with the artificial potential force canceled by an external force. The 4^{th} order equivalence-preserving discretization is indistinguishable from the exact solution, while the 2^{nd} order non-equivalence preserving discretization veers wildly away. The drastic qualitative difference in the two solutions cannot be explained only by the difference in order.

2.4 Dirac variational integrators with forces

We now lay out the generalization of Dirac variational integrators to include forces. We begin from the variational perspective, where we can directly apply the ideas of forced variational integrators. We then formulate the resulting integrators from the perspective of discrete Dirac structures and finish with a basic numerical implementation.

2.4.1 Variational formulation

(+)-discrete Dirac mechanics

In [12], the discrete variational principle for a Dirac system without external forces is the (+)-discrete Lagrange-d'Alembert-Pontryagin principle, given by

$$\delta \sum_{k=0}^{N-1} [L_d(q_k, q_k^+) + p_{k+1}(q_{k+1} - q_k^+)] = 0, \tag{2.35}$$

where the variations vanish at the endpoints and are constrained to lie on a constraint distribution, and pairs of consecutive points in the discrete solution lie in a discrete constraint distribution. We define the forced principle in direct analogy to (2.8) as

$$\delta \sum_{k=0}^{N-1} [L_d(q_k, q_k^+) + p_{k+1}(q_{k+1} - q_k^+)] + \sum_{k=0}^{N-1} [f_d^-(q_k, q_k^+) \cdot \delta q_k + f_d^+(q_k, q_k^+) \cdot \delta q_k^+] = 0, \tag{2.36}$$

where the second sum represents the virtual work associated with the external forces. We have chosen the arguments of $f_d^\pm$ to match those of L_d, and we constrain the variations in the same way as [12]. Thus, δp_k and δq_k^+ are arbitrary and $\delta q_0 = \delta q_n = 0$. We impose $\delta q_k \in \Delta_Q(q_k)$ on the remaining δq_k after taking variations inside the sum, and we insist that $(q_k, q_{k+1}) \in \Delta_Q^{d+}$. For the forced

principle (2.36) these constraints yield

$$0 = \omega^a_{d+}(q_k, q_{k+1}), \tag{2.37a}$$

$$q_{k+1} = q_k^+, \tag{2.37b}$$

$$p_{k+1} = D_2 L_d(q_k, q_k^+) + f_d^+(q_k, q_k^+), \tag{2.37c}$$

$$p_k = -D_1 L_d(q_k, q_k^+) - f_d^-(q_k, q_k^+) + \mu_a \omega^a(q_k). \tag{2.37d}$$

These equations recover the (+)-discrete Lagrange–Dirac equations of [12] when $f_d^\pm = 0$ and the forced discrete Euler–Lagrange equations [15] in the absence of constraints. When both the forces and constraints are zero, we recover the classic discrete Euler–Lagrange equations.

(-)-discrete Dirac mechanics

In [12], (-)-discrete Dirac mechanics derives from the (-)-discrete Lagrange-d'Alembert principle,

$$\delta \sum_{k=0}^{N-1} [L_d(q_{k+1}^-, q_{k+1}) - p_k(q_k - q_{k+1}^-)] = 0, \tag{2.38}$$

with constraints on the variations, and the pairs of sequential points as before. We add forces to this principle as

$$\begin{aligned} \delta \sum_{k=0}^{N-1} &[L_d(q_{k+1}^-, q_{k+1}) - p_k(q_k - q_{k+1}^-)] \\ &+ \sum_{k=0}^{N-1} [f_d^-(q_{k+1}^-, q_{k+1}) \cdot \delta q_{k+1}^- + f_d^+(q_{k+1}^-, q_{k+1}) \cdot \delta q_{k+1}] = 0, \end{aligned} \tag{2.39}$$

again choosing the arguments of $f_d^\pm$ to match those of L_d and constraining the variations as in [12]. In this case, then, δp_k and δq_k^- are arbitrary and $\delta q_0 = \delta q_N = 0$. We impose $\delta q_k \in \Delta_Q(q_k)$ on the remaining δq_k after taking variations inside the sums, and we insist that $(q_k, q_{k+1}) \in \Delta_Q^{d-}$. With these conditions, computing

variations of the principle (2.39) yields

$$0 = \omega^a_{d-}(q_k, q_{k+1}), \tag{2.40a}$$

$$q_k = q^-_{k+1}, \tag{2.40b}$$

$$p_k = -D_1 L_d(q^-_{k+1}, q_{k+1}) - f^-_d(q^-_{k+1}, q_{k+1}), \tag{2.40c}$$

$$p_{k+1} = D_2 L_d(q^-_{k+1}, q_{k+1}) + f^+_d(q^-_{k+1}, q_{k+1}) + \mu_a \omega^a(q_{k+1}). \tag{2.40d}$$

In the unforced case, these equations recover the (-)-discrete Dirac equations of [12]. In the unconstrained case, we recover the forced discrete Euler–Lagrange equations of [15]. In the absence of both we again recover the classic discrete Euler–Lagrange equations.

2.4.2 Discrete Dirac structure formulation

The dynamics of an unforced, continuous Lagrange–Dirac dynamical system can be expressed in terms of Dirac structures as $(X, \mathfrak{D}L) \in D$, where X is the partial vector field of the motion, $\mathfrak{D}L$ the Dirac differential of the Lagrangian L and D a Dirac structure on T^*Q. To accomodate forces in the continuous case, the force $F : TQ \to T^*Q$ is lifted to a map $\tilde{F} : TQ \to T^*T^*Q$ such that

$$\langle \tilde{F}(q, v), w \rangle = \langle F(q, v), T\pi_Q(w) \rangle \ . \tag{2.41}$$

Locally, $\tilde{F}$ is given by $\tilde{F}(q, v) = (q, p, F(q, v), 0)$. The forced Lagrange–Dirac dynamical system is then given by

$$(X, \mathfrak{D}L(q, v) - \tilde{F}(q, v)) \in D_{\Delta_Q}(q, p) \ . \tag{2.42}$$

Without forces, we can express (+) and (-)-discrete Dirac mechanics in terms of discrete Dirac structures as

$$(X^k_d, \mathfrak{D}^+ L_d(q_k, q^+_k)) \in D^{d+}_{\Delta Q}, \tag{2.43}$$

and

$$(X^k_d, \mathfrak{D}^- L_d(q^-_{k+1}, q_{k+1})) \in D^{d-}_{\Delta Q}, \tag{2.44}$$

which amount to the conditions

$$(q_k, D_2L_d, -D_1L_d, q_k^+) - (q_k, p_{k+1}, p_k, q_{k+1}) \in \Delta^\circ_{Q\times Q^*}, \tag{2.45a}$$

$$(-D_1L_d, q_{k+1}, -q_{k+1}^-, -D_2L_d) - (p_k, q_{k+1}, -q_k, -p_{k+1}) \in \Delta^\circ_{Q^*\times Q}. \tag{2.45b}$$

To introduce forces into these expressions in a manner that is consistent with the discrete equations of motion that are derived variationally, we require

$$(q_k, D_2L_d + f_d^+, -D_1L_d - f_d^-, q_k^+) - (q_k, p_{k+1}, p_k, q_{k+1}) \in \Delta^\circ_{Q\times Q^*}, \tag{2.46a}$$

$$(-D_1L_d - f_d^-, q_{k+1}, -q_{k+1}^-, -D_2L_d - f_d^+) - (p_k, q_{k+1}, -q_k, -p_{k+1}) \in \Delta^\circ_{Q^*\times Q}. \tag{2.46b}$$

To this end, define $\tilde{F}_{d+}$ and $\tilde{F}_{d-}$ as

$$\tilde{F}_{d+}(q_k, q_k^+) = (0, -f_d^+(q_k, q_k^+), f_d^-(q_k, q_k^+), 0), \tag{2.47a}$$

$$\tilde{F}_{d-}(q_{k+1}^-, q_{k+1}) = (f_d^-(q_{k+1}^-, q_{k+1}), 0, 0, f_d^+(q_{k+1}^-, q_{k+1})). \tag{2.47b}$$

Then, we can write conditions (2.46) as

$$(X_d^k, \mathfrak{D}^+L_d(q_k, q_k^+) - \tilde{F}_{d+}(q_k, q_k^+)) \in D^{d+}_{\Delta Q} \tag{2.48a}$$

$$(X_d^k, \mathfrak{D}^-L_d(q_{k+1}^-, q_{k+1}) - \tilde{F}_{d-}(q_{k+1}^-, q_{k+1})) \in D^{d-}_{\Delta Q}. \tag{2.48b}$$

mimicking the continuous expression (2.42). In (2.48) we regard $\mathfrak{D}^\pm L_d - \tilde{F}_{d\pm}$ as an abstract expression and impose base-point matching after the subtraction.

2.4.3 Numerical Example

We close with a simple implementation of the (+) forced discrete Dirac equations. We simulate a basic RLC resonator with a single resistor, inductor, and capacitor. We assume some existing voltage in the system but no replenishing voltage source.

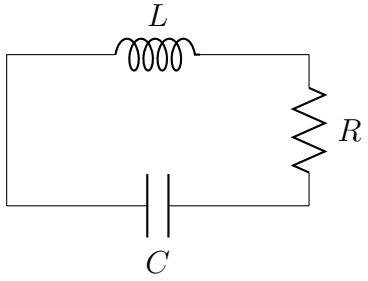

The system is described as a Lagrange–Dirac system in terms of the charges and currents in each component, $(q^C, q^L, q^R, i^C, i^L, i^R)$. Let L, R, and C denote the inductance, resistance, and capacitance of the components. Then the system has Lagrangian function

$$L(q,i) = \frac{L}{2}(i^L)^2 - \frac{(q^C)^2}{2C} \tag{2.49}$$

and force

$$f(q,i) = -i^R R. \tag{2.50}$$

Kirchhoff's current law imposes the following constraints,

$$i^L - i^R = 0, \tag{2.51a}$$

$$i^R - i^C = 0. \tag{2.51b}$$

Thus, our constraints can be described in terms of the annihilator distribution $\Delta_Q^\circ = span\{\omega^1, \omega^2\}$ for $\omega^1 = dq^L - dq^R$ and $\omega^2 = dq^R - dq^C$. We follow the discretization in [12] to construct $\omega_{d+}^{1,2}$ as $\omega_{d+}^a(q_k, q_{k+1}) = \omega^a(q_k, \mathcal{R}_{q_k}^{-1}(q_{k+1}))$ for $\mathcal{R}_q(v) = q + vh$.

Existence of exact discrete quantities in the Dirac setting has not yet been established, so we cannot turn to them to guide the discretization for L_d and $f_d^\pm$. Establishing such quantities is obviously desirable and a topic for future work. For now, we choose a simple L_d and $f_d^\pm$ shown to work well in both the forced, non-Dirac setting [15] as well as the nonholonomic integrator setting [4]. Namely, we choose L_d and $f_d^\pm$ to be

$$L_d^{1/2}(q_k, q_k^+) = hL\left(\frac{q_k^+ + q_k}{2}, \frac{q_k^+ - q_k}{h}\right), \tag{2.52}$$

and

$$f_d^{1/2\pm} = \frac{h}{2} f\left(\frac{q_k^+ + q_k}{2}, \frac{q_k^+ - q_k}{h}\right). \tag{2.53}$$

[15] introduces these forces as the natural complement to $L_d^{1/2}$. The discretizations $L_d^{1/2}$ and $f_d^{1/2\pm}$ both correspond to choosing midpoint quadrature and a linear boundary-value solution to approximate L_d^E and $f_d^{E\pm}$ in the forced, non-Dirac setting. Thus, the set $(L_d^{1/2}, f_d^{1/2\pm})$ is natural and equivalence-preserving by our earlier analysis as well.

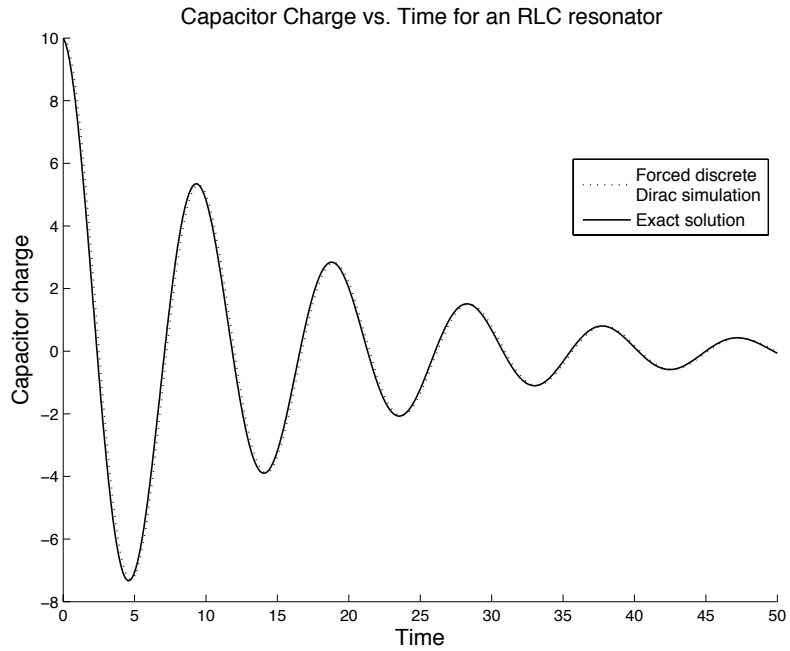

Figure 2.3: A forced discrete Dirac integrator accurately simulates the decaying charge oscillations of a capacitor in an RLC resonator. The resonator consists of a single loop with one inductor ($L = 0.75$), one capacitor ($C = 3$), and one resistor ($R = 0.1$). The step size is $h = 0.05$.

Figure 2.3 shows that the simulated charge in the capacitor over time (dotted line) is almost identical to the exact solution (solid line) using a time-step of $h = 0.05$ for 1000 time-steps.

2.5 Conclusions and future work

In this work we have successfully integrated the presence of external forcing into the discrete Dirac framework originally presented in [12] so that our forced discrete Dirac integrators recover the forced DEL integrators of [15]. We have also studied the effects of shifting forced representations on the accuracy of numerical simulations and presented a straightforward method for constructing integrators that avoid these spurious effects.

The work was conducted with an eye toward future work on in the interconnection of discrete Dirac mechanics. Continuous interconnections can be

equivalently represented as either constraints or interaction forces acting between subsystems. One would hope to obtain a similar equivalence at the discrete level. In ongoing work, presented in the next chapter, we have derived discrete interconnections from the point of view of constraints. However, we do not yet have an equivalent representation in terms of discrete interaction forces. There is a lack of equivalence between forced and constrained representations throughout the discrete literature, though recent work has rectified this issue on vectors spaces through Hamel's formalism.

2.6 Acknowledgements

This work was conducted with Professor Melvin Leok at UC San Diego and was generously funded through the National Science Foundation Graduate Research Fellowship grant number DGE-1144086. This work is currently being prepared for publication.

Chapter 3

Variational integrators for interconnected Lagrange-Dirac systems

In this chapter, we develop a framework for the interconnection of discrete Dirac mechanical systems. This work builds on previous work on the interconnection of continuous Dirac systems [10] and discrete Dirac variational integrators [12]. We test our results by simulating some of the continuous examples given in [10].

3.1 Introduction

This work is motivated in part by a desire to develop a structure-preserving simulation framework with which to study control by interconnection. The need for robust control of mechanical systems is perhaps one of the most common reasons for viewing a system in terms of interconnections. We have a plant system whose behavior we wish to control, so it must be mechanically or electrically joined to a controller system. Hence, we have an interconnected system. Considering that the controlling device is often itself a mechanical system, we have the interconnection of two mechanical systems, and we can begin to study the structure of the interconnected, controlled system as it relates to the structures of the starting plant

and controller. The field of port-controlled Hamiltonian systems undertakes just such a study and has produced extensive results [18, 6].

As the name suggests, port-Hamiltonian systems look at mechanical structure from the Hamiltonian perspective. In [19] and [20] Yoshimura and Marsden develop Lagrange-Dirac mechanics as a way of understanding the implicit systems central to port-Hamiltonian systems from the Lagrangian perspective. That aim is rooted partially in the natural desire to understand implicit systems from both classical perspectives. It also moves toward the goal of studying interconnections and control by interconnection using structured computations via variational integrators. Variational integrators cover a wide range of numerical schemes but are most often derived from the Lagrangian perspective.

The next steps were taken in [10], in which Jacobs and Yoshimura develop continuous interconnections of Lagrange-Dirac systems, and in [12], where Leok and Ohsawa extended variational integrators to the Lagrange-Dirac case. In the present chapter we discretize the interconnections of [10] in accordance with the framework laid out in [12].

While our study of interconnected systems has very specific roots, we have abstracted our way to general interconnections (following [10]) and believe that our results have useful applications outside the realm of plant/controller interconnection. It is natural to approach the modeling of a large, complex system by breaking it into smaller, more easily understood components. The full system can then be modeled as the interconnection of several simpler, component-wise models. Sometimes our engineering objectives themselves are modular, such as with a robot in need of several different appendages, each with a specific function. Here, too, interconnection may be useful by providing the ability to alter the models of each appendage individually with only minimal effort to re-construct a full system model.

3.2 Background

3.2.1 Dirac structures and Langrange-Dirac mechanics

We begin with a review of Dirac structures and their role in Lagrange-Dirac mechanics. Then we revisit the continuous interconnection process.

Dirac structures

Let V be a finite dimensional vector space with dual V^*. Denote the natural pairing between V and V^* by $\langle\cdot,\cdot\rangle$, and define the symmetric pairing $\langle\langle\cdot,\cdot\rangle\rangle$ on $V \oplus V^*$ by

$$\langle\langle(v_1,\alpha_1),(v_2,\alpha_2)\rangle\rangle = \langle\alpha_1, v_2\rangle + \langle\alpha_2, v_1\rangle \tag{3.1}$$

for $(v_1,\alpha_1),(v_2,\alpha_2) \in V \oplus V^*$. A Dirac structure on V is a subset $D \subset V \oplus V^*$ such that $D = D^\perp$ with respect to $\langle\langle\cdot,\cdot\rangle\rangle$.

Now let M be a smooth manifold. Denote by $TM \oplus T^*M$ the Pontryagin bundle over M, so the fiber over $x \in M$ is $T_xM \oplus T_x^*M$. Then a *Dirac structure on* M is a subbundle $D \subset TM \oplus T^*M$ such that every fiber $D(x)$ is a Dirac structure on T_xM. Every manifold Dirac structure D has an associated distribution defined by

$$\Delta_D(x) = \{v \in T_xM \mid (v,\alpha) \in D(x) \text{ for some } \alpha\}. \tag{3.2}$$

The Dirac structure D also defines a bilinear map on Δ_D,

$$\omega_{\Delta_D}(v,w) = \langle\alpha_v, w\rangle. \tag{3.3}$$

This holds for any α_v such that $(v,\alpha_v) \in D(x)$ and any $w \in \Delta_D(x)$. The form ω_{Δ_D} is well-defined on Δ_D even if there exist multiple such α_v due to $D = D^\perp$ with respect to the symmetric pairing above.

Conversely, given a two-form ω on M and a regular distribution $\Delta \subset TM$, we can define a Dirac structure D on M fiber-wise as

$$\begin{aligned} D(x) = \{(v,\alpha) \in T_xM \oplus T_x^*M \mid v \in \Delta(x) \text{ and } \langle\alpha, w\rangle = \omega_x(v,w) \\ \text{for all } w \in \Delta(x)\}. \end{aligned} \tag{3.4}$$

Clearly, in this case $\Delta_D = \Delta$ and $\omega_{\Delta_D} = \omega|_{\Delta_D}$. We use this idea to connect Dirac structures with constraint distributions.

Induced Dirac structures

Dirac structures are especially relevant in the case of Lagrangian systems with linear nonholonomic constraints, i.e. constraints of the form $\omega^a(q) \cdot \dot{q} = 0$, $a = 1, \ldots, m$ for $\{\omega^a\}$ one forms on Q. Such constraints can be equivalently expressed using the regular distribution $\Delta_Q \subset TQ$ defined by $\Delta_Q(q) = \cap_a \ker(\omega^a(q))$. Thus, the annihilator codistribution of Δ_Q is given by $\Delta_Q^\circ(q) = \text{span}\{\omega^a(q)\}$. The constraints are then written $\dot{q} \in \Delta_Q(q)$ or simply $\dot{q} \in \Delta_Q$. Nonholonomic constraints such as these cause the motion on T^*Q to be pre-symplectic rather than symplectic. The Dirac structure induced by Δ_Q gives a precise description of this pre-symplectic structure. Note that we may also have primary constraints on T^*Q if L is degenerate.

The constraints Δ_Q induce a Dirac structure on T^*Q as follows. From Δ_Q, define $\Delta_{T^*Q} \subset TT^*Q$ as

$$\Delta_{T^*Q} = (T\pi_Q)^{-1}(\Delta_Q) \tag{3.5}$$

for $\pi_Q : T^*Q \to Q$ the canonical projection and $T\pi_Q$ its tangent lift. We now apply the construction described in (3.4) using Δ_{T^*Q} and the canonical symplectic form Ω on T^*Q. This gives the following fiber-wise definition of D_{Δ_Q}, the Dirac structure on T^*Q induced by the constraint distribution Δ_Q.

$$\begin{aligned} D_{\Delta_Q}(q,p) = \{(v,\alpha) \in T_{(q,p)}T^*Q \oplus T^*_{(q,p)}T^*Q \mid v \in \Delta_{T^*Q}(q,p) \text{ and} \\ \langle \alpha, w \rangle = \Omega(v,w) \text{ for all } w \in \Delta_{T^*Q}(q,p)\}. \end{aligned} \tag{3.6}$$

Canonical local coordinate expressions

It will be useful to have expressions for $\Delta_{T^*Q}, \Delta^\circ_{T^*Q}$, and D_{Δ_Q} in terms of local canonical coordinates. Let V be a model vector space for the configuration manifold Q, and let $U \subset V$ be a chart around $q \in Q$. Then we have the following

local representations near q,

$$\begin{aligned} TQ &\mapsto U \times V, \\ T^*Q &\mapsto U \times V^*, \\ TTQ &\mapsto (U \times V) \times (V \times V), \\ TT^*Q &\mapsto (U \times V^*) \times (V \times V^*), \\ T^*T^*Q &\mapsto (U \times V^*) \times (V^* \times V). \end{aligned}$$

In these coordinates $\pi_Q : (q,p) \mapsto q$ and $T\pi_Q : (q,p,\delta q,\delta p) \mapsto (q,\delta q)$, so that

$$\Delta_{T^*Q} = \{(q,p,\delta q,\delta p) \in T_{(q,p)}T^*Q \mid (q,\delta q) \in \Delta_Q\} \tag{3.7}$$

with the annihilator distribution

$$\Delta^\circ_{T^*Q}(q,p) = \{(q,p,\alpha_q,\alpha_p) \in T^*_{(q,p)}T^*Q \mid (q,\alpha_q) \in \Delta^\circ_Q \text{ and } \alpha_p = 0\}. \tag{3.8}$$

As indicated above, any $v \in T_{(q,p)}T^*Q$ has two coordinate components. We will write these as $(\delta q, \delta p)$ in the abstract case or (v_q, v_p) when referring to a particular v. Similarly, we will write $\alpha = (\alpha_q, \alpha_p)$ for $\alpha \in T^*_{(q,p)}T^*Q$. In this notation, $\Omega(v,w) = v_q \cdot w_p - v_p \cdot w_q$. So the condition $\langle \alpha, w\rangle = \Omega(v,w)$ for all $w \in \Delta_{T^*Q}$ translates to $(\alpha_q + v_p, \alpha_p - v_q) \in \Delta^\circ_{T^*Q}$. Thus the induced Dirac structure in (3.6) has the coordinate expression

$$\begin{aligned} D_{\Delta_Q}(q,p) = \{(v_q,v_p,\alpha_q,\alpha_p) \in T_{(q,p)}T^*Q \oplus T^*_{(q,p)}T^*Q \mid v_q \in \Delta_Q(q), \\ \alpha_p = v_q, \text{ and } \alpha_q + v_p \in \Delta^\circ_Q(q)\}. \end{aligned} \tag{3.9}$$

The Tulczyjew triple

The Tulczyjew triple relates the spaces T^*T^*Q, TT^*Q, and T^*TQ and helps bridge the gap between Lagrangian and Hamiltonian mechanics. These maps were first studied by Tulczyjew in the context of a generalized Legendre transform in [17]. The first map is the usual flat map derived from the symplectic form Ω on T^*Q. We write $\Omega^\flat : TT^*Q \to T^*T^*Q$ defined by

$$\Omega^\flat(v) \cdot w = \Omega(v,w). \tag{3.10}$$

In coordinates,

$$\Omega^\flat(v) = (-v_p, v_q) \in T^*T^*Q. \tag{3.11}$$

The second map, $\kappa_Q : TT^*Q \to T^*TQ$ is given locally by a simple coordinate shuffling,

$$\kappa_Q : (q, p, \delta q, \delta p) \mapsto (q, \delta q, \delta p, p). \tag{3.12}$$

A global definition of κ_Q can be found in [19]. A unique diffeomorphism κ_Q exists for any manifold Q [19]. The third map, $\gamma_Q : T^*TQ \to T^*T^*Q$ is defined in terms of the first two,

$$\gamma_Q := \Omega^\flat_{T^*Q} \circ \kappa_Q^{-1}. \tag{3.13}$$

Lagrange-Dirac dynamical systems

We are now equipped to define a Lagrange-Dirac dynamical system. Let $L : TQ \to \mathbb{R}$ be a given, possibly degenerate, Lagrangian. We define the Dirac differential of L to be

$$\mathfrak{D}L(q, v) := \gamma_Q \circ \mathbf{d} : TQ \to T^*T^*Q. \tag{3.14}$$

Here $\mathbf{d}$ denotes the usual exterior derivative operator so that $\mathbf{d}L : TTQ \to T^*TQ$. For a curve $(q(t), v(t), p(t)) \in TQ \oplus T^*Q$, we define X_D to be the following partial vector field

$$X_D(q(t), v(t), p(t)) = (q(t), p(t), \dot{q}(t), \dot{p}(t)) \in TT^*Q. \tag{3.15}$$

Then the equations of motion for a Lagrange-Dirac dynamical system with Lagrangian L and constraint distribution Δ_Q are given by

$$(X_D(q(t), v(t), p(t)), \mathfrak{D}L(q(t), v(t))) \in D_{\Delta_Q}(q(t), p(t)). \tag{3.16}$$

In local coordinates $\mathbf{d}L(q, v) = (q, v, \frac{\partial L}{\partial q}, \frac{\partial L}{\partial v})$ and

$$\gamma_Q : (q, \delta q, \delta p, p) \mapsto (q, p, -\delta p, \delta q), \tag{3.17}$$

so we have

$$\mathfrak{D}L(q, v) = (q, \frac{\partial L}{\partial v}, -\frac{\partial L}{\partial q}, v). \tag{3.18}$$

Then using the coordinate expressions from (3.9), the equations determined by (3.16) are

$$\dot{q} = v \in \Delta_Q(q),\ \dot{p} - \frac{\partial L}{\partial q} \in \Delta_Q^\circ(q),\ p = \frac{\partial L}{\partial v}. \tag{3.19}$$

The last equation comes from matching the basepoints of $X_D(q,p)$ and $\mathfrak{D}L(q,v)$. This is a set of differential algebraic equations on $TQ \oplus T^*Q$ whereas the Euler-Lagrange equations give an ODE system on TQ. We see that the first and last equations explicitly enforce the second order curve condition and the Legendre transform, respectively. The middle equation reduces to the Euler-Lagrange equations in the absence of constraints. With constraints, the Euler-Lagrange relationship holds along the permissible directions. Explicit enforcement of the Legendre transform serves to enforce any primary constraints on the system.

The Hamilton-Pontryagin principle

Rather than the usual Hamilton's principle for curves on TQ, we apply the Hamilton-Pontryagin principle for curves on $TQ \oplus T^*Q$. This automatically incorporates a constraint distribution Δ_Q and any primary constraints coming from a degenerate Lagrangian. We have

$$\delta \int_0^T L(q(t), v(t)) - \langle p(t), \dot{q}(t) - v(t) \rangle \, dt = 0 \tag{3.20}$$

for variations $\delta q \in \Delta_Q(q)$ with fixed endpoints and arbitrary variations $\delta v, \delta p$ together with the constraint $\dot{q} \in \Delta_Q(q)$. This principle yields precisely the Lagrange-Dirac equations of motion (3.19).

The Lagrange-d'Alembert Pontryagin principle and Lagrange-Dirac systems with external forces

Suppose we have an external force field $F : TQ \to T^*Q$ acting on the system. As in the classical Lagrangian case [14], we take the horizontal lift of F to define $\tilde{F} : TQ \to T^*T^*Q$ by

$$\langle \tilde{F}(q,v), w \rangle = \langle F(q,v), T\pi_Q(w) \rangle. \tag{3.21}$$

In local coordinates $\tilde{F}(q,v) = (q,p,F(q,v),0)$. The equations of motion for the forced system are given by

$$(X_D(q,v,p), \mathfrak{D}L(q,v) - \tilde{F}(q,v)) \in D_{\Delta_Q}(q,p). \tag{3.22}$$

As before, we can derive the local coordinate equations from this, producing

$$\dot{q} = v \in \Delta_Q(q),\ \dot{p} - \frac{\partial L}{\partial q} - F \in \Delta_Q^\circ(q),\ p = \frac{\partial L}{\partial v}. \tag{3.23}$$

So only the second equation changes with the forcing. Equations (3.23) reduce to the usual forced Euler-Lagrange equations in the absence of constraints.

We must also incorporate the work of the forces into the variational principle. This is done in exactly the same way as forces are appended to Hamilton's principle in the usual forced Lagrangian setting [15]. In that setting, one obtains the Lagrange-d'Alembert principle. Here we arrive at the *Lagrange-d'Alembert-Pontryagin principle*,

$$\delta \int_0^T L(q,v) + \langle p, \dot{q} - v \rangle \ dt + \int_0^T \langle F(q,v), \delta q \rangle \ dt = 0 \tag{3.24}$$

for variations $\delta q \in \Delta_Q(q)$ with fixed endpoints and arbitrary variations $\delta v, \delta p$ together with the constraint $\dot{q} \in \Delta_Q(q)$. The addition of the forcing terms here again produces (3.23).

3.2.2 Interconnection of Lagrange-Dirac systems

In this section we review the interconnection of continuous Lagrange-Dirac systems laid out in [10]. Throughout this section we assume that we are connecting two systems (L_1, Δ_{Q_1}) on Q_1 and (L_2, Δ_{Q_2}) on Q_2. The results easily extend to the interconnection of a finite number of systems, as shown in [10]. The interconnected system will then evolve on $Q = Q_1 \times Q_2$. The interconnection of the two systems has both a variational formulation and a formulation in terms of the interconnection of the two starting Dirac structures, $D_{\Delta_{Q_1}}$ and $D_{\Delta_{Q_2}}$. This interconnection of Dirac structures in turn involves the direct sum of $D_{\Delta_{Q_1}}$ and $D_{\Delta_{Q_2}}$, a product on Dirac structures, and an interaction Dirac structure D_{int}.

Standard interaction Dirac structures

Let $\Sigma_Q \subset TQ$ be a regular distribution on Q describing the interaction between systems 1 and 2. Lift this distribution to T^*Q to define

$$\Sigma_{\text{int}} = (T\pi_Q)^{-1}(\Sigma_Q) \subset TT^*Q. \tag{3.25}$$

Then the *standard interaction Dirac structure* D_{int} on T^*Q is given by

$$D_{\text{int}}(q,p) = \Sigma_{\text{int}}(q,p) \oplus \Sigma_{\text{int}}^{\circ}(q,p) \tag{3.26}$$

for $\Sigma_{\text{int}}^{\circ}$ the annihilator of Σ_{int}.

As mentioned above, any Dirac structure on a manifold M defines an associated distribution $\Delta_M \subset TM$ and bilinear map $\omega_{\Delta_M} : \Delta_M \times \Delta_M \to \mathbb{R}$ defined on Δ_M. Taking $D = \Delta \oplus \Delta^\circ$ produces $\Delta_M = \Delta$ and $\omega_{\Delta_M} \equiv 0$. Thus, the distribution associated with D_{int} is Σ_{int}, and the associated two-form is the zero form. The zero form obviously extends to the whole of T^*Q, so D_{int} can equivalently be generated from Σ_{int} and $\omega \equiv 0$.

The direct sum of Dirac structures

Given two Dirac structures D_1 and D_2 on M_1 and M_2, the direct sum $D_1 \oplus D_2$ is the vector bundle over $M_1 \times M_2$ given by

$$\begin{aligned} &D_1 \oplus D_2(x_1,x_2) = \\ &\quad \{((v_1,v_2),(\alpha_1,\alpha_2)) \in T_{(x_1,x_2)}(M_1 \times M_2) \oplus T^*_{(x_1,x_2)}(M_1 \times M_2) \mid \\ &\quad (v_1,\alpha_1) \in D_1(x_1) \text{ and } (v_2,\alpha_2) \in D_2(x_2)\}. \end{aligned} \tag{3.27}$$

From [10] we have that $D_1 \oplus D_2$ is itself a Dirac structure over $M_1 \times M_2$. In the particular case of induced Dirac structures, $D_{\Delta_{Q_1}} \oplus D_{\Delta_{Q_2}} = D_{\Delta_{Q_1} \oplus \Delta_{Q_2}}$ [10].

The tensor product of Dirac structures

The interconnection of Dirac structures relies on a product operation on Dirac structures referred to as the *Dirac tensor product*. We have the following characterization of the Dirac tensor product.

Definition 2. ([10]). Let D_a, D_b be Dirac structures on M. We define the Dirac tensor product

$$\begin{aligned} D_a \boxtimes D_b = \{(v,\alpha) \in TM \oplus T^*M \mid \exists \beta \in T^*M \\ \text{such that } (v, \alpha+\beta) \in D_a, (v,-\beta) \in D_b\}. \end{aligned} \tag{3.28}$$

An equivalent definition is given in [8]. Let D_Δ be an induced Dirac structure on Q and D_{int} the standard interaction Dirac structure defined above. Then $D_\Delta \boxtimes D_{\text{int}}$ is a Dirac structure when $\Delta \cap \Sigma_Q$ is a regular distribution [10].

Interconnection of Dirac structures

Recall that we wish to connect the systems (L^1, Δ_{Q_1}) and (L^2, Δ_{Q_2}) with associated Dirac structures $D_{\Delta_{Q_1}}$ and $D_{\Delta_{Q_2}}$. The smooth distribution Σ_Q describes their interaction and is used to define the interaction Dirac structure $D_{\text{int}} = \Sigma_{\text{int}} \oplus \Sigma_{\text{int}}^\circ$ for $\Sigma_{\text{int}} = (T\pi_Q)^{-1}(\Sigma_Q)$. As before, $Q = Q_1 \times Q_2$ will be the configuration manifold of the interconnected system.

Given two Dirac structures D_a and D_b on Q_a and Q_b and an interaction Dirac structure D_{int} on $Q = Q_a \times Q_b$, the *interconnection of D_a and D_b through D_{int}* is

$$(D_a \oplus D_b) \boxtimes D_{\text{int}}. \tag{3.29}$$

We noted above that $D_{\Delta_{Q_1}} \oplus D_{\Delta_{Q_2}} = D_{\Delta_{Q_1} \oplus \Delta_{Q_2}}$. We have the following proposition for the interconnection of $D_{\Delta_{Q_1}}$ and $D_{\Delta_{Q_2}}$ through the standard interaction Dirac structure $D_{\text{int}} = \Sigma_{\text{int}} \oplus \Sigma_{\text{int}}^\circ$. (Recall that $\Sigma_Q \subset TQ$ and $\Sigma_{\text{int}} = (T\pi_Q)^{-1}(\Sigma_Q) \subset TT^*Q$.)

Proposition 3. ([10]). If $\Delta_{Q_1} \oplus \Delta_{Q_2}$ and Σ_Q intersect cleanly [i.e. $(\Delta_{Q_2} \oplus \Delta_{Q_2}) \cap \Sigma_Q$ has locally constant rank], then the interconnection of $D_{\Delta_{Q_1}}$ and $D_{\Delta_{Q_2}}$ through D_{int} is locally given by the Dirac structure induced from $(\Delta_{Q_2} \oplus \Delta_{Q_2}) \cap \Sigma_Q$ as, for each $(q,p) \in T^*Q$,

$$\begin{aligned} (D_{\Delta_{Q_1}} \oplus D_{\Delta_{Q_2}}) \boxtimes D_{\text{int}}(q,p) = \{(w,\alpha) \in T_{(q,p)}T^*Q \times T^*_{(q,p)}T^*Q \mid \\ w \in \Delta_{T^*Q}(q,p) \text{ and } \alpha - \Omega^\flat(q,p)\cdot w \in \Delta^\circ_{T^*Q}(q,p)\}, \end{aligned} \tag{3.30}$$

where $\Delta_{T^*Q} = (T\pi_Q)^{-1}((\Delta_{Q_2} \oplus \Delta_{Q_2}) \cap \Sigma_Q)$ and $\Omega = \Omega_1 \oplus \Omega_2$, where Ω_1 and Ω_2 are the canonical symplectic structures on T^*Q_1 and T^*Q_2.

Note that for $Q = Q_1 \times Q_2$, the canonical symplectic form $\Omega_{T^*Q} = \Omega_{T^*Q_1} \oplus \Omega_{T^*Q_2}$. Thus, if we define

$$\Delta_Q = (\Delta_{Q_1} \oplus \Delta_{Q_2}) \cap \Sigma_Q, \tag{3.31}$$

the previous proposition amounts to

$$(D_{\Delta_{Q_1}} \oplus D_{\Delta_{Q_2}}) \boxtimes D_{\text{int}} = D_{\Delta_Q}. \tag{3.32}$$

Interconnection of Lagrange-Dirac systems

Set $L(q, v) = L_1(q_1, v_1) + L_2(q_2, v_2)$ and $\Delta_Q = (\Delta_{Q_1} \oplus \Delta_{Q_2}) \cap \Sigma_Q$. Here, as usual, $(q, v) = (q_1, q_2, v_1, v_2) \in TQ = T(Q_1 \times Q_2)$ in coordinates. Then the interconnected system satisfies

$$(X_D(q, v, p), \mathfrak{D}L(q, v)) \in D_{\Delta_Q}(q, p). \tag{3.33}$$

The interconnected system also satisfies the usual Hamilton-Pontryagin principle (3.20) for L and Δ_Q.

Should there be any external forces $F_i : TQ_i \to T^*Q_i$ acting on either subsystem, those can be lifted to Q as $\tilde{F}_i = \pi_{Q_i}^* F_i$. Then $F = \sum_i \tilde{F}_i$ represents the external forces acting on the interconnected system, and the total system solves the equations

$$(X_D(q, v, p), \mathfrak{D}L(q, v) - F) \in D_{\Delta_Q}(q, p) \tag{3.34}$$

and satisfies the Lagrange-d'Alembert-Pontryagin principle (3.24).

Note that in [10] the forces considered in the interconnection process are interaction forces between subsystems, not external forces. As demonstrated in [10] the constraints imposed by Σ_Q have an equivalent representation as the effect of internal interaction forces. We ignore the interaction force perspective for now, viewing interconnections as governed wholly by constraints Σ_Q. We will say more about bringing the interaction force perspective into discrete interconnections in the concluding sections.

3.2.3 Discrete Dirac mechanics

In this section we review the discrete Dirac mechanics of [12]. We begin with a Lagrangian function $L : TQ \to \mathbb{R}$ and a continuous constraint distribution $\Delta_Q \subset TQ$.

A discrete Tulczyjew triple

Recall the continuous Tulczyjew triple, summarized in the following diagram.

$$T^*TQ \xleftarrow{\kappa_Q} TT^*Q \xrightarrow{\Omega^\flat_{T^*Q}} T^*T^*Q \qquad \gamma_Q : TT^*Q \to T^*T^*Q \tag{3.35}$$

This is used to define the continuous Dirac differential $\mathfrak{D}L = (\gamma_Q \circ \mathbf{d})L$.

In [12] the authors define a discrete Tulczyjew triple using generating functions of a symplectic map $F : T^*Q \to T^*Q$. In coordinates, these are

$$\kappa^d_Q : ((q_0, p_0), (q_1, p_1)) \mapsto (q_0, q_1, -p_0, p_1), \tag{3.36}$$

$$\Omega^\flat_{d+} : ((q_0, p_0), (q_1, p_1)) \mapsto (q_0, p_1, p_0, q_1), \tag{3.37}$$

$$\Omega^\flat_{d-} : ((q_0, p_0), (q_1, p_1)) \mapsto (p_0, q_1, -q_0, -p_1). \tag{3.38}$$

The distinction between $\Omega^\flat_{d\pm}$ comes from choosing either the type 2 or type 3 generating function in its definition.

These maps define the (+) and (-) discrete Tulczyjew triples,

$$T^*(Q \times Q) \xleftarrow{\kappa_Q} T^*Q \times T^*Q \xrightarrow{\Omega^\flat_{d+}} T^*(Q \times Q^*) \qquad \gamma^{d+}_Q : T^*Q \times T^*Q \to T^*(Q \times Q^*) \tag{3.39}$$

and

$$T^*(Q \times Q) \xleftarrow{\kappa_Q} T^*Q \times T^*Q \xrightarrow{\Omega^\flat_{d-}} T^*(Q^* \times Q). \qquad \gamma^{d-}_Q : T^*Q \times T^*Q \to T^*(Q^* \times Q) \tag{3.40}$$

We use $\gamma^{d\pm}_Q$ to define a ($\pm$) discrete Dirac differential on L_d and $\Omega^\flat_{d\pm}$ to define ($\pm$) discrete induced Dirac structures.

Discrete constraint distributions and discrete induced Dirac structures

Recall that a continuous Lagrange-Dirac system on a manifold Q has an associated constraint distribution $\Delta_Q \subset TQ$. With this we have a set of associated constraint one-forms $\{\omega^a\}$ such that

$$\Delta_Q^\circ(q) = \text{span}\{\omega^a(q)\}_{a=1}^m, \quad \text{i.e.} \quad \Delta_Q = \cap_a \ker(\omega^a(q)). \tag{3.41}$$

We define a discrete constraint distribution by discretizing these constraint one-forms. In the theory of [12], we do this using a retraction $R : TQ \to Q$. As with the Tulczyjew triple, we have a (+) and a (-) way of doing this, resulting in discrete forms $\omega_{d\pm}^a : Q \times Q \to \mathbb{R}$.

$$\omega_{d+}^a(q_0, q_1) = \omega^a(q_0)\left(R_{q_0}^{-1}(q_1)\right), \quad \omega_{d-}^a(q_0, q_1) = \omega^a(q_1)\left(-R_{q_1}^{-1}(q_0)\right). \tag{3.42}$$

The discrete constraint distribution is then defined as

$$\Delta_Q^{d\pm} = \{(q_0, q_1) \in Q \times Q \mid \omega_{d\pm}(q_0, q_1) = 0,\ a = 1, \ldots, m\}. \tag{3.43}$$

In classical variational integrator theory, the pair (q_0, q_1) is thought of as the discrete analogue to a tangent vector in TQ. The $(\pm)$ formulation here can be thought of as a right and left formulation based on treating one of q_0, q_1 as the basepoint and the other as a representative of the velocity. Indeed, the distribution Δ_Q^{d+} constrains only q_1, while Δ_Q^{d-} constrains only q_0 [12].

Recall that a continuous Dirac structure on T^*Q relies on the distribution $\Delta_{T^*Q} = (T\pi_Q)^{-1}(\Delta_Q) \subset TT^*Q$ for π_Q the canonical projection on T^*Q. At the discrete level, we define

$$\begin{aligned} \Delta_{T^*Q}^{d+} &= (\pi_Q \times \pi_Q)^{-1}(\Delta_Q^{d\pm}) \\ &= \left\{((q_0, p_0), (q_1, p_1)) \in T^*Q \times T^*Q \mid (q_0, q_1) \in \Delta_Q^{d\pm}\right\} \end{aligned} \tag{3.44}$$

and

$$\begin{aligned} \Delta_{Q\times Q^*}^\circ &= \left\{(q, p, \alpha_q, 0) \in T^*(Q \times Q^*) \mid \alpha_q \mathrm{d}q \in \Delta_Q^\circ(q)\right\}, \\ \Delta_{Q^*\times Q}^\circ &= \left\{(q, p, 0, \alpha_q) \in T^*(Q^* \times Q) \mid \alpha_q \mathrm{d}q \in \Delta_Q^\circ(q)\right\} \end{aligned} \tag{3.45}$$

The distributions $\Delta_{T^*Q}^{d\pm}$ serve as the discrete analogues of Δ_{T^*Q}, while $\Delta_{Q\times Q^*}^\circ$ and $\Delta_{Q^*\times Q}^\circ$ are the (+) and (-) discrete analogues of $\Delta_{T^*Q}^\circ$, respectively.

We then define discrete induced Dirac structures using these discrete distributions and the discrete maps $\Omega^{\flat}_{d\pm}$ defined earlier. We have

$$\begin{aligned} D^{d+}_{\Delta_Q} =&\{\big((z,z^+),\alpha_{\hat{z}}\big) \in (T^*Q \times T^*Q) \times T^*(Q \times Q^*) \mid \\ &(z,z^+) \in \Delta^{d+}_{T^*Q},\ \alpha_{\hat{z}} - \Omega^{\flat}_{d+}(z,z^+) \in \Delta_{Q\times Q^*}\} \end{aligned} \tag{3.46}$$

and

$$\begin{aligned} D^{d-}_{\Delta_Q} =&\{\big((z^-,z),\alpha_{\tilde{z}}\big) \in (T^*Q \times T^*Q) \times T^*(Q^* \times Q) \mid \\ &(z^-,z) \in \Delta^{d-}_{T^*Q},\ \alpha_{\tilde{z}} - \Omega^{\flat}_{d-}(z^-,z) \in \Delta_{Q^*\times Q}\}. \end{aligned} \tag{3.47}$$

Given $z = (q,p)$ and $z^+ = (q^+,p^+)$ then $\hat{z} = (q,p^+)$. Given $z^- = (q^-,p^-)$ and $z = (q,p)$ then $\tilde{z} = (p^-,q)$.

The discrete Dirac differential and discrete Dirac mechanics

We have two versions of the discrete Dirac differential,

$$\mathfrak{D}^+ L_d = \gamma^{d+}_Q \circ \mathbf{d}L_d \quad \text{and} \quad \mathfrak{D}^- L_d = \gamma^{d-}_Q \circ \mathbf{d}L_d. \tag{3.48}$$

Using the discrete vector field

$$X^k_d = ((q_k,p_k),(q_{k+1},p_{k+1})) \in T^*Q \times T^*Q \tag{3.49}$$

we then have the following systems. A *(+)-discrete Lagrange-Dirac system* satisfies

$$(X^k_d, \mathfrak{D}^+ L_d(q_k,q^+_k)) \in D^{d+}_{\Delta_Q}. \tag{3.50}$$

A *(-)-discrete Lagrange-Dirac system* satisfies

$$(X^k_d, \mathfrak{D}^- L_d(q^-_{k+1},q_{k+1})) \in D^{d-}_{\Delta_Q}. \tag{3.51}$$

The variables q^+_k and q^-_{k+1} are the discrete analogues of the velocity variable. In coordinates, equation (3.50) produces the *(+)-discrete Lagrange–Dirac equations of motion*,

$$0 = \omega^a_{d+}(q_k,q_{k+1}), \tag{3.52a}$$

$$q_{k+1} = q^+_k \tag{3.52b}$$

$$p_{k+1} = D_2 L_d(q_k,q^+_k), \tag{3.52c}$$

$$p_k = -D_1 L_d(q_k,q^+_k) + \mu_a \omega^a(q_k), \tag{3.52d}$$

where μ_a are Lagrange multipliers, and the last equation uses the Einstein summation convention. Equation (3.51) produces the *(-)-discrete Lagrange–Dirac equations of motion*,

$$0 = \omega^a_{d-}(q_k, q_{k+1}), \tag{3.53a}$$

$$q_k = q^-_{k+1} \tag{3.53b}$$

$$p_k = -D_1 L_d(q^-_{k+1}, q_{k+1}), \tag{3.53c}$$

$$p_{k+1} = D_2 L_d(q^-_{k+1}, q_{k+1}) + \mu_a \omega^a(q_{k+1}). \tag{3.53d}$$

Again, μ_a are Lagrange multipliers, and the last equation makes use of the Einstein summation convention. Later we will write these equations with the q^+_k and q^-_{k+1} variables eliminated for simplicity.

Both $(\pm)$ equations simplify to the DEL equations in the unconstrained case, and they recover the nonholonomic integrators of [4].

Variational discrete Dirac mechanics

The (+)-discrete Lagrange–d'Alembert–Pontryagin principle is

$$\delta \sum_{k=0}^{N-1} [L_d(q_k, q^+_k) + p_{k+1}(q_{k+1} - q^+_k)] = 0, \tag{3.54}$$

with variations that vanish at the endpoints, i.e. $\delta q_0 = \delta q_N = 0$, and the discrete constraints $(q_k, q_{k+1}) \in \Delta^{d+}_Q$. We also impose the constraint $\delta q_k \in \Delta_Q(q_k)$ after computing variations inside the sum. The variable q^+_k serves as the discrete analog to the introduction of v in the continuous principle.

The (-)-discrete Lagrange-d'Alembert-Pontryagin principle is

$$\delta \sum_{k=0}^{N-1} [L_d(q^-_{k+1}, q_{k+1}) - p_k(q_k - q^-_{k+1})] = 0 \ . \tag{3.55}$$

The variable q^-_k now plays the role of the discrete velocity. Again we take variations that vanish at the endpoints and impose the constraint $\delta q_k \in \Delta_Q(q_k)$. We now impose the discrete constraints $(q_k, q_{k+1}) \in \Delta^{d-}_Q$.

Computing variations of (3.54) yields (3.52). Computing variations for (3.55) yields (3.53) [12]. Thus, in direct analogy with the continuous case, we have

equivalent variational and Dirac structure formulations of discrete Lagrange-Dirac mechanics.

3.3 (+) vs. (-) Discrete Dirac mechanics

Before getting to the interconnected systems results, we say a few words about the distinction between the (+) and (-) formulations of discrete Dirac mechanics laid out in [12]. Later sections will focus on interconnections of (+) discrete Dirac systems as that turns out to be the proper formulation for simulating forward in time.

In their full form, the (+) discrete Dirac equations are only generally solvable for forward time integration (moving forward in index), and the (-) discrete Dirac equations are only generally solvable for backward time integration (moving backward in index). This follows from the implicit function theorem. It also mirrors the case of the augmented approach to holonomic constraints laid out in [15], which has a similar form.

In momentum-matched form, the discrete Dirac equations become

$$\begin{aligned} &D_2L_d(q_{k-1},q_k)+D_1L_d(q_k,q_{k+1})+\mu_a\omega^a(q_k)=0,\ k=1,\dots,N-1\\ &\omega^a_{d\pm}(q_k,q_{k+1})=0, k=0,\dots,N-1. \end{aligned}$$

So the only distinction between the position trajectories of (+) and (-) is, potentially, in the way the constraints are discretized. The two methods generate the same trajectory when

$$\omega^a_{d+}(q_k,q_{k+1})=0 \iff \omega^a_{d-}(q_k,q_{k+1})=0. \tag{3.56}$$

For the retraction based definition of ω^a_{d+} in [12], this requires

$$\omega^a(q_k)\cdot R^{-1}_{q_k}(q_{k+1})=0 \iff \omega^a(q_{k+1})\cdot -R^{-1}_{q_{k+1}}(q_k)=0. \tag{3.57}$$

This holds, for instance, for a base point-independent force and an antisymmetric inverse retraction. For example, an equality constraint between two redundant

variables will be basepoint independent, and the vector space retraction $R_q(v) = q + hv$ has an inverse antisymmetric in (q_k, q_{k+1}).

$$R_{q_k}^{-1}(q_{k+1}) = (q_{k+1} - q_k)/h = -R_{q_{k+1}}^{-1}(q_k). \tag{3.58}$$

If we consider more general discretizations for $\omega_{d\pm}^a$, we could purposefully choose symmetric discretizations so that the (+) and (-) formulations generate the same position trajectories.

3.4 Discrete Dirac interconnections

In this section we present results for interconnecting a finite number of systems on $Q_1, \ldots, Q_n$ to form a system on $Q = Q_1 \times \cdots \times Q_n$. Here and throughout the section, let π_{Q_i} denote the projection from Q onto Q_i and $T\pi_{Q_i}$ denote the tangent lift of π_{Q_i}. In coordinates, we have $q = (q_1, \ldots, q_n), v_q = (q_1, \ldots, q_n, v_{q_1}, \ldots, v_{q_n})$ with $\pi_{Q_i}(q) = q_i$ and $T\pi_{Q_i}(v_q) = (q_i, v_{q_i})$. At the continuous level, we have two equivalent views Dirac interconnections: through variational principles and through preservation of Dirac structures [10]. We always have an interconnection distribution $\Sigma_Q \subset TQ$ describing the interaction between the two systems. We can think of the interconnected system as the system generated variationally by $L(q, \dot{q}) = L^1(T\pi^1(q, \dot{q})) + L^2(T\pi^2(q, \dot{q}))$ and $\Delta_Q = (\Delta_{Q_1} \oplus \Delta_{Q_2}) \cap \Sigma_Q$. To view interconnection in terms of Dirac structure preservation, we write $(X_D, d_D L(q, v)) \in (D_{\Delta_{Q_1}} \oplus D_{\Delta_{Q_2}}) \boxtimes D_{\text{int}}$ for the same Lagrangian. Here D_{int} is a Dirac structure on T^*Q derived from Σ_Q and $\boxtimes$ is the Dirac tensor product defined earlier.

These two views of interconnection are completely equivalent, so that, in particular, $(D_{\Delta_{Q_1}} \oplus D_{\Delta_{Q_2}}) \boxtimes D_{\text{int}} = D_{\Delta_Q}$ for $\Delta_Q = (\Delta_{Q_1} \oplus \Delta_{Q_2}) \cap \Sigma_Q$. We mimic each viewpoint at the discrete level, producing an analogous equivalence between the two.

3.4.1 Interconnecting two discrete Dirac systems variationally through Σ_Q

Suppose we have two systems (L^1, Δ_{Q_1}) and (L^2, Δ_{Q_2}) with configuration manifolds Q_1 and Q_2. Suppose we also have a distribution $\Sigma_Q \subset TQ$ for $Q = Q_1 \times Q_2$ describing the interconnection of systems 1 and 2. Then from [10] we know that the interconnected system is again a Dirac system with Lagrangian $L(q, v) = L^1(q_1, v_1) + L^2(q_2, v_2)$ and distribution $\Delta_Q = (\Delta_{Q_1} \oplus \Delta_{Q_2}) \cap \Sigma_Q$. To discretize any of these systems in the way laid out in [12] we must choose a discretization scheme $L \mapsto L_d$ and a retraction $R : TQ \to Q$. We will assume our discretization scheme is linear in L, i.e. for $L = L^1(T\pi_{Q_1}(q, v)) + L^2(T\pi_{Q_2}(q, v))$ we get $L_d(q_k, q_{k+1}) = L_d^1(q_k^1, q_{k+1}^1) + L_d^2(q_k^2, q_{k+1}^2)$. This is a relatively weak assumption. Schemes for constructing L_d are based on approximating the exact discrete Lagrangian given, with some assumptions on the curve $q(t)$, by

$$L_d^E(q_0, q_1; h) = \int_0^h L(q(t), \dot{q}(t))dt. \tag{3.59}$$

Since the exact discrete Lagrangian is linear in L discretizations are most often linear as well. For instance, discretization based on applying quadrature to the integral in L_d^E will satisfy linearity in L.

Compatible constraint discretizations

The relevant constraint distributions in interconnection are $\Delta_{Q_1}, \ldots, \Delta_{Q_n}$, Σ_Q and $\Delta_Q = (\Delta_{Q_1} \oplus \cdots \oplus \Delta_{Q_n}) \cap \Sigma_Q$. To get equivalence between interconnecting systems before and after discretization, we need to make a particular choice of basis for Δ_Q° and assume a *compatible* constraint discretization, defined below.

From $\Delta_Q = (\Delta_{Q_1} \oplus \cdots \oplus \Delta_{Q_n}) \cap \Sigma_Q$, we have $\Delta_Q^\circ = (\Delta_{Q_1} \oplus \cdots \oplus \Delta_{Q_n})^\circ \cup \Sigma_Q^\circ$. Thus, we can construct a basis for Δ_Q° from the bases of Δ_{Q_i} and Σ_{int}. Let $\{\omega_i^a(q^i)\}_{a=1}^{m_i}$ denote a basis for $\Delta_{Q_i}^\circ(q^i)$. We construct a basis for $(\Delta_{Q_1} \oplus \cdots \oplus \Delta_{Q_n})^\circ(q)$ from the individual bases $\{\omega_i^a(q^i)\}_{a=1}^{m_i}$. Let $\pi_{Q_i}(q) \in Q_i$ denote the i^{th} component projection of $q \in Q$. Define $\tilde{\omega}_i^a(q)$ by $\tilde{\omega}_i^a(q) \cdot v_q = \omega_i^a(\pi_{Q_i}(q)) \cdot T\pi_{Q_i}(v_q)$. Then $\{\{\tilde{\omega}_i^a(q)\}_{a=1}^{m_i}\}_{i=1}^n$ forms a basis for $(\Delta_{Q_1} \oplus \cdots \oplus \Delta_{Q_n})^\circ(q)$. Select a basis

for Σ_Q as $\Sigma_Q^\circ(q) = \text{span}\{\alpha^b(q)\}_{b=1}^l$. Then $\Delta_Q^\circ(q) = \text{span}\{\tilde{\omega}_i^a(q), \alpha^b(q)\}$ (with the appropriate ranging of indices). This will always be our chosen basis for Δ_Q°.

We will call a constraint discretization *compatible* if

$$\tilde{\omega}_{d+,i}^a(q_k, q_{k+1}) = \omega_{d+,i}^a(q_k^i, q_{k+1}^i). \tag{3.60}$$

We use the notation q_k^i to mean the i^{th} portion at the k^{th} time-step. So the full coordinate at t_k is $q_k = (q_k^1, \ldots, q_k^n)$ with $q_k^i \in Q_i$. For retraction-based discretizations, we make use of the following lemma.

Lemma 1. For $R_1, \ldots, R_n$ retractions on $Q_1, \ldots, Q_n$, $R_1 \times \cdots \times R_n$ is a retraction on $Q = Q_1 \times \cdots \times Q_n$.

Compatibility of retraction-based discretizations requires the use of $R_1 \times R_2$ as the retraction on $Q = Q_1, \ldots, Q_n$.

Discrete interconnections using compatible constraint discretizations

Discretizing individual systems before interconnection yields

$$p_{k+1}^i = D_2 L_d^i(q_k^i, q_{k+1}^i), \tag{3.61a}$$

$$p_k^i = -D_1 L_d^i(q_k^i, q_{k+1}^i) + \mu_a \omega_i^a(q_k^i), \tag{3.61b}$$

$$\omega_{d+,i}^a(q_k^i, q_{k+1}^i) = 0,\ a = 1, \ldots, m. \tag{3.61c}$$

Here L_d^i have been discretized according to some scheme linear in L, and

$$\omega_{d+,i}^a(q_k^i, q_{k+1}^i) = \omega^a(q_k)(R_{i,q_k^i}^{-1}(q_{k+1}^i)). \tag{3.62}$$

As above, take $\Sigma_Q^\circ(q) = \text{span}\{\alpha^b(q)\}_{b=1}^l$, so each $\alpha^b(q) \in T_q^*Q$. Define $\alpha_i^b(q) \in T^*Q_i$ by $\alpha_i^b(q) \cdot v_{q_i} = \alpha^b(q) \cdot v_{q_i}^h$ for $v_{q_i}^h$ the horizontal lift of v_{q_i}. To interconnect the discrete systems above, we need to append an $\alpha_i^b(q)$ term to each p_k^i calculation and α_{d+}^b terms to whole set. That is, the interconnected system is

$$p_{k+1}^i = D_2 L_d^i(q_k^i, q_{k+1}^i), \tag{3.63a}$$

$$p_k^i = -D_1 L_d^i(q_k^i, q_{k+1}^i) + \mu_a \omega_i^a(q_k^i) + \lambda_b \alpha_i^b(q_k), \tag{3.63b}$$

$$\omega_{d+,i}^a(q_k^i, q_{k+1}^i) = 0,\ a = 1, \ldots, m_i, \tag{3.63c}$$

$$\alpha_{d+}^b(q_k, q_{k+1}) = 0,\ b = 1, \ldots, l. \tag{3.63d}$$

Note that all of the α terms depend on the entire coordinate $q_k = (q_k^1, \ldots, q_k^n)$, not just on the i^{th} section q_k^i.

Theorem 5. Assume $\phi : L \to L_d$ is linear and the constraint discretization is compatible. Then the discretely interconnected equations (3.63a)-(3.63d) are equivalent to the discrete (+)-Dirac equations for $(L, \Delta_Q) = (L^1 + \cdots + L^n, (\Delta_{Q_1} \oplus \cdots \oplus \Delta_{Q_n}) \cap \Sigma_Q)$.

Proof. We just have to look at the discretization of (L, Δ_Q) by components. The discretization of the monolithic system using ϕ and R yields the usual (+)-discrete Dirac equations,

$$p_{k+1} = D_2 L_d(q_k, q_{k+1}), \tag{3.64a}$$

$$p_k = -D_1 L_d(q_k, q_{k+1}) + \eta_c \beta^c(q_k), \tag{3.64b}$$

$$\beta^c_{d+}(q_k, q_{k+1}) = 0 \ \forall \ c. \tag{3.64c}$$

From our assumptions on ϕ, the first equation splits to give equation (3.63a).

In this notation, $\{\beta^c(q_k)\}_c$ are some basis for $\Delta_Q^\circ(q_k) = ((\Delta_{Q_1} \oplus \cdots \oplus \Delta_{Q_n}) \cap \Sigma_Q)^\circ$. Choosing the appropriate basis leads to equations (3.63b)-(3.63d). As above, define $\beta_i^c(q) \in T^*Q_i$ by $\beta_i^c(q) \cdot v_{q_i} = \beta^c(q) \cdot v_{q_i}^h$ for $v_{q_i}^h$ the horizontal lift of v_{q_i}. Then equation (3.64b) splits as

$$p_k^i = -D_1 L_d^i(q_k^i, q_{k+1}^i) + \eta_c \beta_i^c(q_k). \tag{3.65}$$

Taking the basis defined above, we have $\{\beta^c\} = \{\tilde{\omega}_i^a(q), \alpha^b(q)\}$, so equation (3.65) becomes equation (3.63b). Assume we construct β^c_{d+} via a compatible discretization. Then equation (3.64c) accounts for equations (3.63c) and (3.63d) $\square$

Thus, given a finite number of systems (L^i, Δ_{Q_i}) together with interconnection constraints Σ_Q, we have shown how to interconnect the discrete systems generated by $(L_d^i, \Delta_{Q_i}^{d+}, \Delta_{Q_i}^\circ)$ through $\Sigma_Q^{d+}, \Sigma_Q^\circ$ to give the discretization of the fully interconnected system.

3.4.2 Discrete interconnections as a product on discrete Dirac structures

To mimic the continuous case, we would like to say that this discrete interconnection process corresponds to a discrete Dirac tensor product on discrete Dirac structures. That is, we would like for the discretization of the interconnected system, which can be expressed as $(X_d^k, \mathfrak{D}^+ L_d(q_k, q_k^+)) \in D_{\Delta_Q}^{d+}$, to be equivalently expressed as $(X_d^k, \mathfrak{D}^+ L_d(q_k, q_k^+)) \in (D_{\Delta_{Q_1}}^{d+} \oplus D_{\Delta_{Q_2}}^{d+}) \boxtimes_d D_{\text{int}}^{d+}$ for D_{int}^{d+} defined from Σ_Q, some definition of $\boxtimes_d$, and the appropriate notion of $\oplus$.

The direct sum of induced discrete Dirac structures

The definition of $\oplus$ for induced discrete Dirac structures is relatively obvious. We make it precise in this section to ensure that the convenient properties of using $\oplus$ on induced Dirac structures carry over to the discrete setting. Suppose, again, that $Q = Q_1 \times Q_2$ and that we have two constraint distributions $\Delta_{Q_1} \subset TQ_1$ and $\Delta_{Q_2} \subset TQ_2$. We can derive each distribution from its annihilator as $\Delta_{Q_i}(q_i) = \cap_a \ker(\omega_i^a(q_i))$ for $\{\omega_i^a(q_i)\}_a$ a basis for $\Delta_{Q_i}^\circ(q_i)$. The direct sum distribution on Q has annihilator given by $(\Delta_{Q_1} \oplus \Delta_{Q_2})^\circ = \Delta_{Q_1}^\circ \oplus \Delta_{Q_2}^\circ$, so we can construct a basis for it by extending the bases of $\Delta_{Q_i}^\circ$. As in the last section, we use $\pi_{Q_i} : Q \to Q_i$ to denote component projections from Q. To extend ω_i^a we denote by $\tilde{\omega}_i^a$ the one form on Q such that $\tilde{\omega}_i^a(q) \cdot v_q = \omega_i^a(\pi_{Q_i}(q)) \cdot T\pi_{Q_i}(v_q)$. In coordinates $\tilde{\omega}_1^a = (\omega_1^a, 0)$ and $\tilde{\omega}_2^b = (0, \omega_2^b)$. Then the distribution $\Delta_{Q_1} \oplus \Delta_{Q_2}$ has a local expression as $(\Delta_{Q_1} \oplus \Delta_{Q_2})(q) = [\cap_a \ker(\tilde{\omega}_1^a(q))] \cap [\cap_b \ker(\tilde{\omega}_2^b(q))]$.

The direct sum of continuous Dirac structures $D_{\Delta_{Q_1}}$ and $D_{\Delta_{Q_2}}$ is given by $D_{\Delta_{Q_1}} \oplus D_{\Delta_{Q_2}} = D_{\Delta_{Q_1} \oplus \Delta_{Q_2}}$. Fiber-wise, this is given by

$$(D_{\Delta_{Q_1}} \oplus D_{\Delta_{Q_2}})(q,p) = D_{\Delta_{Q_1}}(T^* i_{Q_1}(q,p)) \oplus D_{\Delta_{Q_2}}(T^* i_{Q_2}(q,p)), \tag{3.66}$$

where $i_{Q_i} : Q_i \hookrightarrow Q$ is the inclusion and $T^* i_{Q_i}$ its tangent lift. In coordinates,

$$\begin{aligned} \{(v,\alpha) =& (v_1, v_2, \alpha_1, \alpha_2) \in T_{(q_1,q_2,p_1,p_2)} T^*Q \mid (v_1, \alpha_1) \in D_{\Delta_{Q_1}}(q_1, p_1) \\ & \text{and } (v_2, \alpha_2) \in D_{\Delta_{Q_2}}(q_2, p_2)\}. \end{aligned} \tag{3.67}$$

We mimic this coordinate expression at the discrete level with the following definition.

Definition 3. Given two discrete induced Dirac structures $D^{d+}_{\Delta_{Q_1}} \subset (T^*Q_1 \times T^*Q_1) \times T^*(Q_1 \times Q_1^*)$ and $D^{d+}_{\Delta_{Q_2}} \subset (T^*Q_2 \times T^*Q_2) \times T^*(Q_2 \times Q_2^*)$, define their direct sum $D^{d+}_{\Delta_{Q_1}} \oplus D^{d+}_{\Delta_{Q_2}} \subset (T^*Q \times T^*Q) \times T^*(Q \times Q^*)$ coordinate-wise as

$$\begin{aligned} D^{d+}_{\Delta_{Q_1}} \oplus D^{d+}_{\Delta_{Q_2}} = \{((z,z+),\alpha_{\hat{z}}) \mid ((q_1,p_1,q_1^+,p_1^+),(q_1,p_1^+,\alpha_{q_1},\alpha_{p_1})) \in D^{d+}_{\Delta_{Q_1}} \\ \text{and } ((q_2,p_2,q_2^+,p_2^+),(q_2,p_2^+,\alpha_{q_2},\alpha_{p_2})) \in D^{d+}_{\Delta_{Q_2}}\} \end{aligned} \tag{3.68}$$

Here we've partitioned the coordinates as

$$(z,z^+) = (q,p,q^+,p^+) = (q_1,q_2,p_1,p_2,q_1^+,q_2^+,p_1^+,p_2^+) \tag{3.69}$$

and

$$\alpha_{\hat{z}} = (q,p^+,\alpha_q,\alpha_p) = (q_1,q_2,p_1^+,p_2^+,\alpha_{q_1},\alpha_{q_2},\alpha_{p_1},\alpha_{p_2}). \tag{3.70}$$

We also make the following straightforward definition of the direct sum of two discrete constraint distributions.

Definition 4. The direct sum of two discrete Dirac structures is given by

$$\begin{aligned} \Delta^{d+}_{Q_1} \oplus \Delta^{d+}_{Q_2} = \{(q_1,&q_2,q_1^+,q_2^+) \in Q \times Q \mid \\ &(q_1,q_1^+) \in \Delta^{d+}_{Q_1} \text{ and } (q_2,q_2^+) \in \Delta^{d+}_{Q_2}\}. \end{aligned} \tag{3.71}$$

We have the following useful lemma.

Lemma 2. Assume we use the same separable discretization scheme to construct $\omega^a_{1,d+}$, $\omega^b_{2,d+}$, $\tilde{\omega}^a_{1,d+}$, and $\tilde{\omega}^b_{2,d+}$. Then $\Delta^{d+}_{Q_1} \oplus \Delta^{d+}_{Q_2} = (\Delta_{Q_1} \oplus \Delta_{Q_2})^{d+}$ and $D^{d+}_{\Delta_{Q_1}} \oplus D^{d+}_{\Delta_{Q_2}} = D^{d+}_{\Delta_{Q_1} \oplus \Delta_{Q_2}}$. Thus, $D^{d+}_{\Delta_{Q_1}} \oplus D^{d+}_{\Delta_{Q_2}}$ is again a discrete induced Dirac structure.

Proof. We have

$$\begin{aligned} (\Delta_{Q_1} \oplus \Delta_{Q_2})^{d+} = \{(q,q^+) \in Q \times Q \mid \tilde{\omega}^a_{1,d+}(q,q^+) = 0 \text{ and} \\ \tilde{\omega}^b_{2,d+}(q,q^+) = 0 \text{ for all } a,b\} \end{aligned} \tag{3.72}$$

and

$$\Delta^{d+}_{Q_i} = \{(q_i,q_i^+) \in Q_i \times Q_i \mid \omega^a_{i,d+}(q_i,q_i^+) = 0 \ \forall a\}. \tag{3.73}$$

By our assumptions, $\tilde{\omega}^a_{i,d+}(q,q^+) = \omega^a_{i,d+}(q_i,q_i^+)$. Thus, $\Delta^{d+}_{Q_1} \oplus \Delta^{d+}_{Q_2} = (\Delta_{Q_1} \oplus \Delta_{Q_2})^{d+}$.

To prove $D^{d+}_{\Delta_{Q_1}} \oplus D^{d+}_{\Delta_{Q_2}} = D^{d+}_{\Delta_{Q_1}\oplus\Delta_{Q_2}}$ we need to show that the conditions

$$(q,q^+) \in (\Delta_{Q_1} \oplus \Delta_{Q_2})^{d+} \tag{3.74}$$

and

$$(q,p^+,\alpha_q - p, \alpha_p - q^+) \in \{(q,p,\beta,0) \mid \beta dq \in (\Delta_{Q_1} \oplus \Delta_{Q_2})^\circ(q)\} \tag{3.75}$$

are equivalent to the conditions

$$((q_1,p_1,q_1^+,p_1^+),(q_1,p_1^+,\alpha_{q_1},\alpha_{p_1})) \in D^{d+}_{\Delta_{Q_1}} \tag{3.76}$$

and

$$((q_2,p_2,q_2^+,p_2^+),(q_2,p_2^+,\alpha_{q_2},\alpha_{p_2})) \in D^{d+}_{\Delta_{Q_2}}. \tag{3.77}$$

Using $\Delta^{d+}_{Q_1} \oplus \Delta^{d+}_{Q_2} = (\Delta_{Q_1} \oplus \Delta_{Q_2})^{d+}$, the distribution conditions implied by (3.76) and (3.77) are equivalent to (3.74). From (3.76) and (3.77) we also have

$$(q_1,p_1^+,\alpha_{q_1} - p_1, \alpha_{p_1} - q_1^+) \in \{(q_1,p_1,\beta,0) \mid \beta dq \in \Delta^\circ_{Q_1}\} \tag{3.78}$$

and

$$(q_2,p_2^+,\alpha_{q_2} - p_2, \alpha_{p_2} - q_2^+) \in \{(q_2,p_2,\beta,0) \mid \beta dq \in \Delta^\circ_{Q_2}\}. \tag{3.79}$$

Thus, $(\alpha_{p_1},\alpha_{p_2}) - (q_1^+,q_2^+) = 0$. From $\alpha_{q_i} - p_i \in \text{span}\{\omega^a_i(q_i)\}$ we have $(\alpha_{q_1} - p_1, 0) \in \text{span}\{\tilde{\omega}^a_1(q)\}$ and $(0,\alpha_{q_2} - p_2) \in \text{span}\{\tilde{\omega}^b_2(q)\}$. Thus, we have $(\alpha_{q_1} - p_1, \alpha_{q_2} - p_2) \in \text{span}\{\tilde{\omega}^a_1(q), \tilde{\omega}^b_2\}$, i.e. $\alpha_q - p \in (\Delta_{Q_1} \oplus \Delta_{Q_2})^\circ$. Hence, conditions (3.76) and (3.77) also give (3.75).

Performing the same checks from the reversed point of view, we can derive (3.76) and (3.77) from (3.74) and (3.75), proving that $D^{d+}_{\Delta_{Q_1}} \oplus D^{d+}_{\Delta_{Q_2}} = D^{d+}_{\Delta_{Q_1}\oplus\Delta_{Q_2}}$. □

For continuous distributions Δ_1 and Δ_2, a similar set of checks shows that

$$\Delta_1^{d+} \cap \Delta_2^{d+} = (\Delta_1 \cap \Delta_2)^{d+}. \tag{3.80}$$

Defining D^{d+}_{int} and $\boxtimes_d$

We begin by defining D^{d+}_{int}. The distribution Σ_Q defines the interconnection constraints on $Q = Q_1 \times Q_2$. Lift Σ_Q to TT^*Q, defining $\Sigma_{\text{int}} = (T\pi)^{-1}(\Sigma_Q)$. Then the continuous interaction Dirac structure is induced by Σ_{int} and $\Omega_{\text{int}} \equiv 0$. To discretize this construction, we define $\Omega^{d+}_{\text{int}}(q, p, q^+, p^+) = (q, p^+, 0, 0)$.

Definition 5. We defined the *standard discrete interaction Dirac structure* to be

$$D^{d+}_{\text{int}} = \{((z, z^+), \alpha_{\hat{z}}) \mid (z, z^+) \in \Sigma^{d+}_{\text{int}}, \alpha_{\hat{z}} - \Omega^{d+}_{\text{int}}(z, z^+) \in \Sigma^{\circ}_{Q\times Q^*}\}(q) \tag{3.81}$$

for $\Omega^{d+}_{\text{int}}(q, p, q^+, p^+) = (q, p^+, 0, 0)$.

Here, as in the original definitions of the discrete Dirac structures, $z = (q, p), z^+ = (q^+, p^+), \hat{z} = (q, p^+)$. This discrete Dirac structure mirrors the induced discrete Dirac structure of [12] with $\Omega^{\flat}_{d\pm}$ replaced by Ω^{d+}_{int}.

Recall, again, the continuous definition of $\boxtimes$.

Definition 6. [10] Let $D_a, D_b \in \text{Dir}(M)$ [i.e. D_a and D_b are Dirac structures on M]. We define the Dirac tensor product

$$\begin{aligned} D_a \boxtimes D_b = \{(v, \alpha) \in & TM \oplus T^*M \mid \exists \beta \in T^*M \text{ such that} \\ & (v, \alpha + \beta) \in D_a, (v, -\beta) \in D_b\}. \end{aligned} \tag{3.82}$$

Mimicking this definition at the discrete level, we define $\boxtimes_d$ as follows.

Definition 7. Define the operation $\boxtimes_d$ on two discrete Dirac structures D_1 and D_2 by

$$\begin{aligned} D_1 \boxtimes D_2 = \{((z, z^+), & \alpha_{\hat{z}}) \mid \exists \beta_{\hat{z}} \in T^*_{\hat{z}}(Q \times Q^*) \\ & \text{with}((z, z^+), \alpha_{\hat{z}} + \beta_{\hat{z}}) \in D_1, ((z, z^+), -\beta_{\hat{z}}) \in D_2\}, \end{aligned} \tag{3.83}$$

where $\beta_{\hat{z}} = (q, p^+, \beta_q, \beta_{p^+}), \alpha_{\hat{z}} = (q, p^+, \alpha_q, \alpha_{p^+}), \alpha_{\hat{z}} + \beta_{\hat{z}} = (q, p^+, \alpha_q + \beta_q, \alpha_{p^+} + \beta_{p^+}), -\beta_{\hat{z}} = (q, p^+, -\beta_q, -\beta_{p^+})$.

Discrete interconnections via Dirac structures

With these definitions in place, we now have the tools to state the main result.

Theorem 6. Given two discrete Dirac structures $D^{d+}_{\Delta_{Q_1}}$ and $D^{d+}_{\Delta_{Q_2}}$ generated from $\Delta_{Q_1} \subset TQ_1$ and $\Delta_{Q_2} \subset TQ_2$ and an interconnection distribution $\Sigma_Q \subset TQ = T(Q_1 \times Q_2)$,

$$(D^{d+}_{\Delta_{Q_1}} \oplus D^{d+}_{\Delta_{Q_2}}) \boxtimes_d D^{d+}_{\text{int}} = D^{d+}_{\Delta_Q} \tag{3.84}$$

for $\Delta_Q = (\Delta_{Q_1} \oplus \Delta_{Q_2}) \cap \Sigma_Q$.

Thus, the statement $(X^k_d, \mathfrak{D}^+ L_d(q_k, q^+_k)) \in (D^{d+}_{\Delta_{Q_1}} \oplus D^{d+}_{\Delta_{Q_2}}) \boxtimes_d D^{d+}_{\text{int}}$ is equivalent to the statement $(X^k_d, \mathfrak{D}^+ L_d(q_k, q^+_k)) \in D^{d+}_{\Delta_Q}$ and to the interconnected equations given in (3.63a)-(3.63d).

Proof. First we recall the definition of a (+)-discrete induced Dirac structure,

$$\begin{aligned} D^{d+}_{\Delta_Q} = \{((z, z^+), \alpha_{\hat{z}}) \in (T^*Q \times T^*Q) \times T^*(Q \times Q^*) \mid \\ (z, z^+) \in \Delta^{d+}_{T^*Q}, \alpha_{\hat{z}} - \Omega^\flat_{d+}(z, z^+) \in \Delta^\circ_{Q \times Q^*}\}. \end{aligned} \tag{3.85}$$

For $Q = Q_1 \times Q_2$ we can write $z = (z_1, z_2)$, $z^+ = (z^+_1, z^+_2)$, $\hat{z} = (\hat{z}_1, \hat{z}_2)$, and $\alpha_{\hat{z}} = (\alpha_{\hat{z}_1}, \alpha_{\hat{z}_2})$. Then

$$\begin{aligned} D^{d+}_{\Delta_{Q_1}} \oplus D^{d+}_{\Delta_{Q_2}} = \{((z, z^+), \alpha_{\hat{z}}) \mid ((z_1, z^+_1), \alpha_{\hat{z}_1}) \in D^{d+}_{\Delta_{Q_1}} \\ \text{and } ((z_2, z^+_2), \alpha_{\hat{z}_2}) \in D^{d+}_{\Delta_{Q_2}}\} \end{aligned} \tag{3.86}$$

and

$$\begin{aligned} (D^{d+}_{\Delta_{Q_1}} \oplus D^{d+}_{\Delta_{Q_2}}) \boxtimes_d D^{d+}_{\text{int}} = \{((z, z^+), \alpha_{\hat{z}}) \mid \exists \beta_{\hat{z}} \in T^*_{\hat{z}}(Q \times Q^*) \text{ with} \\ ((z, z^+), \alpha_{\hat{z}} + \beta_{\hat{z}}) \in D^{d+}_{\Delta_{Q_1}} \oplus D^{d+}_{\Delta_{Q_2}}, ((z, z^+), -\beta_{\hat{z}}) \in D^{d+}_{\text{int}}\}. \end{aligned} \tag{3.87}$$

From the first condition we have $((z_1, z^+_1), \alpha_{\hat{z}_1} + \beta_{\hat{z}_1}) \in D^{d+}_{\Delta_{Q_1}}$ and $((z_2, z^+_2), \alpha_{\hat{z}_2} + \beta_{\hat{z}_2}) \in D^{d+}_{\Delta_{Q_2}}$.

Consider the distribution conditions first. The distribution condition for $D^{d+}_{\Delta_Q}$ is that $(z, z^+) \in \Delta^{d+}_{T^*Q}$. We can break the distribution condition down as

$$\begin{aligned} ((q, p), (q^+, p^+)) &\in \{((q, p), (q^+, p^+)) \in T^*Q \times T^*Q \mid (q, q^+) \in \Delta^{d+}_Q\} \\ &= \{((q, p), (q^+, p^+)) \mid (q, q^+) \in (\Delta^{d+}_{Q_1} \oplus \Delta^{d+}_{Q_2}) \cap \Sigma^{d+}_Q\} \\ &= \{((q, p), (q^+, p^+)) \mid (q, q^+) \in \Sigma^{d+}_Q, (q_1, q^+_1) \in D^{d+}_{\Delta_{Q_1}}, \\ &\qquad \text{and } (q_2, q^+_2) \in D^{d+}_{\Delta_{Q_2}}\}. \end{aligned} \tag{3.88}$$

We now derive the distribution condition from $((z,z^+),\alpha_{\hat{z}}) \in (D^{d+}_{\Delta_{Q_1}} \oplus D^{d+}_{\Delta_{Q_2}}) \boxtimes_d D^{d+}_{\text{int}}$. From $((z_1,z_1^+),\alpha_{\hat{z}_1}+\beta_{\hat{z}_1}) \in D^{d+}_{\Delta_{Q_1}}$ and $((z_2,z_2^+),\alpha_{\hat{z}_2}+\beta_{\hat{z}_2}) \in D^{d+}_{\Delta_{Q_2}}$, we get $(q_1,q_1^+) \in D^{d+}_{\Delta_{Q_1}}$ and $(q_2,q_2^+) \in D^{d+}_{\Delta_{Q_2}}$. From $((z,z^+),-\beta_{\hat{z}}) \in D^{d+}_{\text{int}}$ we have $(q,q^+) \in \Sigma^{d+}_Q$. Thus, the distribution conditions derived from $((z,z^+),\alpha_{\hat{z}}) \in D^{d+}_{\Delta_Q}$ and $((z,z^+),\alpha_{\hat{z}}) \in (D^{d+}_{\Delta_{Q_1}} \oplus D^{d+}_{\Delta_{Q_2}}) \boxtimes_d D^{d+}_{\text{int}}$ are equivalent.

Now we consider the second condition, coming from $\alpha_{\hat{z}} - \Omega^\flat_{d+}(z,z^+) \in \Delta^\circ_{Q\times Q^*}$ in the general definition. Recalling the definitions of $\Delta^\circ_{Q\times Q^*}$, $\hat{z}=(q,p^+)$, and $\Omega^\flat_{d+}(z,z^+)=(q,p^+,p,q^+)$ gives

$$(q,p^+,\alpha_q,\alpha_{p^+}) - (q,p^+,p,q^+) \in \{(q,p,\alpha_q,0) \in T^*(Q\times Q^*) \mid \alpha_q dq \in \Delta^\circ_Q(q)\}. \tag{3.89}$$

In the case of $\Delta_Q = (\Delta_{Q_1} \oplus \Delta_{Q_2}) \cap \Sigma_Q$ we can rewrite this condition explicitly as

$$\alpha_q - p \in [(\Delta_{Q_1} \oplus \Delta_{Q_2}) \cap \Sigma_Q]^\circ(q_0), \tag{3.90}$$

$$\alpha_{p^+} - q^+ = 0. \tag{3.91}$$

Now consider the statement $((z,z^+),\alpha_{\hat{z}}) \in (D^{d+}_{\Delta_{Q_1}} \oplus D^{d+}_{\Delta_{Q_2}}) \boxtimes_d D^{d+}_{\text{int}}$. First examine $((z,z^+),-\beta_{\hat{z}}) \in D^{d+}_{\text{int}}$. This implies that $-\beta_{\hat{z}} - \Omega^{d+}_{\text{int}}(z,z^+) \in \Sigma^\circ_{Q\times Q^*}$, i.e. $(q,p^+,-\beta_q,-\beta_{p^+}) \in \{(q,p,\alpha_q,0) | \alpha_q dq \in \Sigma^\circ_Q(q)\}$. Thus, we must have $-\beta_{p^+}=0$ and $-\beta_q \in \Sigma^\circ_Q(q)$. Now we examine $((z,z^+),\alpha_{\hat{z}}+\beta_{\hat{z}}) \in D^{d+}_{\Delta_{Q_1}} \oplus D^{d+}_{\Delta_{Q_2}}$. From the subsection above, we then have that $((z_i,z_i^+),\alpha_{\hat{z}_i}+\beta_{\hat{z}_i}) \in D^{d+}_{\Delta_{Q_i}}$ which gives the conditions

$$(q_i,p_i^+,\alpha_{q_i}+\beta_{q_i}-p_i,\alpha_{p_i^+}+\beta_{p_i^+}-q_i^+) \in \{(q,p,\alpha,0) | \alpha dq \in \Delta^\circ_{Q_i}\}. \tag{3.92}$$

We already know that $\beta_{p^+}=0$, so these conditions become

$$\alpha_{p_i^+} - q_i^+ = 0, \tag{3.93}$$

$$\alpha_{q_i} + \beta_{q_i} - p_i \in \Delta^\circ_{Q_i}. \tag{3.94}$$

Putting the two indices together gives

$$\alpha_{p^+} - q^+ = 0, \tag{3.95}$$

$$\alpha_q - p + \beta_q \in \Delta^\circ_{Q_1} \oplus \Delta^\circ_{Q_2}. \tag{3.96}$$

We've already established that $\beta_q \in \Sigma_Q^\circ(q)$, so (3.96) becomes

$$\alpha_q - p \in (\Delta_{Q_1}^\circ \oplus \Delta_{Q_2}^\circ)(q) \cup \Sigma_Q^\circ(q), \tag{3.97}$$

i.e.

$$\alpha_q - p \in [(\Delta_{Q_1} \oplus \Delta_{Q_2}) \cap \Sigma_Q]^\circ(q). \tag{3.98}$$

Thus, we derive precisely the same conditions from both $D_{\Delta_Q}^{d+}$ and $(D_{\Delta_{Q_1}}^{d+} \oplus D_{\Delta_{Q_2}}^{d+}) \boxtimes_d D_{\text{int}}^{d+}$ and the two structures are equivalent. □

We have now shown that we can interconnect discrete Dirac systems in a way consistent with the variational discretization of the full system and that the Dirac structure preserved by the interconnected discrete system can be viewed as a product of $D_{\Delta_{Q_1}}^{d+} \oplus D_{\Delta_{Q_2}}^{d+}$ with a discrete interaction Dirac structure, analogous to the continuous case. In defining D_{int}^{d+}, we have extended the notion of discrete Dirac structures beyond the induced structures of [12]. This extension as well as the definition of $\boxtimes_d$, which is agnostic to whether its operands are induced structures, raises the question of whether we can make a more general definition of discrete Dirac structures for which induced structures are just a special case. We discuss this more in the future work section below.

3.5 Numerical Examples

Continuing the theme of reproducing [10] discretely, we now work through the simulation of some of the interconnected examples presented there. We will rehash the setup of each example.

3.5.1 A chain of spring masses

The first example is a chain of three spring masses attached to a wall. We consider it to be the interconnection of a chain of two spring masses with the third spring/mass pair. Thus we have two primitive systems with configuration spaces $Q_1 = Q_2 = \mathbb{R}^2$. The first system has coordinates (q_1, q_2), the second $(\bar{q}_2, q_3)$. Figures 3.1 and 3.2 illustrate these two viewpoints. Note that in the torn case we introduce an extra variable, $\bar{q}_2$, to mark the position of the left end of the spring.

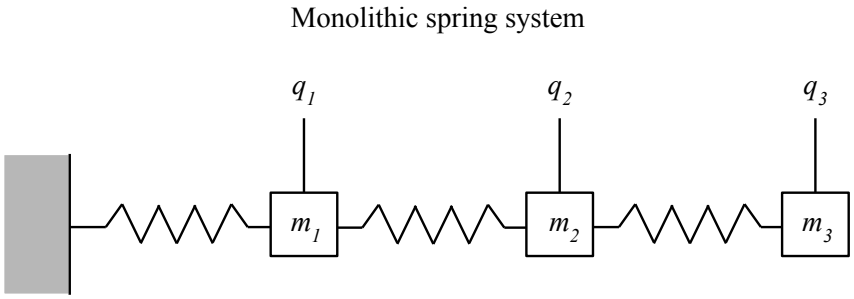

Figure 3.1: A chain of spring masses like that presented in [10].

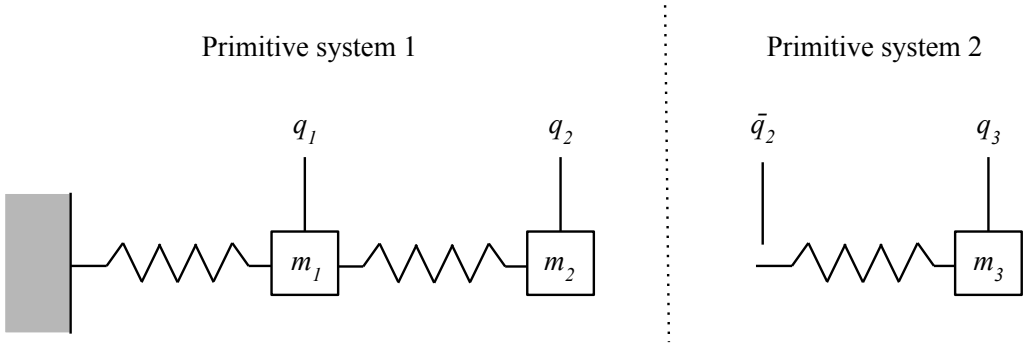

Figure 3.2: The chain of springs as two primitive systems [10].

Viewed separately, the two primitive systems each have the trivial constraint distribution $\Delta_{Q_i} = TQ_i$ and Lagragians

$$L_1(q_1, q_2, v_1, v_2) = \frac{1}{2}m_1 v_1^2 + \frac{1}{2}m_2 v_2^2 - \frac{1}{2}k_1 q_1^2 - \frac{1}{2}k_2(q_2 - q_1)^2 \tag{3.99}$$

and

$$L_2(\bar{q}_2, q_3, \bar{v}_2, v_3) = \frac{1}{2}m_3 v_3^2 - \frac{1}{2}(q_3 - \bar{q}_2)^2. \tag{3.100}$$

To interconnect the systems into the chain in Figure 3.1, we need to enforce the constraint $q_2 = \bar{q}_2$. This is a holonomic constraint, but within the framework of Dirac systems we enforce it with a compatible initial condition and a distribution constraint $\Sigma_{\text{int}}(q) = \{v \in T_qQ \mid v_2 = \bar{v}_2\}$. Thus $\Sigma_{\text{int}}^\circ = \text{span}\{\omega\}$ for $\omega = dq_2 - d\bar{q}_2 \in T_q^*Q$. In coordinates $\omega = (0, 1, -1, 0)$.

We discretized both the simple chain of springs in Figure 3.1 and the interconnected version described above using the retraction-based methodology laid out in [12] and used in the circuit example therein. Namely, we choose the vector space retraction $R_q(v) = q + vh$ for h the timestep, giving $R_{q_0}^{-1}(q_1) = \frac{1}{h}(q_1 - q_0)$. Then we set

$$L_d(q_k, q_{k+1}) = hL(q_k, R_{q_k}^{-1}(q_{k+1})), \tag{3.101}$$

$$\omega_{d+}(q_k, q_{k+1}) = \langle \omega(q_k), R_{q_k}^{-1}(q_{k+1}) \rangle. \tag{3.102}$$

Figures 3.3 through 3.6 show the results of this numerical experiment.

Figures 3.3 and 3.4 compare the interconnected discretization with the discretization of the full system. Note that we are more concerned with reproducing the behavior of the full discretization than with the overall accuracy of the simulation. We have excellent agreement between the two discretizations, with the interconnected results obscuring the full discretization in the figures by lying directly on top. It is also difficult to distinguish in Figure 3.3 between the trajectories of q_2 and $\bar{q}_2$. This is because, as shown in Figure 3.5, the interconnected discretization preserves the $q_2 = \bar{q}_2$ constraint to machine precision. Thus, the trajectories lie atop one another in Figure 3.3. Figure 3.4 shows good agreement between the energy of the full system discretization and that of the interconnected discretization. Lastly, Figure 3.6 shows that the interconnected discretization exhibits the oscillatory energy behavior characteristic of variational integrators.

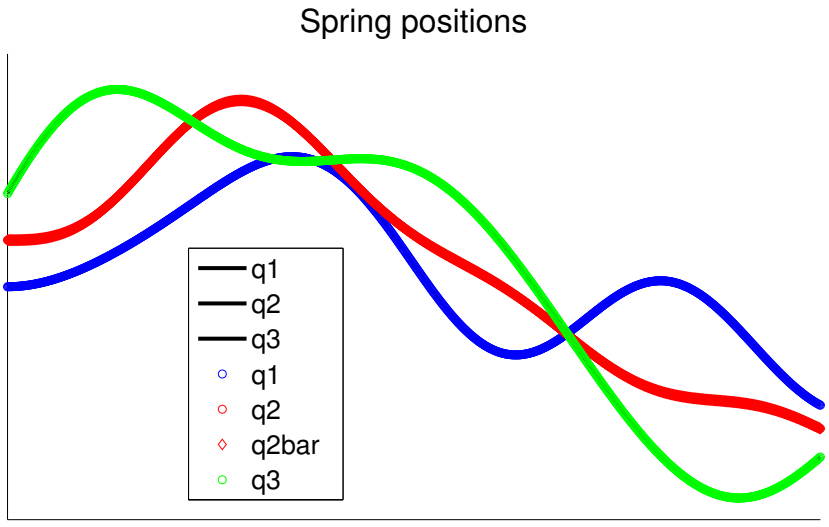

Figure 3.3: A comparison of spring positions over time. Solutions from discretizing the full system are plotted as lines. Solutions from discretizing as two interconnected systems are plotted as hollow shapes. The shapes lie directly over the lines.

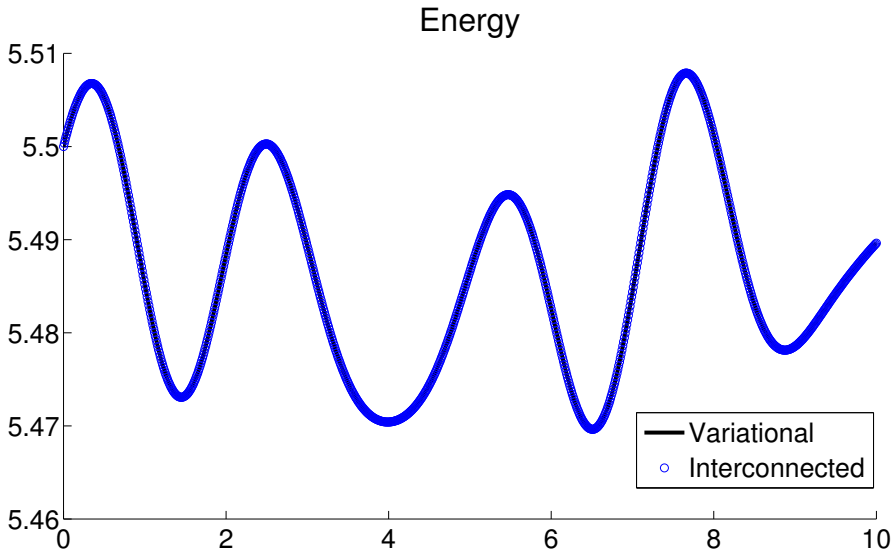

Figure 3.4: A comparison of the spring system energy over time. The line labeled "variational" is the energy of the full-system discretization. The hollow circles show the energy for the discretization as two interconnected systems. The hollow circles lie directly on top of the line. Note also the small scale of the vertical axis.

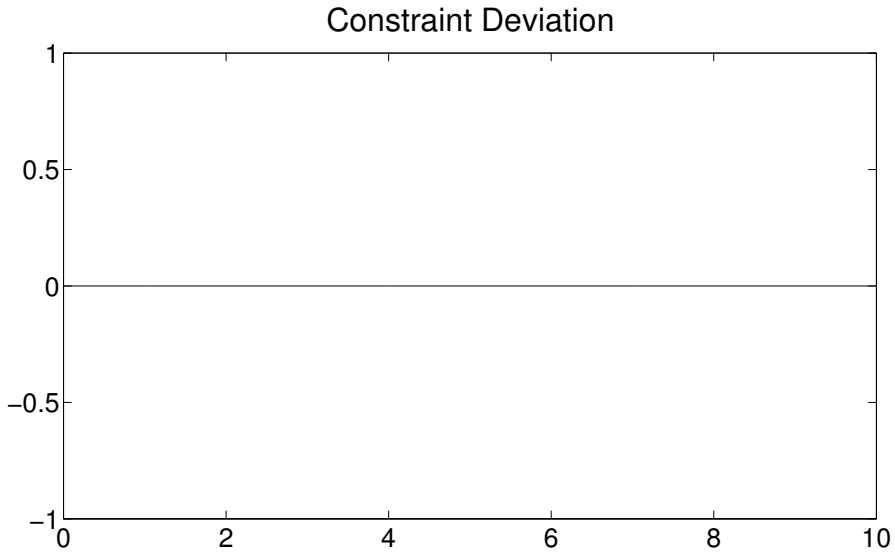

Figure 3.5: Deviation of the interconnected discretization from the constraint $q_2 = \bar{q}_2$ over time. We see that the constraint is preserved to machine precision.

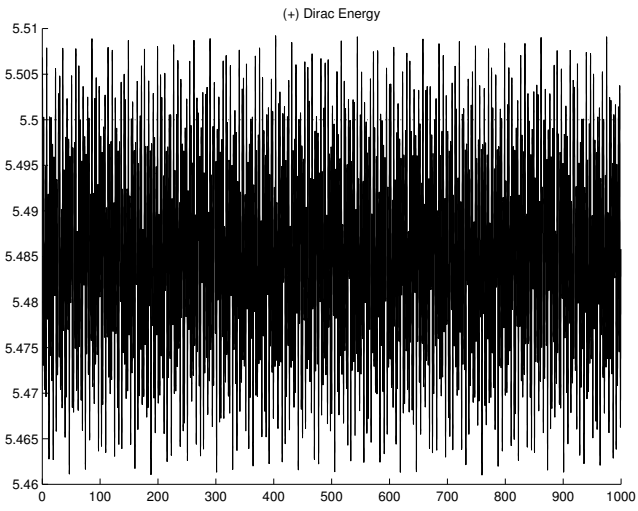

Figure 3.6: The interconnected discretization's energy oscillates over very long times, much like the energy of classical variational discretization.

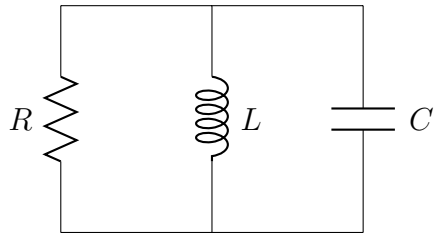

Figure 3.7: A simple parallel RLC circuit [10].

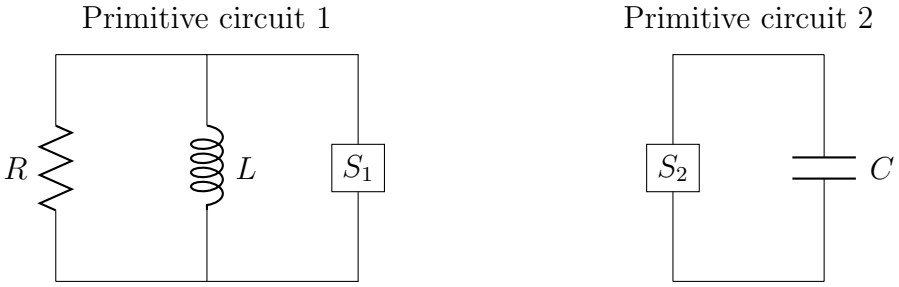

Figure 3.8: Considering the circuit as two primitive circuits. The S_i boxes show the possible points of connection and represent the influence of any connected circuit components [10].

3.5.2 An LC circuit

The next example is a very simple parallel RLC circuit which we consider as the joining of a capacitor to the RL loop component. We borrow the illustrations of this idea from [10] in Figures 3.7 and 3.8.

When considering electric circuits as Lagrangian, Hamiltonian or Lagrange-Dirac systems we take the charges as the configuration variables. So the configuration space for the undivided circuit is $\mathbb{R}^3$ with coordinates (q_R, q_L, q_C) representing the charge in the resistor, inductor and capacitor, respectively. Then $\dot{q}$ represents the currents in each component. The Lagrangian for any circuit is given by the magnetic energy stored in any inductors minus the electric potential energy of any capacitors. For the first primitive circuit we have $Q_1 = \mathbb{R}^3$ with local coordinates $q_1 = (q_R, q_L, q_{S_1})$. The q_{S_1} variable represents the possible point of connection shown in Figure 3.8 and represents the influence of any connected circuit compo-

nents. The Lagrangian is just the magnetic energy,

$$L_1(q_1, v_1) = \frac{1}{2} l v_L^2, \tag{3.103}$$

for l the inductance. The circuit has a nontrivial constraint distribution given by Kirchoff's circuit law,

$$\Delta_{Q_1}(q_1) = \{v_1 = (v_R, v_L, v_C) \in T_{q_1} Q_1 \mid v_R - v_L + v_{S_1} = 0\}. \tag{3.104}$$

Thus, $\Delta_{Q_1}^\circ = \text{span}\{\omega_1\}$ for $\omega_1 = dq_R - dq_L + dq_{S_1}$. In coordinates, $\omega_1 = (1, -1, 1)$. This circuit also has an external force due to the resistor, given by $f_r = -R dq_R = (-R, 0, 0)$.

The second primitive circuit has configuration space $Q_2 = \mathbb{R}^2$ with local coordinates $q_2 = (q_{S_2}, q_C)$. Here the Lagrangian is given by

$$L_2(q_2, v_2) = -\frac{1}{2C} q_C^2 \tag{3.105}$$

for C the capacitance. Again, we have a nontrivial constraint coming from circuit laws,

$$\Delta_{Q_2}(q_2) = \{v_2 = (v_{S_2}, v_C) \in T_{q_2} Q_2 \mid v_C - v_{S_2} = 0\}. \tag{3.106}$$

Hence, $\Delta_{Q_2}^\circ = \text{span}\{\omega_2\}$ for $\omega_2 = -dq_{S_2} + dq_C = (-1, 1)$.

To interconnect the two circuits, we set $Q = Q_1 \times Q_2, L = L_1 + L_2$ and use

$$\Sigma_{\text{int}} = \{(v_R, v_L, v_{S_1}, v_{S_2}, v_C) \in TQ \mid v_{S_1} = v_{S_2}\}. \tag{3.107}$$

Again we compare the numerical results of a discretization of the full circuit as shown in Figure 3.7 to those from a discretization of the primitive circuits shown in Figure 3.8 and interconnected via Σ_{int}. Figures 3.9 through 3.11 show the results.

Figure 3.9 shows that the capacitor charge of the interconnected discretization correctly replicates that of the full system discretization. In Figure 3.10 we see that the same is true for the overall circuit energy. Lastly, Figure 3.11 shows preservation of the constraint to machine precision in this case as well. Thus, once again, our interconnected discretization behaves equivalently to the full system discretization.

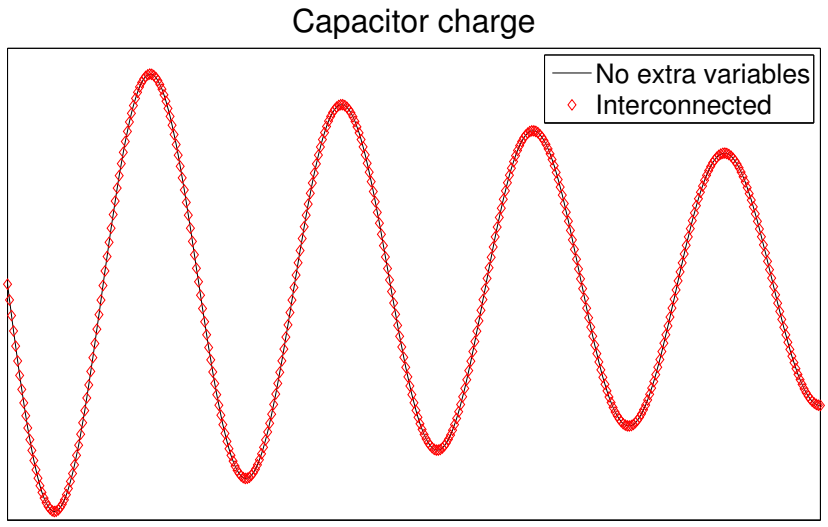

Figure 3.9: A comparison of the capacitor charge in the system generated by the monolithic and interconnected models. The two agree very closely.

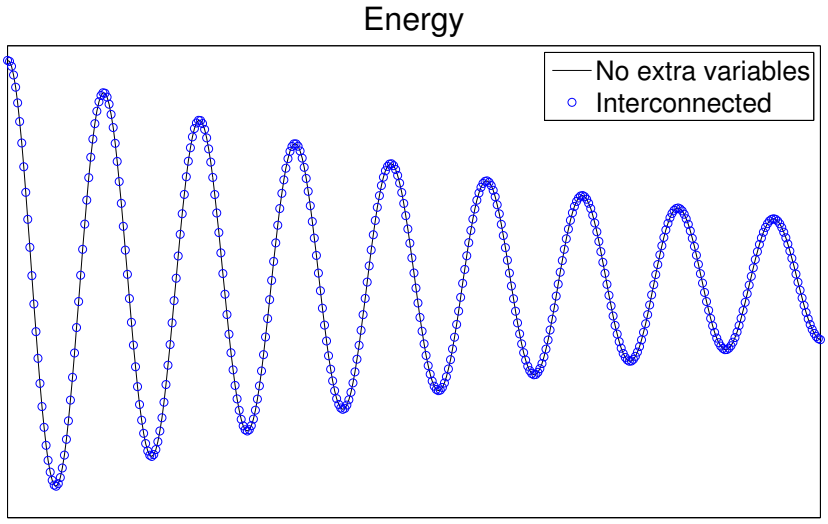

Figure 3.10: The energy in the circuit system generated by the monolithic vs. the interconnected model. The two agree very closely.

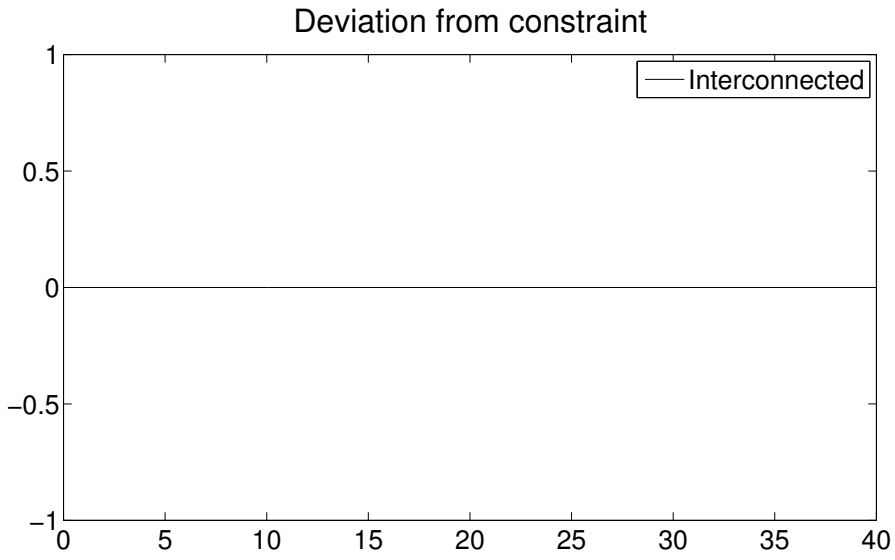

Figure 3.11: The interconnected model preserves the interconnection constraint to machine precision.

3.6 Conclusions and future work

We have presented a framework for interconnecting discrete Lagrange-Dirac systems, extending the work of [12]. Our view of interconnections is based on the perspective presented in [10]. In [10], the authors emphasize the equivalence between the constrained view and the interaction force view of interconnections. Our discrete interconnections so far take the constrained point of view. In future work, we would like to see an equivalent interaction-force perspective at the discrete level.

We would also like to further investigate the relationship between discrete Dirac integrators and the vast literature on nonholonomic integrators. With any luck, the two approaches to nonholonomic constraints will mutually shed light on one another.

As a practical consideration, the tearing of systems like those in the examples here can lead to new, redundant variables in the interconnected system. Those extra variables have been dealt with on a case by case basis in this study, and our numerical experiments confirm the the monolithic interconnected system with extra variables produces the same results as the full system without extra

variables in these cases. We would of course prefer to have a theoretical justification for introducing and working with extra variables in this way. We leave this as future work.

3.7 Acknowledgements

This work was conducted with Professor Melvin Leok at UC San Diego and was generously funded through the National Science Foundation Graduate Research Fellowship grant number DGE-1144086. This work is currently being prepared for publication.

Chapter 4

Structured model reduction on Lie groups: A preliminary study

This chapter details preliminary results on structured model reduction methods for systems evolving on Lie groups. Most model reduction methods assume a linear structure for the underlying configuration space. This is true of the Principal Orthogonal Decomposition (POD) method, which is one of the most commonly used model reduction techniques and the one we focus on extending in this work. This underlying assumption of linearity means ignoring much of the geometric structure of the system and often destroying that structure in the reduction process. This has negative implications for the overall performance of the reduced model. In this work, our goal is to improve the final performance of the reduced model by considering the geometry of the starting system. This work is inspired by [11], in which the authors use an embedding to associate a linear space with the underlying configuration manifold and extend reduction techniques on the linear space to the manifold. Following a suggestion in [11], we consider the case when the configuration manifold is a Lie group. We use canonical coordinates of the first kind as a way to associate a linear space with the configuration manifold. We work through an extended example of our proposed techniques applied to a molecular dynamics system from the literature. Our method drastically improves the performance of the reduced model on our chosen example system as compared to a reduced model generated by standard POD applied to the system in embedded

matrix coordinates.

Both this work and its impetus in [11] seek to adapt the method of model reduction by Principal Orthogonal Decomposition (POD) on snapshots so that the reduced model has Lagrangian or Hamiltonian structure when the full model does. While the method is often referred to as POD with snapshots or just POD, it is the Galerkin projection of the full dynamics onto the POD basis that actually produces the reduced model, and it is that step which we wish to alter. Following the ideas in [11], the hope is to leverage the computational efficiency of POD in finding a representative subspace for the dynamics but then to generate a reduced model using that subspace in such a way that the reduced model is again a mechanical system. Mechanical structure in a system is both sufficiently powerful in determining dynamics and sufficiently general in terms of applications that it may be worth the extra effort of using a slightly more specialized POD-based method to generate reduced models.

The authors of [11] emphasize the freedom in choosing the linear embedding $\eta : Q \to V$ and suggest the possible use of canonical coordinates of the first kind on $SO(3)$ for systems of coupled rigid bodies. Part of the purpose of this project was to investigate the feasibility of this suggestion. We've conducted this investigation using a simple molecular dynamics model to define a coupling between rigid bodies in 3D space.

4.1 Background

In this section we review some relevant background material on POD and mechanics on Lie groups.

4.1.1 Principal Orthogonal Decomposition with snapshots

Model reduction via POD is widely used in fluid dynamics, but it has also been applied in other areas, including control. POD, also known as the Karhunen-Loève expansion and Principal Component Analysis, produces a least-squares optimally ordered basis for a given set of data. In model reduction applications,

POD is used to identify an ordered basis of (linear) phase space from a set of data points called snapshots. Truncating the POD basis and projecting the dynamics onto that subspace provides a lower-dimensional model of the system.

This POD method, with snapshots and subsequent projection, uses only linear operations but produces a nonlinear reduced model. This provides computational efficiency while leaving hope that the important nonlinear effects of the full system will persist in the reduced system. The method is also entirely data driven, so it requires no specialized knowledge of the system dynamics to implement, making it widely and easily applicable.

POD with snapshots begins by considering a system $\dot{y} = f(y)$. The snapshots are taken as $y_j = y(t_j)$ from either experiments or a simulation of the full model. Letting $Y = [y_1, \ldots, y_m]$ be the matrix whose columns are the snapshots y_j, the POD basis of dimension d is $\{u_1, \ldots, u_d\}$, the first d left singular vectors of Y. The reduced dynamics are then $\dot{y}_d = \Pi_d f(y_d(t))$ for Π_d the projection onto $\text{span}\{u_1, \ldots, u_d\}$.

The data-driven nature of POD with snapshots makes it easy to use but also presents a drawback if you want your reduced model to preserve specific mechanical structures. The POD process is agnostic to the underlying model attributes, and it may destroy the mechanical nature of a given model, even if the reduced model is again nonlinear.

4.1.2 A structured model reduction scheme

In [11], Lall, Krysl and Marsden advocate an approach to model reduction of mechancial systems that produces a reduced model which again has a Lagrangian mechanical structure. Their approach first embeds the configuration manifold Q inside a vector space V. Standard, computationally efficient methods like POD can be used within V to identify a reduced basis spanning some subspace V_r. The configuration space for the reduced model is then taken to be $Q_r = Q \cap V_r$, the intersection of the original configuration manifold with the reduced linear space. The pair $(Q_r, L|_{Q_r})$, given by the reduced manifold and the original Lagrangian restricted to the reduced manifold, define the reduced Lagrangian mechanical model.

Some properties of the parent Lagrangian system may be directly inherited by the reduced system. For instance, the reduced system will always preserve a symplectic form ($\Omega_{L_r} = (Ti)^*\Omega_L$ for $i : Q_r \to Q$ the inclusion) and will conserve energy when the parent system does. More general symmetries of the parent system will be preserved only if the action of the symmetry group leaves Q_r invariant.

In [11], the authors apply this method to a finite-element elasticity model with great success. For that model, the configuration space Q is actually a vector space. In this case you do not need an embedding, and the overall method amounts to doing a principal component analysis on position-only snapshots and using the restricted Lagrangian to define a system on the resultant subspace.

We encountered some practical difficulties in trying to apply this method to our Lie group examples. Namely, there is no obvious practical way in which to project a given initial condition onto the reduced system submanifold. This is the main reason for which we do not compare our methods directly to this method in the current work.

4.1.3 Left-trivialized Hamilton-Pontryagin motion on Lie groups

Suppose we have a Lie group G with corresponding Lie algebra $\mathfrak{g}$ and Lie algebra dual $\mathfrak{g}^*$. Given a Lagrangian function on G, i.e. $L : TQ \to \mathbb{R}$, a left-trivialized Lagrangian $l : G \times \mathfrak{g} \to \mathbb{R}$ is defined by

$$l(g, \xi) = L(g, g\xi). \tag{4.1}$$

We have the following theorem.

Theorem 7. ([2]). Consider a Lagrangian system on a Lie group G with Lagrangian $L : TQ \to \mathbb{R}$. Let $l : G \times \mathfrak{g} \to \mathbb{R}$ be its left-trivialization. Then the following are equivalent:

1. Hamilton's principle for L on G

$$\delta \int_a^b L(g, \dot{g}) \mathrm{d}t = 0 \tag{4.2}$$

holds, for arbitrary variations [of] $g(t)$ with endpoint conditions $g(a)$ and $g(b)$ fixed.

2. The following variational principle holds on $G \times \mathfrak{g}$:

$$\delta \int_a^b l(g, \xi) \mathrm{d}t = 0 \tag{4.3}$$

using variations of the form

$$\delta\xi = \dot{\eta} + \mathrm{ad}_\xi \eta \tag{4.4}$$

where $\eta(a) = \eta(b) = 0$ and $\xi = g^{-1}\dot{g}$, i.e. $\xi = TL_{g^{-1}}\dot{g}$.

3. The HP [Hamilton-Pontryagin] principle

$$\delta \int_a^b [L(g, v) + \langle p, \dot{g} - v \rangle] \mathrm{d}t = 0 \tag{4.5}$$

holds, where $(g(t), v(t), p(t)) \in PG$ [$PG = TG \oplus T^*G$.] can be varied arbitrarily and independently with endpoint conditions $g(a)$ and $g(b)$ fixed.

4. The left-trivialized HP principle

$$\delta \int_a^b [l(g, \xi) + \langle \mu, g^{-1}\dot{g} - \xi \rangle] \mathrm{d}t = 0 \tag{4.6}$$

holds, where $(g(t), \xi(t), \mu(t)) \in G \times \mathfrak{g} \oplus \mathfrak{g}^*$ can be varied arbitrarily and independently with endpoint conditions $g(a)$ and $g(b)$ fixed.

Here ad : $\mathfrak{g} \to \mathfrak{g}^*$ denotes the adjoint action of $\mathfrak{g}$ on itself, also known as the adjoint representation of $\mathfrak{g}$. We have

$$\mathrm{ad}_\xi \eta = [\xi, \eta] \tag{4.7}$$

for $[\cdot, \cdot]$ the Lie bracket on $\mathfrak{g}$. The Hamilton-Pontryagin principle on $G \times \mathfrak{g} \oplus \mathfrak{g}^*$ produces the following set of equations.

$$\frac{d}{dt} g = g\xi, \tag{4.8}$$

$$\frac{d}{dt} \mu = \mathrm{ad}^*_\xi \mu + g \frac{\partial l}{\partial g}, \tag{4.9}$$

$$\mu = \frac{\partial l}{\partial \xi}(g, \xi). \tag{4.10}$$

These equations encompass both the left-trivialized Euler-Lagrange equations and the left-trivialized Hamilton's equations. We use them in the analysis of our model problem below.

4.2 Our example system

Following the suggestion of [11], we begin by considering a system of coupled rigid bodies. We focus on molecular dynamics as a test application because it involves simulating a very large number of coupled rigid bodies (the molecules), and often simulations need to be run many times. The desired result is a reduced model that preserves mechanical structure and qualitative behavior of the full model. We start with the model presented in [3] (originally from [7]), which is

$$\dot{\mathbf{q}}_i = \frac{\mathbf{p}_i}{m_i} \tag{4.11}$$

$$\dot{\mathbf{p}}_i = -\frac{\partial V}{\partial \mathbf{q}_i} \tag{4.12}$$

$$\dot{\mathbf{m}}_i = \mathbf{m}_i \times (I_i^{-1}\mathbf{m}_i) - \mathrm{rot}\left(\mathbf{Q}_i^T \frac{\partial V}{\partial \mathbf{Q}_i}\right) \tag{4.13}$$

$$\dot{\mathbf{Q}}_i = \mathbf{Q}_i(\widehat{I_i^{-1}\mathbf{m}_i}). \tag{4.14}$$

Here the index i denotes the i^{th} particle in the system, and the quantities are

$$\mathbf{q} \in \mathbb{R}^3 \text{ position} \tag{4.15}$$

$$\mathbf{p} \in \mathbb{R}^3 \text{ linear momentum} \tag{4.16}$$

$$\mathbf{m} \in \mathbb{R}^3 \text{ angular momentum} \tag{4.17}$$

$$\mathbf{Q} \in SO(3) \text{ attitude matrix} \tag{4.18}$$

$$V : \{\mathbf{q}_i, \mathbf{Q}_i\}_{i=1}^N \to \mathbb{R} \text{ interaction potential.} \tag{4.19}$$

The rot map is defined as $\mathrm{rot}(A) = v \in \mathbb{R}^3$ such that $\hat{v} = \begin{bmatrix} 0 & -v_3 & v_2 \\ v_3 & 0 & -v_1 \\ -v_2 & v_1 & 0 \end{bmatrix} = A - A^T$. This map is sometimes referred to as "check" in the literature and written $\mathrm{rot}(A) = \check{A}$.

First we need to understand the underlying Lie group of the system. Individual rigid bodies are modeled on either $SE(3) = SO(3) \rtimes \mathbb{R}^3$ or $SO(3) \times \mathbb{R}^3$, so our total group should be $G = P^N$ for P either $SE(3)$ or $SO(3) \times \mathbb{R}^3$ and N the number of particles. The equations provided also look like left-reduced equations, with the telltale reconstruction equation for $\dot{\boldsymbol{Q}}$. These are in fact the left-trivialized equations of motion on $G = (SO(3) \times \mathbb{R}^3)^N$. The next section shows this explicitly.

4.2.1 The molecular dynamics system as a left-trivialized Hamilton-Pontryagin system

We have the following (reduced) Hamiltonian for the system [3].

$$H(\mathbf{q}, \mathbf{p}, \boldsymbol{m}, \boldsymbol{Q}) = T(\mathbf{p}, \boldsymbol{m}) + V(\mathbf{q}, \boldsymbol{Q}) \tag{4.20}$$

for kinetic energy

$$T(\mathbf{p}, \boldsymbol{m}) = \sum_{i=1}^{N} \frac{1}{2} \left(\frac{||\mathbf{p}_i||^2}{m_i} + \boldsymbol{m}_i \cdot (I_i^{-1} \boldsymbol{m}_i) \right). \tag{4.21}$$

The interaction potential is given by $V = \sum_{i>j} V_{i,j}$ with

$$V_{i,j}(\mathbf{q}_i, \mathbf{Q}_i, \mathbf{q}_j, \mathbf{Q}_j) = V_{i,j}^{short} + V_{i,j}^{dip} \tag{4.22}$$

where $V_{i,j}^{short}$ describes short-range interactions and $V_{i,j}^{dipole}$ describes dipole-dipole interactions. These are in turn given by

$$V_{i,j}^{short} = 4\epsilon \left(\frac{\sigma}{r_{i,j}} \right)^{12}, \ \mathbf{r}_{i,j} = \mathbf{q}_i - \mathbf{q}_j, \ r_{i,j} = ||\mathbf{r}_{i,j}|| \tag{4.23}$$

and

$$V_{i,j}^{dip} = \frac{1}{r_{i,j}^3} \boldsymbol{\mu}_i \cdot \boldsymbol{\mu}_j - \frac{3}{r_{i,j}^5} (\boldsymbol{\mu}_i \cdot \mathbf{r}_{i,j})(\boldsymbol{\mu}_j \cdot \mathbf{r}_{i,j}). \tag{4.24}$$

The variable $\boldsymbol{\mu}_i$ gives the orientation of the i^{th} dipole vector, with $\boldsymbol{\mu}_i = \mathbf{Q}_i \bar{\boldsymbol{\mu}}_i$ for $\bar{\boldsymbol{\mu}}_i$ a fixed reference orientation of the i^{th} dipole.

With this potential, the Hamiltonian is invariant under a left diagonal action of $SE(3)$. (The term $(\boldsymbol{\mu}_i \cdot \mathbf{r}_{i,j})(\boldsymbol{\mu}_j \cdot \mathbf{r}_{i,j})$ in the potential is invariant under a left diagonal action by $SE(3)$ but not under a left diagonal action of $SO(3) \times \mathbb{R}^3$.) Note that this Hamiltonian is *not* invariant under the left action of the full group $G = P^N$. So the equations of motion may be left-trivialized, but they are not symmetry reduced Lie-Poisson equations. We now confirm that, with the proper definition of $l(g, \xi), \xi$, and μ, these are the left-trivialized Hamilton-Pontryagin equations on $G = (SO(3) \times \mathbb{R}^3)^N$. That is, they have the form

$$\frac{d}{dt} g = g\xi, \tag{4.25}$$

$$\frac{d}{dt} \mu = \mathrm{ad}_\xi^* \mu + g \frac{\partial l}{\partial g}, \tag{4.26}$$

$$\mu = \frac{\partial l}{\partial \xi}(g, \xi). \tag{4.27}$$

In this notation, $g\xi$ and $g\frac{\partial l}{\partial g}$ denote the tangent and cotangent lifted left actions by g, respectively. More explicitly, $g\xi = TL_g\xi$ and $g\frac{\partial l}{\partial g} = T^*L_g\frac{\partial l}{\partial g}$.

Multiplication in the group $SO(3)\times\mathbb{R}^3$ is $(A,a)(B,b) = (AB, a+b)$. The tangent lift of this multiplication is $TL_{(Q,q)}(\xi,u) = (Q\xi,u)$. The cotangent lift of this multiplication is $T^*L_{(Q,q)}(\beta,y) = (Q^T\beta,y)$ when β is an arbitrary element of $T^*SO(3)$ represented as a matrix. In the special case that $\beta\in T^*_QSO(3)$, then $T^*L_Q\beta \in T^*_{\mathrm{Id}}SO(3)\cong\mathfrak{g}^*$. Then $T^*L_Q\beta$ has an equivalent representation as $\mathrm{rot}(Q^T\beta)$.

The Lie bracket on $\mathfrak{so}(3)\times\mathbb{R}^3\cong\mathbb{R}^3\times\mathbb{R}^3$ is

$$[(\xi,u),(\eta,v)] = (\xi\times\eta, 0), \tag{4.28}$$

and the pairing between $\mathfrak{so}(3)\times\mathbb{R}^3$ and $(\mathfrak{so}(3)\times\mathbb{R}^3)^*$ is given by

$$\langle(\alpha,x),(\xi,v)\rangle = \alpha^T\xi + x^Tv. \tag{4.29}$$

Thus, $\mathrm{ad}^*_{(\xi,u)}(\alpha,x) = (\alpha\times\xi,0)$. The product Lie structure on $(SO(3)\times\mathbb{R}^3)^N$ uses the same operations acting component-wise.

In the notation of the left-trivialized Hamilton-Pontryagin equations above, $\xi = g^{-1}\dot{g}$. In this example then

$$\xi_i = (\hat{\xi}_i^Q, \xi_i^q) = (\boldsymbol{Q}_i^T, -\mathbf{q})(\dot{\boldsymbol{Q}}_i, \dot{\mathbf{q}}_i) \tag{4.30}$$

$$= (\boldsymbol{Q}_i^T\dot{\boldsymbol{Q}}_i, \dot{\mathbf{q}}_i) \tag{4.31}$$

$$= \left(\widehat{I_i^{-1}\boldsymbol{m}_i}, \frac{\mathbf{p}_i}{m_i}\right). \tag{4.32}$$

Our left-trivialized Lagrangian is $L = T - V$ written in terms of $g = (\boldsymbol{Q},\mathbf{q})$ and ξ. That is,

$$l(g,\xi) = l(\mathbf{q},\boldsymbol{Q},\xi^Q,\xi^q) \tag{4.33}$$

$$= \sum_{i=1}^N \frac{1}{2}\left(m_i||\xi_i^q||^2 + I_i\xi_i^Q\cdot(\xi_i^Q)\right) - V(\boldsymbol{Q},\mathbf{q}). \tag{4.34}$$

Thus,

$$\frac{\partial l}{\partial\xi_i} = (I_i\xi_i^Q, m_i\xi_i^q). \tag{4.35}$$

Notice also that

$$(I_i\xi_i^Q, m_i\xi_i^q) = (\boldsymbol{m}_i, \mathbf{p}_i). \tag{4.36}$$

So, μ in the reduced H-P equations corresponds to

$$\mu_i = (\boldsymbol{m}_i, \mathbf{p}_i). \tag{4.37}$$

We just need to confirm that equation (4.26) agrees with the given equations of motion.

$$\dot{\mu_i} = (\dot{\boldsymbol{m}}_i, \dot{\mathbf{p}}_i) \tag{4.38}$$

$$= \mathrm{ad}^*_{\xi_i}\mu + T^*L_{g_i}\frac{\partial l}{\partial g_i} \tag{4.39}$$

$$= \mathrm{ad}^*_{(\xi_i^Q,\xi_i^q)}(\boldsymbol{m}_i, \mathbf{p}_i) + T^*L_{(\boldsymbol{Q}_i,\mathbf{q}_i)}\left(-\frac{\partial V}{\partial \boldsymbol{Q}_i}, -\frac{\partial V}{\partial \mathbf{q}_i}\right) \tag{4.40}$$

$$= (\boldsymbol{m}_i \times \xi_i^Q, 0) + \left(\mathrm{rot}\left(-\boldsymbol{Q}_i^T\frac{\partial V}{\partial \boldsymbol{Q}_i}\right), -\frac{\partial V}{\partial \mathbf{q}_i}\right). \tag{4.41}$$

In summary,

$$\dot{\boldsymbol{m}}_i = \boldsymbol{m}_i \times (I_i^{-1}\boldsymbol{m}_i) - \mathrm{rot}\left(-\boldsymbol{Q}_i^T\frac{\partial V}{\partial \boldsymbol{Q}_i}\right), \tag{4.42}$$

and

$$\dot{\mathbf{p}}_i = -\frac{\partial V}{\partial \mathbf{q}_i}. \tag{4.43}$$

Thus, we realized equations (4.11)-(4.14) as the left-trivialized Hamilton-Pontryagin equations for $G = (SO(3) \times \mathbb{R}^3)^N$. Note that the assumption $G = SE(3)^N$ results in different tangent-lifted group actions and does not recover the provided equations.

4.3 Model reduction methods applied to this example

We now consider the application of several model reduction methods to this example. In each method we select a section of the system variables to sample as snapshots. Call this section y and take $y_j \approx y(t_j), j = 1, \ldots, m$. We then form a snapshot matrix $Y = [y_1 \cdots y_m]$, i.e. Y has columns y_j. Suppose the SVD of

our snapshot matrix is $Y = \tilde{U}\Sigma V$. Define U to be the $cN \times d$ matrix of first d singular vectors, i.e. $U = \tilde{U}(:, 1:d)$ in Matlab notation. We take U as the basis of the reduced system, referred to as the reduced basis. The constant c will depend on which variables are included in y. Let $\bar{U}$ be a $cN \times (cN - d)$ matrix whose columns form a basis for range$(U)^{\perp}$. This matrix can be found easily in Matlab using `null`(U^T). We present four options for our model reduction corresponding to y being the full phase configuration in embedded coordinates, configurations only in embedded coordinates, configurations only in exponential coordinates, or the full phase configuration with the positions in exponential coordinates.

4.3.1 Full phase configuration in embedded coordinates

This is the classic POD approach applied to the provided equations (4.11)-(4.14). In this case y consists of the full state of the system, i.e.

$$y = [\ldots, q_i, p_i, Q_i, \mathbf{m}_i, \ldots]^T \in \mathbb{R}^{18N}. \tag{4.44}$$

We can rewrite our original equations as $\dot{y} = F(y)$. We now approximate y by $U\lambda$ for some $\lambda \in \mathbb{R}^d, d << 18N$, and we solve the equations $\dot{\lambda} = U^T F(U\lambda) = \tilde{F}(\lambda)$.

4.3.2 Configurations only in embedded coordinates

This is the approach described in [11]. In this case y consists only of configuration variables, i.e.

$$y = [\ldots, q_i, Q_i, \ldots]^T \in \mathbb{R}^{12N} \tag{4.45}$$

denotes the position vector of the entire system. (Here we are thinking of Q_i as a vector embedded in $\mathbb{R}^9$.) The constraint is then $g(y) = \bar{U}^T y = 0$ and the constraint derivative is $\bar{U}^T \dot{y} = 0$. This is equivalent to the constraint $y \in$ range(U). The left-

trivialized H-P equations with holonomic constraints are

$$\xi = g^{-1}\dot{g}, \tag{4.46}$$

$$\mu = \frac{\partial l}{\partial \xi}, \tag{4.47}$$

$$\dot{\mu} = \mathrm{ad}^*_\xi \mu + g\frac{\partial l}{\partial g} - g\nabla\varphi(g)\lambda, \tag{4.48}$$

$$0 = \phi(g). \tag{4.49}$$

Using this general form, our particular equations become

$$\dot{\mathbf{q}}_i = \frac{\mathbf{p}_i}{m_i} \tag{4.50}$$

$$\dot{\mathbf{p}}_i = -\frac{\partial V}{\partial \mathbf{q}_i} + \frac{1}{m_i}\bar{U}_i\lambda \tag{4.51}$$

$$\dot{\mathbf{m}}_i = \mathbf{m}_i \times (I_i^{-1}\mathbf{m}_i) - \mathrm{rot}\left(\mathbf{Q}_i^T \frac{\partial V}{\partial \mathbf{Q}_i}\right) - \mathrm{rot}\left(\mathbf{q}_i^T \frac{\partial \varphi}{\partial \boldsymbol{Q}_i}\right)\lambda \tag{4.52}$$

$$\dot{\mathbf{Q}}_i = \mathbf{Q}_i\widehat{(I_i^{-1}\mathbf{m}_i)} \tag{4.53}$$

$$\bar{U}^T y = 0 \tag{4.54}$$

$$\bar{U}_i^T \frac{p_i}{m_i} = 0 \tag{4.55}$$

$$r_j(Q_i)^T(I_i^{-1}\mathbf{m}_i \times v_i^{j,l}) = 0, j = 1, \ldots, 3, l = 1, \ldots, 12N - d. \tag{4.56}$$

The final equations comes from differentiating the constraint $\bar{U}^T y = 0$. If we let $\bar{U}^T = \begin{bmatrix} \cdots & \bar{U}_i^T & \bar{U}_i^T & \cdots \end{bmatrix}$ where $\bar{U}_i^T \in \mathbb{R}^{12N-d\times 3}$ and $\bar{U}_i^T \in \mathbb{R}^{12N-d\times 9}$, then the constraints on each particle are

$$\bar{U}_i^T q_i = 0 \tag{4.57}$$

$$\bar{U}_i^T Q_i^v = 0, \tag{4.58}$$

$$Q_i^v = \begin{bmatrix} Q_{11} & Q_{12} & Q_{13} & Q_{21} & \cdots & Q_{33} \end{bmatrix}^T. \tag{4.59}$$

The differentiated center of mass constraint is then (4.55). Further partition $\bar{U}_i^T$ as $\bar{U}_i^T = \begin{bmatrix} (\bar{U}_i^T)_1 & (\bar{U}_i^T)_2 & (\bar{U}_i^T)_3 \end{bmatrix}$ with each $(\bar{U}_i^T)_j \in \mathbb{R}^{12N-d\times 3}$. The differentiated orientation constraint can be written in matrix-vector form as $(\bar{U}_i^T)_j \dot{\boldsymbol{Q}}_i^T e_j = 0$. We then obtain the $3(12N - d)$ scalar constraints in (4.56) using (4.53) and labeling the rows of $(\bar{U}_i^T)_j$ by $v_i^{j,l}, l = 1, \ldots, 12N - d$.

4.3.3 Position-only snapshots in exponential coordinates

In this case we use only position data to construct the snapshots y_j, but we represent Q_i by v_i such that $\exp(\hat{v}_i) = Q_i$. Then each y_j is given by $y_j = \begin{bmatrix} \cdots & q_i^j & v_i^j & \cdots \end{bmatrix}$. (This is, in the end, a column vector). We then take the SVD of the snapshot matrix $Y = \begin{bmatrix} y_1 & \cdots & y_m \end{bmatrix}$ to get $Y = \tilde{U}\Sigma V$ and take $U = \tilde{U}(:, 1:d)$ as the reduced basis. The "constraint" is then that $y = U\lambda$ for $\lambda \in \mathbb{R}^d$. Partitioning U horizontally, this can be written as

$$q_i = U_i^q \lambda, \;\; v_i = U_i^v \lambda, \tag{4.60}$$

where U_i^q and U_i^v are $3 \times d$ matrices. We say "constraint" above because, for this formulation, we will rewrite the equations of motion directly in terms of λ rather than formulating the problem as having an additional constraint.

This formulation has the advantage that given a reduced state $\lambda^{(k)}$, the corresponding full state is given by $q_i = U_i^q \lambda^{(k)}, Q_i = \exp(\widehat{U_i^v \lambda^{(k)}})$. Thus, the solution of the reduced system is guaranteed to lie on $\mathbb{R}^3 \times SO(3)$ without having to impose any constraints on the state λ. This simplifies the form of the final equations and avoids the logistical difficulties of intersecting a vector subspace with the original manifold.

We start from the given equations of motion.

$$\dot{\mathbf{q}}_i = \mathbf{p}_i \tag{4.61}$$

$$\dot{\mathbf{p}}_i = -\frac{\partial V}{\partial \mathbf{q}_i} \tag{4.62}$$

$$\dot{\mathbf{m}}_i = \mathbf{m}_i \times (I_i^{-1}\mathbf{m}_i) - \text{rot}\left(\mathbf{Q}_i^T \frac{\partial V}{\partial \mathbf{Q}_i}\right) \tag{4.63}$$

$$\dot{\mathbf{Q}}_i = \mathbf{Q}_i(\widehat{I_i^{-1}\mathbf{m}_i}). \tag{4.64}$$

We will assume in our simulations later that $m_i = 1$ and that $\epsilon = \sigma = 1$ in $V(q, Q)$.

In this case, the derivatives of the potential are

$$\begin{aligned}\frac{\partial V}{\partial q_i} = \sum_{j>i}\Bigg[&- \frac{48}{r_{ij}^{14}} - \frac{3\mu_i^T\mu_j}{r_{ij}^5} + \left(\frac{15\mu_i^T\mathbf{r}_{ij}\mu_j^T\mathbf{r}_{ij}}{r_{ij}^7}\right)\mathbf{r}_{ij} \\ &- \left(\frac{3\mu_j^T\mathbf{r}_{ij}}{r_{ij}^5}\right)\mu_i - \left(\frac{3\mu_i^T\mathbf{r}_{ij}}{r_{ij}^5}\right)\mu_j\Bigg] \\ + \sum_{l<i}\Bigg[&\frac{48}{r_{li}^{14}} + \frac{3\mu_l^T\mu_i}{r_{li}^5} - \left(\frac{15\mu_l^T\mathbf{r}_{li}\mu_i^T\mathbf{r}_{li}}{r_{li}^7}\right)\mathbf{r}_{li} \\ &+ \left(\frac{3\mu_i^T\mathbf{r}_{li}}{r_{li}^5}\right)\mu_l + \left(\frac{3\mu_l^T\mathbf{r}_{li}}{r_{li}^5}\right)\mu_i\Bigg]\end{aligned} \tag{4.65}$$

$$\frac{\partial V}{\partial Q_i} = \sum_{j\neq i}\left[\frac{1}{r_{ij}^3}\mu_j\bar{\mu}_i^T - \left(\frac{3\mu_j^T\mathbf{r}_{ij}}{r_{ij}^5}\right)\mathbf{r}_{ij}\bar{\mu}_i{}^T\right] \tag{4.66}$$

where we have

$$\mathbf{r}_{ij} = q_i - q_j,\ r_{ij} = ||\mathbf{r}_{ij}||,\ \mu_i = Q_i\bar{\mu}_i. \tag{4.67}$$

The variable $\bar{\mu}_i$ is a fixed reference orientation for the dipole vector of the ith body. In simulations we initialize Q_i randomly, set $\mu_i = (0,1,1)^T$, and solve for $\bar{\mu}_i$.

In terms of the variables q, v we have

$$q_i = q_i,\ p_i = m_i\dot{q}_i = \dot{q}_i,\ Q_i = \exp(\hat{v}_i),\ \mathbf{m}_i = I_i d\exp_{v_i}(\dot{v}_i), \tag{4.68}$$

so we get, in terms of λ,

$$q_i = U_i^q\lambda,\ p_i = U_i^q\dot{\lambda},\ Q_i = \exp(\widehat{U_i^v\lambda}),\ \mathbf{m}_i = I_i d\exp_{U_i^v\lambda}(U_i^v\dot{\lambda}). \tag{4.69}$$

We are using the left-trivialized definition of $d\exp$ here.

For each given equation of motion, we take the appropriate time derivative on the left hand side and substitute in the appropriate definitions on the right hand side. We begin with rewriting the equations in (q, v) variables, i.e. in exponential coordinates. For equations (4.104) and (4.64) we get

$$\dot{q}_i = \dot{q}_i \tag{4.70}$$

$$\frac{d}{dt}\exp(v_i) = \exp(v_i)d\exp_{v_i}(\dot{v}_i). \tag{4.71}$$

For equations (4.106) and (4.63), we get

$$\ddot{q}_i = -\frac{\partial V}{\partial q_i}(q, v) \tag{4.72}$$

$$\frac{d}{dt}(I_i d\exp_{v_i}(\dot{v}_i)) = (I_i d\exp_{v_i}(\dot{v}_i)) \times (d\exp_{v_i}(\dot{v}_i)) - rot\left(\exp(v_i)^T \frac{\partial V}{\partial Q_i}(q, v)\right). \tag{4.73}$$

We could also rearrange the equations to obtain a system in (q, v, p, m) rather than (q, Q, p, m), where $Q = \exp(\hat{v})$. This gives

$$\dot{\mathbf{q}}_i = \mathbf{p}_i \tag{4.74}$$

$$\dot{\mathbf{p}}_i = -\frac{\partial V}{\partial \mathbf{q}_i}(q, v) \tag{4.75}$$

$$\dot{\mathbf{m}}_i = \mathbf{m}_i \times (I_i^{-1}\mathbf{m}_i) - \text{rot}\left(\exp(v_i)^T \frac{\partial V}{\partial \mathbf{Q}_i}(q, v)\right) \tag{4.76}$$

$$\dot{v}_i = d\exp_{v_i}^{-1}(I_i^{-1}\mathbf{m}_i) \tag{4.77}$$

Equation (4.77) comes from observing that $\dot{Q}_i = \frac{d}{dt}\exp(v_i) = Q_i(\widehat{I_i^{-1}\mathbf{m}_i})$.

For the reduced system, we will rewrite the equations as a second order equation in λ. We can express $q_i, \dot{q}_i, v_i$ and $\dot{v}_i$ in terms of $\lambda, \dot{\lambda}$. Equation (4.72) becomes

$$U_i^q \ddot{\lambda} = -\frac{\partial V}{\partial q_i}(q(\lambda), v(\lambda)). \tag{4.78}$$

Equation (4.73) becomes

$$\begin{aligned}\frac{d}{dt}(I_i d\exp_{U_i^v\lambda}(U_i^v\dot{\lambda})) =&(I_i d\exp_{U_i^v\lambda}(U_i^v\dot{\lambda})) \times (d\exp_{U_i^v\lambda}(U_i^v\dot{\lambda})) \\ &- \text{rot}\left(\exp(U_i^v\lambda)^T \frac{\partial V}{\partial Q_i}(q(\lambda), v(\lambda))\right).\end{aligned} \tag{4.79}$$

Because we are working on $SO(3)$ and $\mathfrak{so}(3)$, $d\exp_u$ has a closed matrix formulation, which comes from Rodrigue's formula,

$$d\exp_u = A(u) = \text{Id} - \left(\frac{1-\cos(\alpha)}{\alpha^2}\right)\hat{u} + \left(\frac{\alpha - \sin(\alpha)}{\alpha^3}\right)\hat{u}^2, \tag{4.80}$$

for $\alpha = ||u||$. We write this as $d\exp_u = A(u) \in \mathbb{R}^{3\times 3}$ for convenience. Then equation (4.81) becomes

$$\begin{aligned}\frac{d}{dt}(I_i A(U_i^v\lambda)(U_i^v\dot{\lambda})) =&(I_i A(U_i^v\lambda)(U_i^v\dot{\lambda})) \times (A(U_i^v\lambda)(U_i^v\dot{\lambda})) \\ &- \text{rot}\left(\exp(U_i^v\lambda)^T \frac{\partial V}{\partial Q_i}(q(\lambda), v(\lambda))\right).\end{aligned} \tag{4.81}$$

The time derivative on the left hand side can be written as

$$\frac{d}{dt}(I_i A(U_i^v\lambda)(U_i^v\dot{\lambda})) = \frac{d}{dt}[M(t)v(t)] \tag{4.82}$$

$$= \dot{M}(t)v(t) + M(t)\dot{v}(t) \tag{4.83}$$

$$= I_i\frac{d}{dt}[A(U_i^v\lambda)]U_i^v\dot{\lambda} + I_i A(U_i^v\lambda)U_i^v\ddot{\lambda}. \tag{4.84}$$

We compute $\frac{d}{dt}[A(U_i^v\lambda)]U_i^v\dot{\lambda}$ below. This allows us to rearrange (4.81) as

$$U_i^v\ddot{\lambda} = A(U_i^v\lambda)^{-1}I_i^{-1}\Bigg[(I_i A(U_i^v\lambda)(U_i^v\dot{\lambda})) \times (A(U_i^v\lambda)(U_i^v\dot{\lambda})) \tag{4.85}$$

$$- \text{rot}\left(\exp(U_i^v\lambda)^T\frac{\partial V}{\partial Q_i}(q(\lambda), v(\lambda))\right) - I_i\frac{d}{dt}[A(U_i^v\lambda)]U_i^v\dot{\lambda}\Bigg]$$

We can now stack equations (4.78) and (4.85) to get a second order equation in λ,

$$U\ddot{\lambda} = F(U\lambda, U\dot{\lambda}). \tag{4.86}$$

Having recovered the full matrix U, we can use its orthogonality to write everything as a second-order equation

$$\ddot{\lambda} = U^T F(U\lambda, U\dot{\lambda}). \tag{4.87}$$

Computing the derivative

In this section we explicitly compute $\frac{d}{dt}[A(U_i^v\lambda)]U_i^v\dot{\lambda}$. To do this, we use the notation $u(t) = U_i^v\lambda(t) \in \mathbb{R}^3$ and $w(t) = U_i^v\dot{\lambda}(t)$ for convenience. With this notation, we need to compute $\frac{d}{dt}[A(u(t))]v(t) \in \mathbb{R}^3$, where the derivative is only being applied to $A(u(t))$. We compute

$$A(u(t))v(t) = \left[\text{Id} - \frac{1-\cos(\alpha)}{\alpha^2}\hat{u} + \frac{\alpha - \sin(\alpha)}{\alpha^3}\hat{u}^2\right]v \tag{4.88}$$

$$= v - \frac{1-\cos(||u||)}{||u||^2}(u\times v) + \frac{||u|| - \sin(||u||)}{||u||^3}[u\times(u\times v)] \tag{4.89}$$

$$= v - \frac{1-\cos(||u||)}{||u||^2}(u\times v) + \frac{||u|| - \sin(||u||)}{||u||^3}(u^T v)u \tag{4.90}$$

$$- \frac{||u|| - \sin(||u||)}{||u||^3}||u||^2 v \tag{4.91}$$

$$= v - c_1(u)(u\times v) + c_2(u)(u^T v)u - c_3(u)v. \tag{4.92}$$

Now we take the time derivative of this vector, treating $v(t)$ as constant. First we find that $\cot c_i(u(t)) = \tilde{c}_i u^T \dot{u}$ for

$$\tilde{c}_1 = \frac{\sin(\alpha)\alpha - 2 + 2\cos(\alpha)}{\alpha^4} \tag{4.93}$$

$$\tilde{c}_2 = \frac{-2\alpha^2 - \alpha^2\cos(\alpha) + 3\alpha\sin(\alpha)}{\alpha^6} \tag{4.94}$$

$$\tilde{c}_3 = \frac{-\alpha\cos(\alpha) + \sin(\alpha)}{\alpha^3}. \tag{4.95}$$

Then

$$\frac{d}{dt}|_{w\equiv\text{constant}}[A(u(t))w] = \frac{d}{dt}[-c_1(t)(u(t)\times w) + c_2(t)(u(t)^T w)u(t) - c_3(t)w] \tag{4.96}$$

$$= -\dot{c}_1(u\times w) - c_1(\dot{u}\times w) + \dot{c}_2(u^T w)u \tag{4.97}$$

$$+ c_2[(\dot{u}^T w)u + (u^T w)\dot{u}] - \dot{c}_3 w \tag{4.98}$$

$$= -\tilde{c}_1(u^T\dot{u})(u\times w) - c_1(\dot{u}\times w) + \tilde{c}_2(u^T\dot{u})(u^T w)u \tag{4.99}$$

$$+ c_2(\dot{u}^T w)u + c_2(u^T w)\dot{u} - \tilde{c}_3(u^T\dot{u})w. \tag{4.100}$$

Replacing $u(t) = U_i^v\lambda(t)$ and $w(t) = U_i^v\dot{\lambda}(t)$, we note that $\dot{u} = w$ in this particular case. This simplifies the equation to

$$\frac{d}{dt}|_{w\equiv\text{constant}}[A(u(t))w] = -\tilde{c}_1(u^T w)(u\times w) + \tilde{c}_2(u^T w)^2 u \tag{4.101}$$

$$+ c_2||w||^2 u + (c_2 - \tilde{c}_3)(u^T w)w \tag{4.102}$$

which we can rewrite directly in terms of $\lambda, \dot{\lambda}$ as

$$\frac{d}{dt}[A(U_i^v\lambda)]U_i^v\dot{\lambda} = -\tilde{c}_1(\lambda^T(U_i^v)^T U_i^v\dot{\lambda})(U_i^v\lambda\times U_i^v\dot{\lambda}) + \tilde{c}_2(\lambda^T(U_i^v)^T U_i^v\dot{\lambda})^2 U_i^v\lambda$$
$$+ c_2||U_i^v\dot{\lambda}||^2 U_i^v\lambda + (c_2 - \tilde{c}_3)(\lambda^T(U_i^v)^T U_i^v\dot{\lambda})U_i^v\dot{\lambda}. \tag{4.103}$$

4.3.4 Full state snapshots with positions in exponential coordinates

Now we begin from the equations

$$\dot{\mathbf{q}}_i = \mathbf{p}_i, \tag{4.104}$$

$$\dot{v}_i = d\exp_{v_i}^{-1}(\widehat{I_i^{-1}\mathbf{m}_i}), \tag{4.105}$$

$$\dot{\mathbf{p}}_i = -\frac{\partial V}{\partial \mathbf{q}_i}(q, v), \tag{4.106}$$

$$\dot{\mathbf{m}}_i = \mathbf{m}_i \times (I_i^{-1}\mathbf{m}_i) - \mathrm{rot}\left(\exp(v_i)^T \frac{\partial V}{\partial \mathbf{Q}_i}(q, v)\right), \tag{4.107}$$

derived in the previous section. Let y denote the full state and $G(y)$ denote the right hand side. We can take samples of the full state $\{(q, v, p, m)_j\}$ and do an SVD of the sample matrix to get $\tilde{U}$, Σ, and then the new basis U. We shift our initial condition to $x_0 = U^T y_0$, and we project the vector field to get

$$\dot{x} = U^T G(Ux). \tag{4.108}$$

Notice that, while similar in form, this is different from the equations for $\ddot{\lambda}$ above. In the equations for $\ddot{\lambda}$ we have maintained the second-order relationship between the variables (q, v) and (p, m). The reduction of the (p, m) variables is derived from the reduction of the (q, v) variables. In this example, that maintaining the second-order relationship produces correction terms in F that are not present in the corresponding sections of G.

4.4 Numerical Results

Figure 4.1 shows the results of solving the full model versus solving a POD reduced model based on the full system state in $\mathbb{R}^{12N}$, i.e. with $SO(3)$ embedded in $\mathbb{R}^9$ as matrices. We solve both systems for $N = 15$ at high tolerances with `ode45` until $T = 20$. The distance between configurations is measured as the root mean square difference between the $\mathbf{q}$ components of $(\mathbf{q}^{(t_k)}, \mathbf{Q}^{(t_k)})$ computed using the full model and the $\mathbf{q}$ components of $(U\lambda^{(t_k)})$ computed using the reduced model. We see that at $t_k \approx 13$ the reduced model solution diverges from the full model

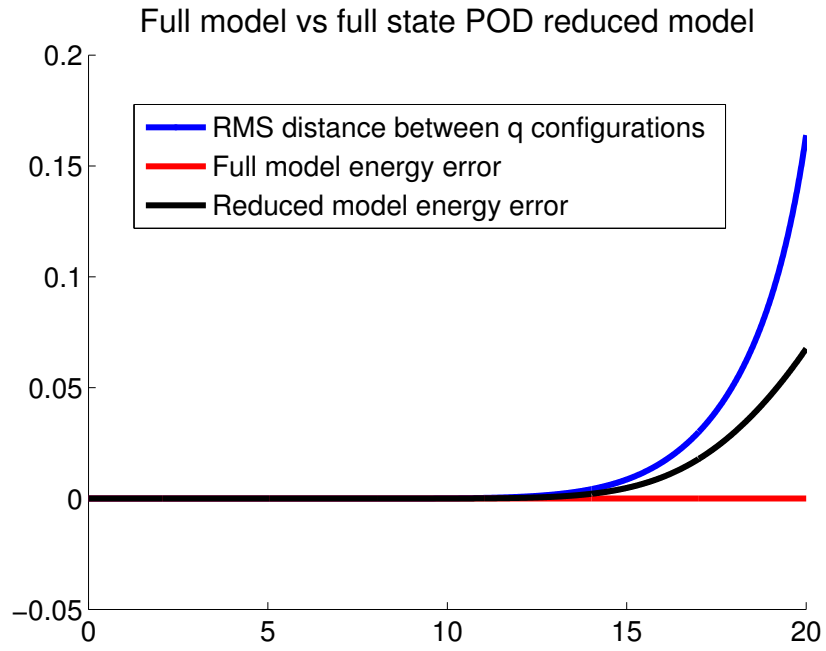

Figure 4.1: Comparing the full model in $\mathbb{R}^{12N}$ to a POD model based on full state snapshots. We see both the configuration and the energy error of the reduced system diverge toward the end of the time interval.

solution. The energy error shortly follows suit. From this experiment, we see that a reduced model produced by classic POD with snapshots will not remain valid over the full time interval. However, we also confirm our suspicions that this model is a good candidate for reducing. Were it not, we would expect to see the two solutions diverge much more quickly. As further confirmation of this, Figure 4.2 shows a steep decline in the singular values of the data matrix, indicating that only a few modes are responsible for most of the system's motion.

Figure 4.3 shows the singular values of the data matrix constructed from position-only snapshots in exponential coordinates. Again, we see a steep decline in magnitude, making the system a good candidate for model reduction. Figure 4.4 shows the full model run on $\mathbb{R}^{12N}$ versus the reduced model derived from a PCA analysis on the exponential position data. This reduced model preserves the second-order, mechanical relationship among the variables. As above, we run the system with $N = 15$ until $t = 20$, solving both systems to very high tolerances with `ode45` in Matlab. Both the $\mathbf{q}$ position error and the energy error of this reduced

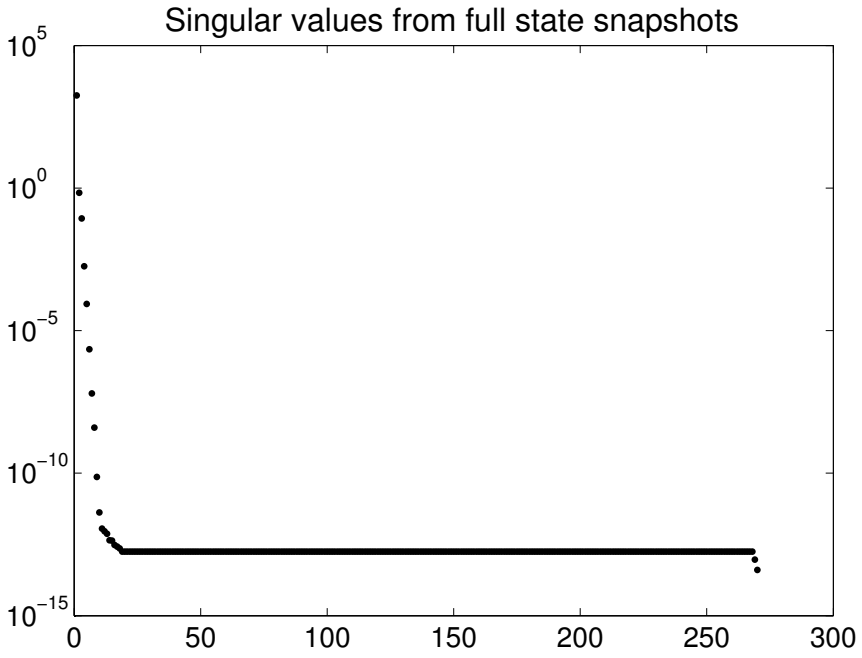

Figure 4.2: Singular values of the data matrix constructed from full state snapshots. Note the steep decline in magnitude, indicating that the system is a good candidate for model reduction.

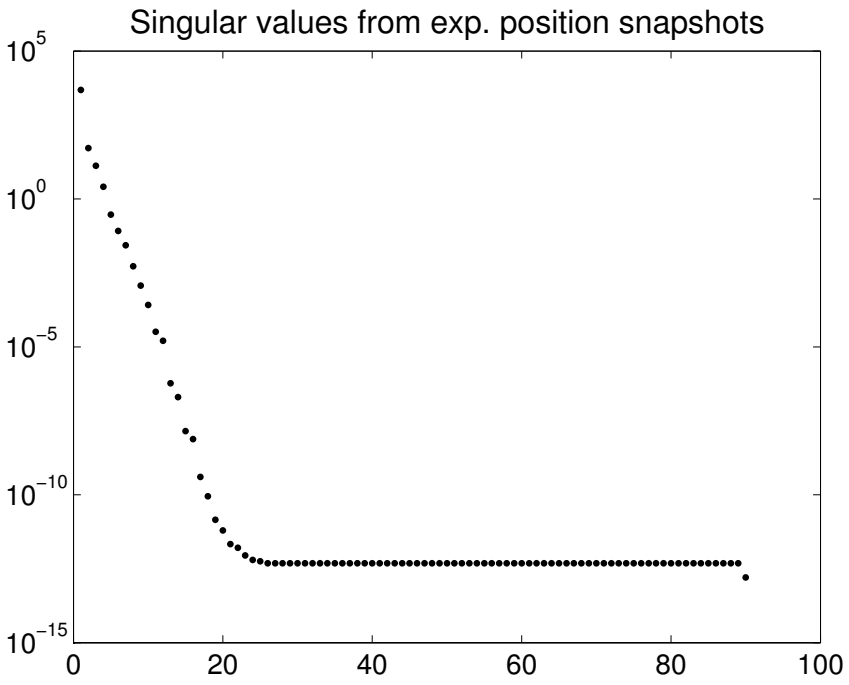

Figure 4.3: Singular values of the data matrix constructed from position snapshots in exponential coordinates. Again, we see a steep decline in magnitude, encouraging us to reduce the model.

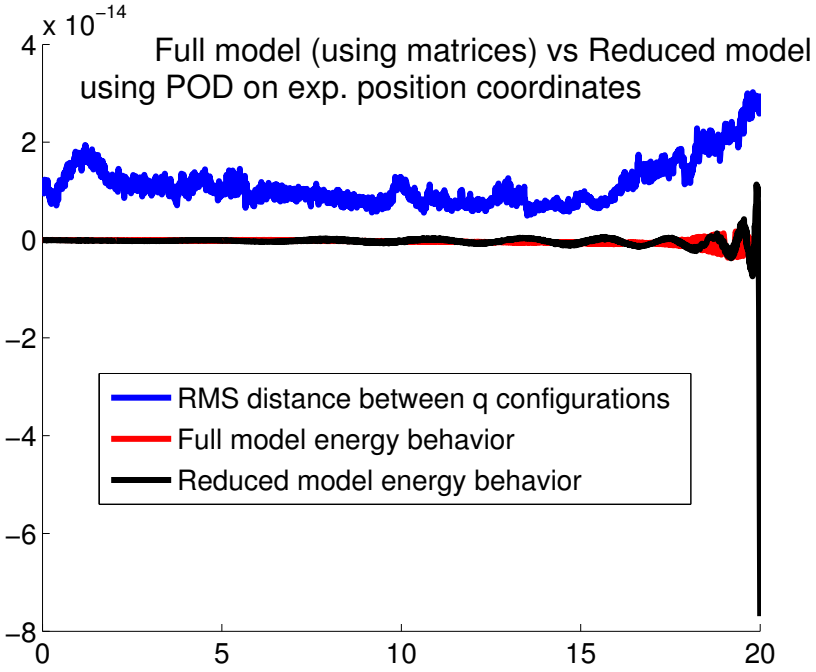

Figure 4.4: A comparison of the full model run in embedded matrix coordinates to a reduced model constructed via POD on position snapshots in exponential coordinates. We see the two models agree very closely for the full time interval.

model remain $O(10^{-14})$ over the entire time interval. This is an $O(10^{13})$ improvement over the reduced model constructed from full state snapshots in embedded matrix coordinates.

Lastly, Figure 4.5 compares the trajectory of the full model versus that of the reduced model constructed from PCA on full-state data with the positions in exponential coordinates. That is, we constructed this reduced model using straightforward POD with snapshots. The only difference from the first reduced model presented is taking the snapshots in exponential rather than embedded matrix coordinates. The model does not preserve any relationship between positions and momenta. Figure 4.5 shows that the error between reduced and full models remains at most $O(10^{-13})$ over the entire interval. This is an $O(10^{12})$ improvement over POD with embedded coordinates and only one order of magnitude worse than the position-reduced model designed to preserve structure. This result suggests that the elimination of extraneous variables by moving from embedded to local coor-

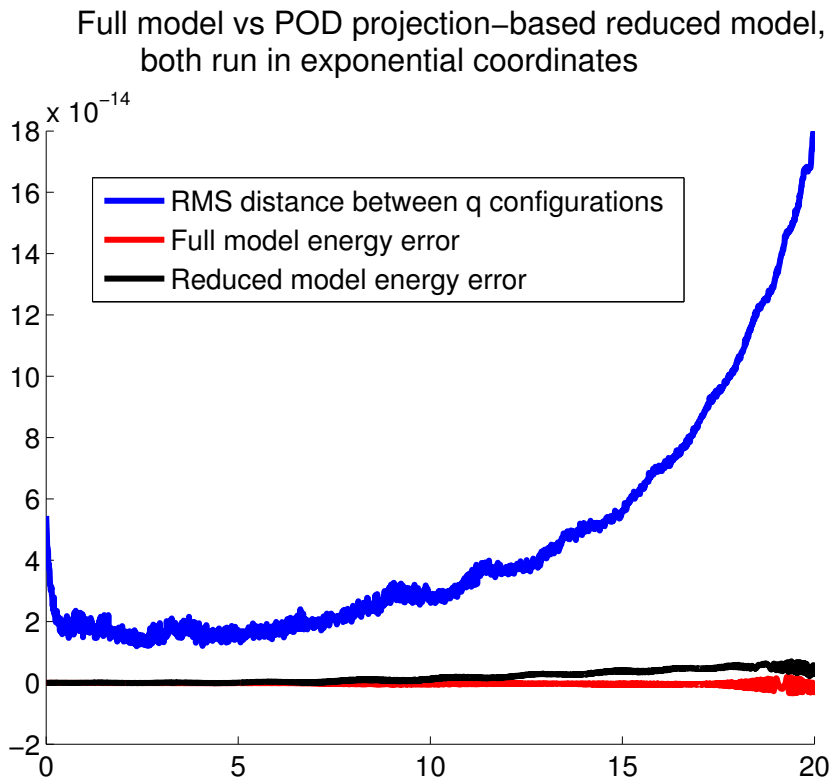

Figure 4.5: A comparison of the full model run in exponential coordinates to a reduced model constructed via POD on full state snapshots in exponential coordinates. The error in the reduced model is slightly larger than for the model using position-only snapshots but much smaller than the model using full state snapshots in embedded coordinates.

dinates could be responsible for most of the gains in the position-reduced system. This is good news from the standpoint of practical implementations. POD on local coordinates is just as data-driven and easily implemented (given a local coordinate model) as POD on embedded coordinates. At the same time, local coordinates present several unique challenges as, over long enough times, we would expect to leave the chart in which we performed the original POD.

4.5 Ongoing and future work

To perform classical SVD-based POD on position snapshots in a manifold requires some sort of coordinate mapping from the manifold to a linear space. using an embedding of Q in some V as done in [11] amounts to using a global coordinate system on Q. In this work we have followed a suggestion of [11] and investigated the use of canonical local coordinates on $(SO(3) \times \mathbb{R}^3)^N$. Our results show a vast improvement over classical techniques on embedded coordinates. (Though, notably, we have not directly compared our methods to the new method suggested in [11].) These results clearly indicate that we should continue to investigate the use of canonical and other local coordinate maps in model reduction.

The matrix exponential and logarithm at the heart of canonical coordinates on $SO(3)$ have particularly large radii of convergence. Thus, in this first work we have assumed there is no need to worry about switching charts. For a straightforward comparison in the SVD between the local coordinates x_1 and x_2 of two sampled positions q_1 and q_2 to be meaningful, x_1 and x_2 should be generated by the same coordinate chart. That is, we should have $x_i = \phi(q_i)$ for some fixed coordinate map $\phi : u_\phi \subset Q \to \mathbb{R}^n$. Similarly, a straightforward POD comparison of $x_1, \ldots, x_n$ will be meaningful only if all n snapshot coordinates are generated by the same chart. This restricts the time horizon over which we can take snapshots.

Even if we take our snapshots over just a short time span and construct a sensible reduced linear space from them, it's unclear what the implications of that reduced space are for the overall system motion. Geometric integration shows its best advantages when using large time steps and/or performing long-time simula-

tions. Both of these scenarios are likely to drive the system's state out of u_ϕ, at which point we'd need to either extrapolate a model for the new chart from the original reduced model or re-perform the reduction process. Dynamically switching among a set of reduced models to obtain the current best fit is not a new idea [1], and perhaps we can borrow some ideas from the literature in this pursuit.

4.6 Acknowledgements

The work presented in this chapter was conducted in collaboration with Professors Elena Celledoni and Brynjulf Owren at the Norwegian University of Science and Technology (NTNU) and is currently being prepared for publication. My heartfelt thanks goes out to them for welcoming me so graciously into the NTNU community and spending their precious time chasing my hare-brained vision for this project. I am also indebted to the National Science Foundation's Graduate Opportunities Worldwide Program and to the Research Council of Norway for funding the project (Forsningsgrådet project number 239684/F11 and NSF Graduate Research Fellowship grant number DGE-1144086).

Bibliography

[1] D. Amsallem, M. J. Zahr, and C. Farhat. Nonlinear model order reduction based on local reduced-order bases. *International Journal for Numerical Methods in Engineering*, 92(10):891–916, 2012.

[2] N. Bou-Rabee and J.E. Marsden. Hamilton-pontryagin integrators on lie groups part i: Introduction and structure-preserving properties. *Foundations of computational mathematics*, 2007.

[3] E. Celledoni, F. Fassò, N. Säfström, and A. Zanna. The exact computation of the free rigid body motion and its use in splitting methods. *SIAM J. Sci. Comp.*, 30(4):2084–2112, 2008.

[4] J. Cortés and S. Martínez. Non-holonomic integrators. *Nonlinearity*, 14(5):1365–1392, 2001.

[5] M. de León, D. Martín de Diego, and A. Santamaría-Merino. Geometric integrators and nonholonomic mechanics. *Journal of Mathematical Physics*, 2004.

[6] V. Duindam, A. Macchelli, S. Stramigioli, and H. Bruyninckx. *Modeling and Control of Complex Physical Systems: The Port-Hamiltonian Approach*. Springer, 2009.

[7] A. Dullweber, B. Leimkuhler, and R. MacLachlan. Symplectic splitting methods for rigid body molecular dynamics. *J. Chem. Phys.*, 105:5840–5851, 1997.

[8] M. Gualtieri. Generalized complex geometry. *Annals of Mathematics*, 174:75–123, 2011.

[9] J. Hall and M. Leok. Spectral variational integrators. *Numer. Math.*, 2014.

[10] H.O. Jacobs and H. Yoshimura. Tensor products of dirac structures and interconection in lagrangian mechanics. *Journal of Geometric Mechanics*, 6(1):67–98, March 2014.

[11] S. Lall, P. Krysl, and J. Marsden. Structure-preserving model reduction for mechanical systems. *Physica D*, 184:304–318, 2003.

[12] M. Leok and T. Ohsawa. Variational and geometric structures of discrete dirac mechanics. *Foundations of computational mathematics*, 11(5):529–562, October 2011.

[13] M. Leok and T. Shingel. General techniques for constructing variational integrators. *Front. Math. China*, 7(2):273–303, 2012. (Special issue on computational mathematics, invited paper).

[14] J.E. Marsden and T.S. Ratiu. *Introduction to Mechanics and Symmetry*. Springer, 2 edition, 1999.

[15] J.E. Marsden and M. West. Discrete mechanics and variational integrators. *Acta Numerica*, 10:357–514, May 2001.

[16] R. McLachlan and M. Perlmutter. Integrators for nonholonomics mechanical systems. *Journal of Nonlinear Science*, 16(4):283–328, 2006.

[17] W.M. Tulczyjew. The legendre transformation. *Annales de l'Institute Henri Poincaré*, 27:101–114, 1977.

[18] A. van der Schaft. Port-hamiltonian systems: an introductory survey. *Proceedings of the International Congress on Mathematicians, Madrid, Spain*, 2006.

[19] H. Yoshimura and J.E. Marsden. Dirac structures in lagrangian mechanics *Part I: Implicit Lagrangian systems. Journal of Geometry and Physics*, 57(1):133–156, 2006.

[20] H. Yoshimura and J.E. Marsden. Dirac structures in lagrangian mechanics *Part II: Variational Structures. Journal of Geometry and Physics*, 57(1):209–250, 2006.